windpark drentse monden oostermoer

Measuring the EMI radiation with Lofar at the test turbine at location DEE-2.1 - Windpark De Drentse Monden en Oostermoer -

Final Report

Table of Contents

Table of Figures

Table of Tables

Change Log

Issue	Author	Affected Section	Reason	Status
1.0		All	Document Creation	Released to Ventolines at 21 October 2019
1.1		Many sections, see: Section 6.4	- Added 6.4 Appendix: Change list - Updates according to change list in appendix section 6.4.1	Released to Ventolines at 29 October 2019
1.2		Refer to appendix section 6.4.2	Updates according to change list in appendix section 6.4.2	Released to Ventolines at 8 November 2019
1.2 Final		Refer to appendix section 6.4.3	Updates according to change list in appendix section 6.4.3	Released to Ventolines at 19 November 2019

1 Management summary

Three to be newly built wind turbine farms, collectively named the "Windpark De Drentse Monden en Oostermoer" (DMO), are located close to ASTRON's LOFAR radio telescope. To minimise the possible effects caused by EMI interference induced by the wind turbines, a covenant has been signed between ASTRON and the three companies building DMO, stipulating maximum emission thresholds and the shared responsibility between the parties. These parties are:

- Raedthuys Windenergie B.V.,
- Duurzame Energieproductie Exloërmond B.V.,
- Windpark Oostermoer Exploitatie B.V.

According to the Covenant the EMI interference level induced by the wind turbines should be at least below -35dB, in relation the reference level defined as the "**Norm**":

> The (equivalent of) the limit value in EMC standard EN55011 for class A group 1, of 50 dBµV / m in a bandwidth of 120 kHz (this corresponds to - 0.8 dBµV / (m · Hz)) at a distance of 10 m from the wind turbine gondola at a height of 100m serves as a reference for the agreements in this covenant ("Norm").

During the first two weeks in September 2019, S&T has conducted a number of so called (pre-)validation measurements to verify that the test wind turbine, designated DEE-2.1, complies with covenant.

These measurements were performed with a measuring instrument built by S&T and ASTRON. During the design and construction of the measuring instrument, ASTRON and AT were kept informed and checked both the design and the code. ASTRON and AT also have been informed and included in the execution of the measurements and in the analysis of the resulting data.

Therefore ASTRON, AT and S&T state together that:

1. The complete measuring instrument, with LOFAR as the measuring instrument, has proven to meet the requirements and conditions described in the system requirements document [SRD] and the functionality as laid down in the Architectural Design Document [ADD], both based on:
   - The Measuring method [MeasMeth], developed by Agentschap Telecom,
   - The Statement Of Objectives [LMEMI], written by ASTRON, for usage or LOFAR as a measurement device and
   - The WTEM Memorandum: L-formula [L-Form-upd], written by ASTRON.
2. The execution of the measurements and the analysis of the resulting data were performed correctly.

The observations that can be made with respect to the measurements and analyses are:

- Based on the measurement uncertainty assessment (section 3.7), the total uncertainty in the measurements is estimated at:
  - Vertical polarized measurements: ±2.0 dB
  - Horizontal polarized measurements: ±2.9 dB
  - Vertical + Horizontal polarized measurements: ±3.3 dB
- All measurements to characterize the behaviour of the WTG have been successfully conducted.
- All data has been backed up so that the results can be re-analysed if necessary.
- With respect to the analysis, the main results per frequency band are:
  - **LBA:**
    - Around 70 MHz (in the LBA frequency band) we seem to have found evidence for a wideband signal whose source is believed to be found inside the WTG.

      Further analysis regarding a suspected UPS shows that indeed it contributes significantly to the measured interference.

- Other signals exceeding the -35 dB limit are either caused by insufficient sensitivity of the equipment, excessive environmental noise, or cannot unambiguously assigned to a source inside the WTG, but more likely to a reflection of a source outside the WTG.
- For the combination of H-pol and V-pol data, we added both H-pol signal and the V-pol signal. We notice then when the UPS is switched off, the H+V signal is at the -35 dB limit, whereas when the UPS is still operational, the H+V signal exceeds the -35 dB limit with 3 dB. Note, the operational version of the DEE-2.1 will be modified such that the UPS will have its impact reduced on the signal strength.

  - **HBA-LOW:**
    - The majority of the HBA-LOW band doesn't show a significant disturbance, except for a set of features originating from the nonlinear character of the LOFAR receiver chain itself. At the higher frequencies, we see the effect of reflections of DAB emissions outside the WTG itself.
  - **HBA-MID**:
    - The HBA-MID is almost completely contaminated by DAB emissions. No disturbances from the WTG have been found.
  - **HBA-HIGH:**
    - The lower frequencies of this band are contaminated by DAB emissions just like the complete HBA-MID band. Other disturbances that can be found in the averaged L-plot cannot be unambiguously assigned to a source inside the WTG, but are more likely to be a reflection of a source outside the WTG.

- The results of the summations of the H-polarization and V-polarization components (H+V) are:
  - For those ranges where there is a signal from the WTG detected (e.g., around the 70 MHz) we notice the expected increase in signal power of approximately 3 dB (the signal being more-or-less unpolarized).
  - In the HBA frequency range there is no signal higher than -35 dB value at the frequencies where the signal in individual H-polarization and V-polarization component is under -35 dB level, i.e., no new exceedances of the -35 dB level are introduced by the summation.

Conclusion:

One signal has been found around the 70 MHz that is believed to originate from the WTG. This issue has been further investigated and it was shown that the signal can be linked to the workings of one of the UPS systems inside the WTG. This has been validated by processing the data for those time period for which it is certain that the UPS was not operative anymore. This analysis resulted indeed in evidence that the UPS contributes to the signal found at 70 MHz.

Other signals exceeding the -35 dB limit are either caused by insufficient sensitivity of the equipment, receiver characteristics, excessive environmental noise, or cannot unambiguously be assigned to a source inside the WTG, but more likely to a reflection of a source outside the WTG.

Also, after the required summation of the polarization components (H-pol and V-pol) we have seen:

- A considerable improvement has been obtained by switching off the UPS as is part of the modification the WTG. The measured signal strength is then at the -35 dB limit for the 70 MHz region.
- Currently, no other frequency is suspected to exceed the -35 dB llimit value where the WTG must be assumed to be the source of the measured signal level.

Figure 1 gives a graphical overview of the main measurement results over entire frequency range.

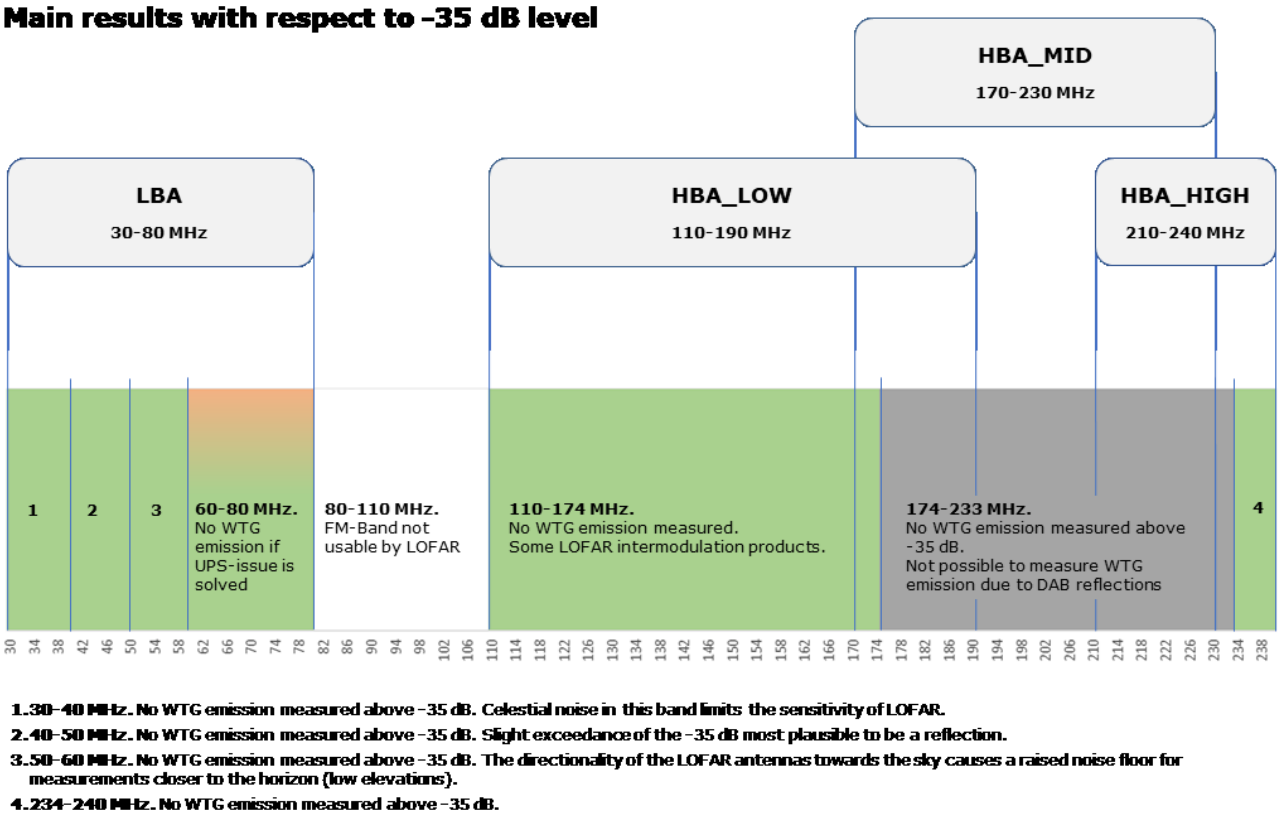

Figure 1: Overview of main measurement results over entire frequency range

2 Introduction

2.1 Purpose and Scope

The purpose of this document is report the outcome for the Measuring the EMI radiation with Lofar at the test turbine at location DEE-2.1 - Windpark De Drentse Monden en Oostermoer - (WTEM_LOFAR) project.

2.2 The project

Three to be newly built wind turbine farms, collectively named the "Windpark De Drentse Monden en Oostermoer" (DMO), are located close to ASTRON's LOFAR radio telescope. To minimise the possible effects caused by EMI interference induced by the WTGs, a covenant [COV] has been signed between ASTRON and the three companies building DMO, stipulating maximum emission thresholds and the shared responsibility between the parties. These parties are:

- Raedthuys Windenergie B.V.,
- Duurzame Energieproductie Exloërmond B.V.,
- Windpark Oostermoer Exploitatie B.V.

According to the Covenant the EMI interference level induced by the WTGs should be at least below -35dB, in relation the reference level defined as the "**Norm**":

> The (equivalent of) the limit value in EMC standard EN55011 for class A group 1, of 50 dBµV / m in a bandwidth of 120 kHz (this corresponds to - 0.8 dBµV / (m · Hz)) at a distance of 10 m from the wind turbine gondola at a height of 100m serves as a reference for the agreements in this covenant ("Norm").

In this project S[&]T has:

- Laid down the requirements for the total measurement instrument in the System Requirements Document [SRD],
- Designed the total measurement instrument conform the Architectural Design Document [ADD],
- Based the design on:
  - The method [MeasMeth] described by Agentschap Telecom (AT)
  - The Statement Of Objectives [LMEMI] written by ASTRON, for usage of LOFAR as a measurement device and
  - The Memorandum of ASTRON [L-Form-upd].

Conform the Covenant, AT is responsible for the final validation of the measuring instrument. Therefore, during the design process, the coding, the actual measurements and the processing of data, S[&]T has informed and included AT (as well as ASTRON) by:

- Submission of requirements and design documentation, code, measurement plans and measurement results for review,
- Regular joint progress and consultancy meetings.

The result of this project and its complete process is laid down in this Final Report.

2.3 Document Overview

The structure of the document is as follows:

- Section 1: Management summary
- Section 2: Introduction
- Section 3: Measurements
- Section 4: Analysis overview
- Section 5: Summary of results and conclusions
- Section 6: Appendices

2.4 Reference Documents

Applicable and reference documents are listed in Table 1.

Table 1: Applicable documents.

AD	Document	Author	Vers.	Issue date
[RFQ]	Request for Quotation, Realisation and Implementation Measurement of Electromagnetic Radiation	Project Wind Farm De Drentse Monden en Oostermoer	01	2017/12/23
[COV]	Agreement coexistence wind farm De Drentse Monden en Oostermoer and the LOFAR radio telescope of ASTRON	ASTRON, Raedthuys Windenergie B.V., Duurzame Energieproductie Exloërmond B.V., Windpark Oostermoer Exploitatie B.V.	01	2016/09/16
[MeasMeth]	Method for measuring the EMI radiation of wind turbines in relation to the LOFAR radio telescope	Agentschap Telecom	1.0	2017/10/08
[VEML]	Verstoring van het elektromagnetische milieu ter plaatse van de LOFAR kern door het windturbinepark Drentse Monden en Oostermoer	Agentschap Telecom		2016/10/19
[LMEMI]	Increasing LOFAR capabilities for measuring wind turbine EMI	ASTRON, Dwingeloo, The Netherlands	1.0	2018/09/18
[L-Form-upd]	WTEM Memorandum: L-formula	ASTRON, Dwingeloo, The Netherlands	-	2019/10/11
[OFFR]	Algorithms for Radio Interference Detection and Removal,	A.R. Offringa, University of Groningen, dissertation.		June 2012
[ANTSOL]	Computation of Antenna Dependent Complex Gains	Sanjay Bhatnagar, document can be found on: http://www.aoc.nrao.edu/~sbhatnag/GMRT_Offline/antsol/antsol.html		Jan, 1999
[ADD]	WTEM Architectural Design Document, ST-WDMO-WTEM-ADD-001	S&T, Delft	1.6	2019/10/18
[SRD]	WTEM System Requirements Document ST-WDMO-WTEM-SRD-001	S&T, Delft	1.4	2019/08/20
[UNCERT]	WTEM Uncertainty Assessment ST-WDMO-WTEM-REP-002	S&T, Delft	1.2 Final	2019/11/19
[CALNPL]	NPL_2018100058 emitter certificate R2	National Physical Laboratory (NPL), Teddinton Middlesex, United Kingdom	2.0	2019/02/12

2.5 Definitions

Terms, acronyms, abbreviations and definitions are listed in Table 2.

Table 2: Terms and Definitions

Term	Explanation
ACM	Antenna Correlation Matrix
ADC	Analog-to-Digital Converter
ADD	Architecture Design Document
ASTRON	Netherlands Institute for Radio Astronomy.
AT	Agentschap Telecom
DAB	Digital Audio Broadcast
DMO	Drentse Monden Oostermoer
EIRP	Effective Isotropic Radiated Power
EMC	Electro Magnetic Compatibility
EMI	Electro Magnetic Interference
HBA	High Band Antenna
IM	Inter Modulation
LBA	Low Band Antenna
LNA	Low Noise Amplfier
LOFAR	LOW Frequency Array; ASTRON's radio telescope in the neighbourhood of the Wind Turbine Park.
NPL	National Physical Laboratory, Hampton Rd, Teddington TW11 0LW, United Kingdom
RCU	Receiver Control Unit (one of the components of the LOFAR infrastructure)
RFI	Radio Frequency Interference
RFQ	Request for Quotation
RS	Reference Source
S[&]T	Science and Technology BV
SDM	EMC ShutDown Mode
Tx	Transmitter
UPS	Uninterruptible Power Supply
UTC	Coordinated Universal Time
WTEM	Wind Turbine Electro Magnetic Interference Measurements
WTG	Wind Turbine Generator

3 Measurements

3.1 Reference source

The reference source [ADD] that has been used for these measurements, emits a well-characterized (i.e., calibrated at the National Physical Laboratory (NPL) [CALNPL]) signal with a known flux density with respect to the covenant limit values. This signal will be emitted sufficiently close to the Wind Turbine Generator (WTG) so that the transmission path of the reference signal corresponds to the one of the WTG signals, yet the position of the reference source is sufficiently separated that the reference source signal doesn't interfere with the WTG signal.

The reference signal that is emitted during the measurement period is a comb signal with a frequency period of 1 MHz.

3.2 H-V-measurements

The measurements are divided into a set of Horizontal polarized (H-pol) and a set of Vertical polarized (V-pol) measurements. For the H-pol measurements, the antenna of the reference source is placed such that Horizontal polarized signals are emitted, and for the V-pol measurements, the Reference Source emits Vertical polarized signals.

The antennas at the receiving stations are also dual-polarized. That is, the antennas receive the signals in two –orthogonal– directions, these directions are called XX and YY. In principle, the XX and YY polarization of the antenna have no direct relationship with the H-pol and V-pol signals from the Reference Source. However, as it turns out:

- The H-pol signal from the Reference Source is dominantly represented by the YY-readings of the antenna.
- The V-pol signal from the Reference Source is dominantly represented by the XX-readings of the antenna.

The signals that are emitted by the WTG will contain both H-pol and V-pol components. To measure the V-component of the total WTG emission, we will take only the XX readings into account, and to measure the H-component of the total WTG emission, the YY readings.

Note that the Measure Method [MeasMeth] as issued by Agentschap Telecom (AT) defined that the behaviour of the WTG had to be measured only for the V-polarized signals, as originally it was hypothesized that the transmission of H-polarized signals and the reception of those signals by the LOFAR antennas would be negligible compared to the V-polarized signals. However, during the test measurements in February 2019 it was noticed, on suggestion of Dick Harberts (Philips) who is supporting WTG project development, that the LOFAR antennas would be sensitive to both H-polarized and V-polarized signals. It was then accepted by all parties that both H-polarized and V-polarized signals will be measured.

3.3 Frequency bands

For the analysis we will distinguish between different frequency bands. The use of these frequency bands is a consequence of using LOFAR as a measurement system. Due to the maximum sample rate, the ADCs of LOFAR cannot digitize the whole frequency band of 30 … 240 MHz in one pass. Instead, the frequency span of 30 - 240 MHz must be divided into four different smaller frequency bands, each of them to be observed separately (refer to Figure 2).

Within this frequency span the band from 90 – 110 MHz is affected by FM radio transmissions, where LOFAR will not measure anyway. The band from 174—230 MHz is affected by Digital Audio Broadcast. This band is included in a separate band to be observed.

The separation results in the following four bands: LBA (Low Band Antenna), HBA (High Band Antenna) and the latter in a division of low, high and mid (refer to Figure 2 and Table 3).

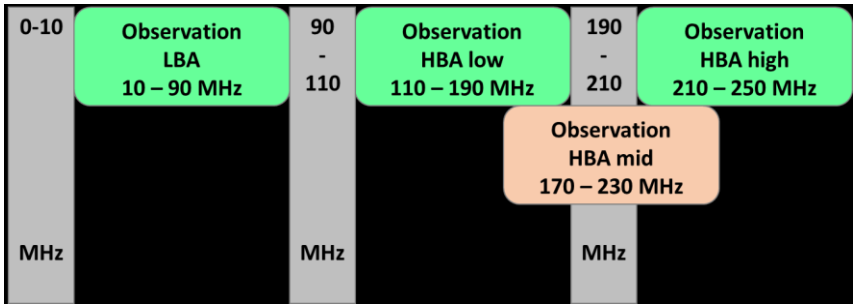

Figure 2: Frequency bands (refer to [ADD])

Table 3: Frequency bands (refer to [ADD])

Frequency band	Frequency range	Description
LBA	10 – 90 MHz	Massive interference below 20 MHz during daytime. Only 30[1] – 80 MHz is considered
HBA_LOW	110 – 180 MHz	HBA band with the least interference
HBA_HIGH	210 – 250 MHz	This band contains many digital audio stations. Only 210 – 240[2] is considered
HBA_ MID	170 – 230 MHz	HBA band affected by interference. It contains several digital audio stations.

3.4 Wind turbine modes

The following wind turbine modes have been measured during the first two weeks in September 2019:

Table 4: Wind turbine modes

Turbine mode	Description
Normal operation	Completely powered and producing wind energy power at least 50 kW, during the entire measurement, corresponding to a wind speed of approximately 3.0 - 3.5 m/s
Wind turbine off	Completely powerless, switching at the sub-station level. Before Switching at the sub-station Nordex will bring the turbine to a stop and will manually switch-off the aviation lights and the aviation light UPS system
EMC Shutdown	Wind turbine is powerless up from the low voltages circuit breaker in the converter. Only system which remains active is the aviation light system by means of his battery package (estimation capacity 8 – 10 hours).
Standby downtime plus	Standby state corresponding to the downtime state with switched off visibility sensor and flickering module, according to the Nordex Downtime Status proposal revision 3.
Standby downtime	Standby state corresponding to the downtime state according to the Nordex Downtime Status proposal revision 3 (without switching off the visibility sensor and shadow flickering module)

Note that the two Standby modes have initially been identified for the stand-still periods, but this has during the measurement period been assigned to a newly defined WTG-mode, called the EMC Shutdown (measured at night and consequently with aviation lights on) mode. As a consequence, the Standby modes have not been included in the analysis in this report.

[1] 30 MHz is the minimum frequency of the "LOFAR" band given in [MeasMeth]

[2] 240 MHz is the maximum frequency of the "LOFAR" band given in [MeasMeth]

3.5 Measurements

As mentioned in Section 3.2 the measurements have taken place for horizontal polarised signals as well as vertical polarised signals from the reference source. This needed a different setup for the horizontal and vertical polarised measurements, which is further explained in the paragraphs below.

3.5.1 Measurement setting

V-measurement:

- Antenna of the Reference in V-position.
- Crane direction: 30 degrees South from West, pointing to the LOFAR core.
- Antenna direction: 30 degrees West from North, pointing to Drouwenermond.

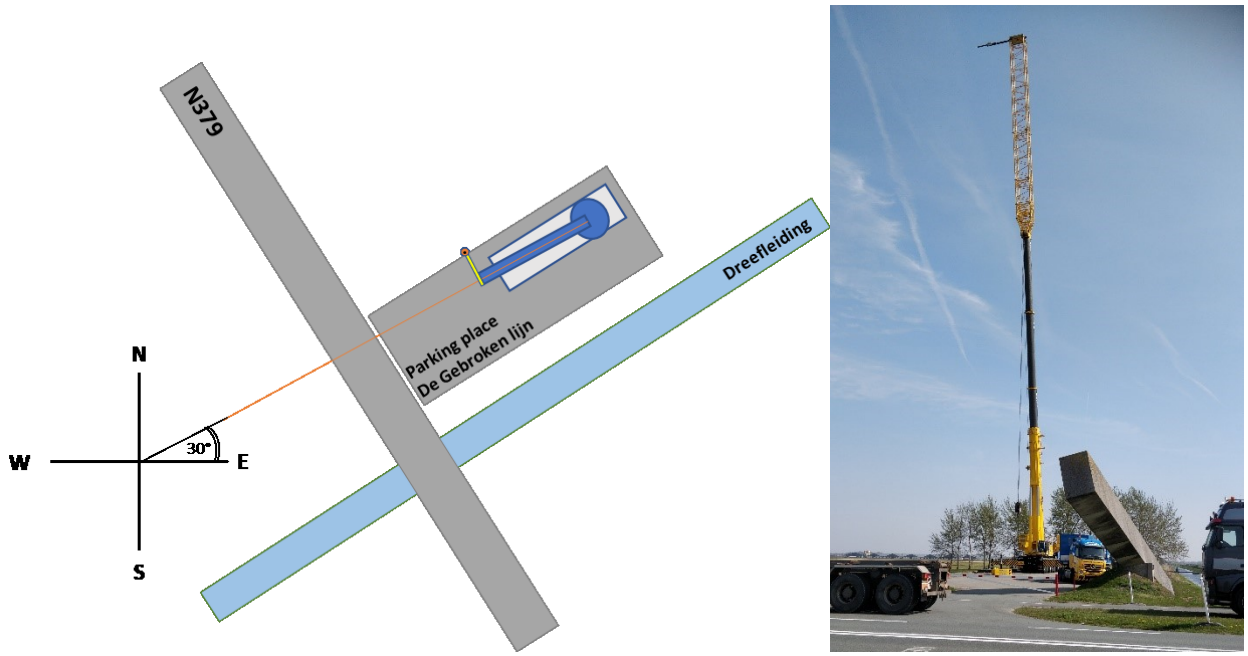

Figure 3: V-measurement directions

H-measurement:

- Antenna of the Reference Source in H-position.
- Crane direction: 30 degrees East from South, pointing to Nieuw-Weerdinge.
- Antenna direction: 30 degrees South from West, pointing to the LOFAR core.

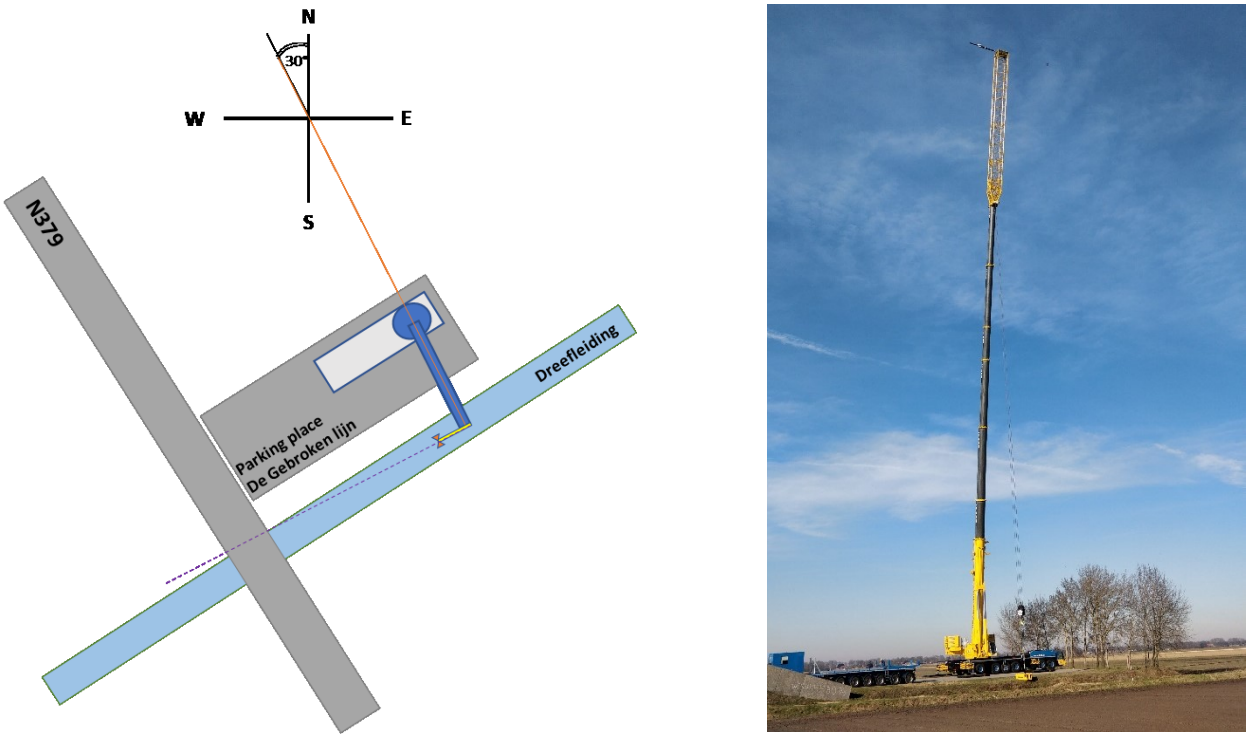

Figure 4: H-measurement directions

Figure 5 provides a geographical sketch of the positions of the different wind turbines and the positions of the LOFAR antennas. The centre of LOFAR antennas is at point (0,0), and the antennas (blue points) are placed in the block defined by the coordinates (-2, 2) (left upper corner) and (2,-2) (right lower corner). The WTG under test DEE 2.1 is placed just left of the coordinate (4,2).

With respect to the crane pointing: For the V-measurements, the crane is pointing towards the LOFAR antennas; for the H-measurements, the crane is pointing perpendicular of the line towards the LOFAR antennas.

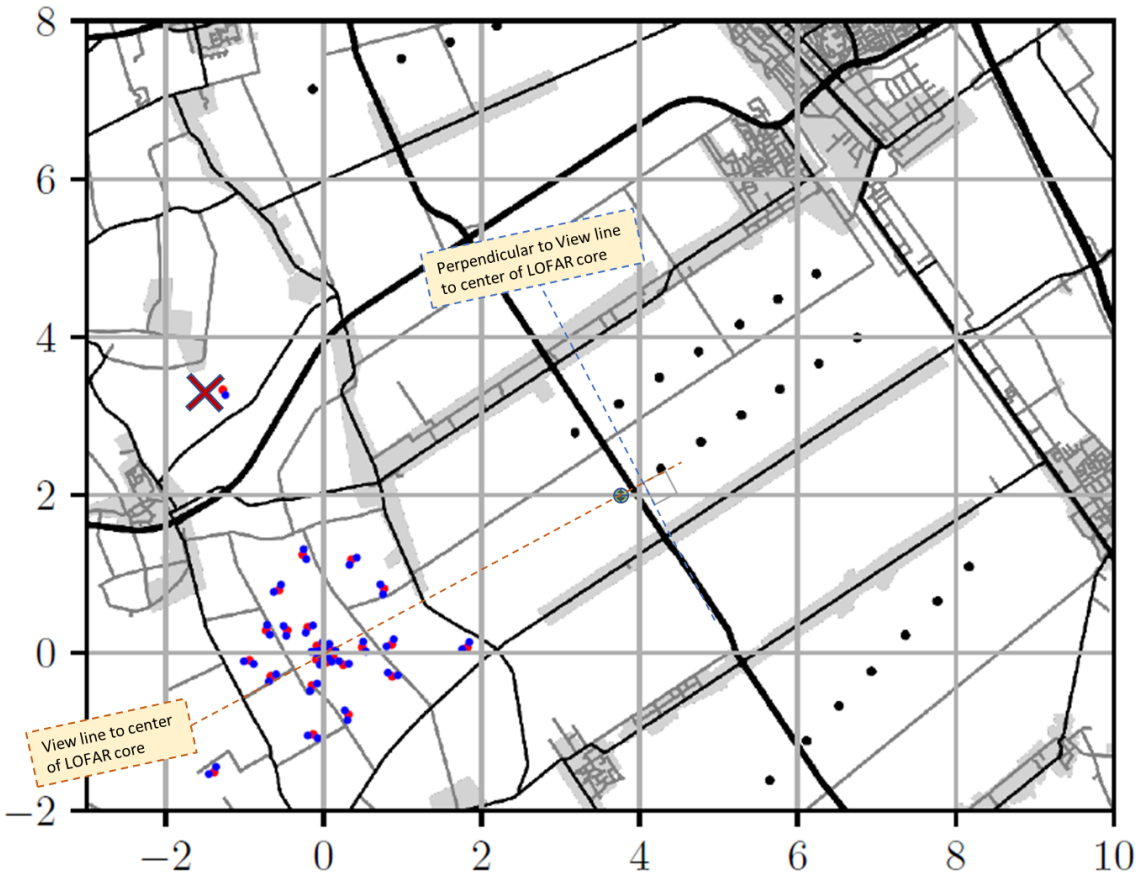

Figure 5: Overview V- and H- measurement directions

3.5.2 Measurement schedule

The following table provides an overview of the measurements that have been performed during the first two weeks of September 2019:

Table 5: Measurement schedule

Night	Start (CEST)	Stop (CEST)	Polarization	WTG-mode	Success
Mon 02/Sep	21:00:00	06:40:00	V	Normal operation	No
Tue 03/Sep	20:56:04	06:36:04	V	Normal operation	Yes
Wed 04/Sep	20:52:08	06:32:08	V	Wind turbine off	Yes
Thu 05/Sep	20:48:12	06:28:12	V	Standby downtime plus	Yes
Fri 06/Sep	20:44:16	06:24:16	V	Standby downtime	Yes
Sat 07/Sep	20:40:20	06:20:20	H	Normal operation	Partly, second half useful
Sun 08/Sep	20:36:25	06:16:25	H	Standby downtime	Yes
Mon 09/Sep	20:32:29	06:12:29	H	Standby downtime plus	Yes
Tue 10/Sep	20:28:33	06:08:33	H	Wind turbine off	Yes
Wed 11/Sep	20:24:37	06:04:37	H	Normal operation	Yes
Thu 12/Sep	20:20:41	06:00:41	H	EMC Shutdown	Yes (additional data processing required to select the red-light mode during the processing)
Fri 13/Sep	20:16:45	05:56:45	V	EMC Shutdown	Yes

3.5.3 Measurement schemes

The measurements have been conducted using measurement schemes. Appendix 6.1 shows the detailed schemes that have been followed.

The measurements have covered all four frequency bands handled in section 3.3, for each of the different wind turbine modes (handled in section 3.4) in the order given in section 3.5.2.

Each of the frequency bands were measured for two hours each in order to cope with thermal and systematic noise. This means that to cover the whole frequency span a measurement duration of 8 hours was necessary.

As an additional constraint, the so-called HBA_LOW measurements were deliberately interrupted for 1.5 hours. Otherwise, the measurements would be affected, by the rising of the celestial source TAURUS-A right behind the WTG, shown by interferences visible in the measurement samples.

Also, the measurements were shifted back in time each day (night), by approximately 3 minutes and 56 seconds, in order to keep the galactic background, with its interfering celestial sources, exactly the same. This can be seen both in the measurement schedule (Table 5 in section 3.5.2) looking at start / stop times and in the measurement schemes (Appendix 6.1) looking at start / end times.

During the measurements the reference source has been operated with an emission pattern of 12 seconds ON and 48 seconds OFF. The measurement data of the reference source OFF period was actually used for measurement of EMI from the wind turbine (integrated over the before mentioned two hours). The measurement data of the reference source ON period was used during processing for compensation of changes in the propagation path, as the signal of the reference source and of the WTG travel approximately the same path. It also was used to calibrate the receiver antenna system for electronic fluctuations. All this is described in Appendix 6.3

3.6 Data processing

The data processing is divided into two steps:

- Step 1: Pre-processing performed by ASTRON. The objective of this pre-processing process is basically to reduce noise:
  - Astronomical sources that have a signal flux in the same order magnitude as the relevant covenant values are being subtracted from the data.
  - The measured samples are being screened (and the samples are being flagged) for RF interference using the Algorithm by Andre Offingra [OFFR].
- Step 2: Final processing at S[&]T. This process involves the estimation of the signal strength of the WTG by a process called the imaging. The processing results in a power spectrum (Power Spectral Density) plot in which the received signal power density is plotted against frequency. The signal powers are retrieved from so-called voxel cubes (for more details see also Appendix 6.3). These voxel cubes are being created by a process called imaging. Starting from the received antenna signals, estimate the location of the source of the signals. A strong signal with respect to the environment will create a clear hotspot; a signal buried in noise will create a less clear image as is shown in the following image.

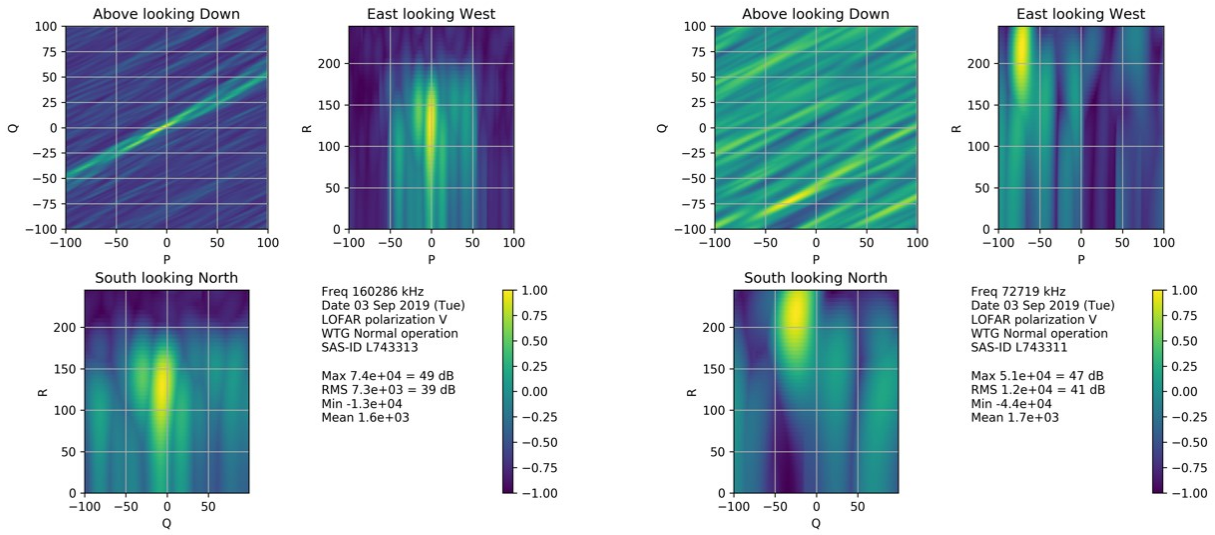

Figure 6 two examples of a voxel cube: Left a strong signal, Right a signal buried in noise.

3.7 Uncertainty analysis

In [UNCERT] a detailed analysis of the uncertainties in both the measurements and the analysis has been provided. Based on the quantitative impact of the summary of the individual contributions, given in Table 6, the result of the estimated total uncertainty in the measurements is:

V-measurements: ±2.0 dB

H-measurements: ±2.9 dB

H+V measurements: ±3.3 dB

Table 6 is the summary of the individual elements that actual contribute to the total measurement uncertainty estimation. This summary is made from an extensive list from possible contributing elements that were explored in detail in [UNCERT]. These values cannot be added linearly. Similarly, to Section 3.1 in [UNCERT], these individual dB values must be added in quadrature. This is a consequence of the dB scale being an inherent combination of values as a ratio, rather than an absolute, discrete value of its own.

Table 6: Summary individual element contributions to the measurement uncertainty

Name	Conclusion	Quantitative Impact	
		Vertical polarization	Horizontal polarization
Transmission, Reference source, Antenna			
Direction	Some gain variation across the antenna pattern	±0.2 dB	±1.0 dB
Transmission, Reference source, Source calibration			
Power (NPL)	Third-party calibration measurements of entire spectral range	±1.5 dB	±1.5 dB
Transmission, Reference source, Crane			
Crane EM properties	Simulations predict a spectral variation due to reflections and resonances.	±1.2 dB	±2.55 dB
Calculation, Calibration at S&T			
Distance proportionality	This question was resolved, and determined to have no influence on uncertainties.	±0.26 dB	±0.26 dB

Polarisation leakage	Incomplete coupling between the transmitted polarisation and LOFAR's dipoles.	±1.0 dB	±1.0 dB
	Total	**±2.0 dB**	**±2.9 dB**
	Total H+V	**±3.3 dB**	

4 Analysis overview

4.1 General analysis introduction

4.1.1 Frequency plot explanation

The main output of the analysis is the set of Power Spectral Density (PSD) plots where the performance of the WTG is depicted in relation to the covenant value. For each of the measurements a separate plot is provided. Each plot contains the following values:

- The so-called "L-value" which describes the Power density of the WTG in relation to the covenant value. The covenant value of 0 dB equals 50 dBµV/m in a BWcov = 120 kHz bandwidth at 10 m distance, or an EIRP density value of 2.8 10-12 W/Hz). The L-value is depicted by black or blue dots in the graph, where
    - A black dot indicates that the maximum flux within the voxel cube is indeed at the location of the WTG.
    - A blue dot indicates that the maximum flux is found at another place than the WTG location. This is an indication of much disturbance at this frequency.
- The noise floor which has been computed by taking the RMS of the voxel cube belonging to the Reference Source, at the time that the reference source is switched off. The noise floor is depicted by the (light) grey dots in the graph. The noise floor is indicated by the grey dots in the graph.
- A curve of 3 times the noise floor. Each WTG power value exceeding this significance level can be considered as being surely originating from the WTG, statistically with 88.9% probability, by Chebyshev's inequality[3]. For unimodal distributions the probability of being within the interval is at least 95% by the Vysochanskij–Petunin inequality[4]. There may be certain assumptions for a distribution that force this probability to be at least 98%[5] and here for 3σ: 99,73%[5].
- The -35 dB limit line. The -35 dB limit is depicted by the dashed line in the graph.

4.1.2 L-value

The "L-value" is defined in the measurement description by AT [MeasMeth] as the value of the WTG output relative to the covenant reference value. Thus, a value of -35 dB indicates a WTG that for that frequency complies to the -35 dB covenant threshold. The L-value is now defined as:

$$L = {}^{P_{WTG}}/_{P_C}.$$

Where P_C is the covenant value, and P_{WTG} the power density of the WTG.

Or, as expressed in dB's, then the L-value becomes: $L[dB] = P_{WTG}[dB] - P_C[dB]$.

We refer to the technical note of ASTRON [L-Form-upd], which serves as an update to [MeasMeth], to provide the exact formula to compute the L-value based on the voxel cube values and the distance of the WTG and the Reference Source to LOFAR. Note that the update was necessary in order to resolve the consequences of the different signal structure of the Reference Source (a comb of very narrow band signals with a frequency spacing of 1 MHz, instead of a broadband signal distributed over some 100 kHz).

4.1.3 Analysis steps

The reasons that the measured Power Spectral Density graph for the Covenant values is higher than the -35 dB limit line can be several:

- A disturbance originating from the WTG.
- The ambient noise is higher than that coming from the WTG.

---

[3] https://en.wikipedia.org/wiki/Chebyshev%27s_inequality#Probabilistic_statement

[4] https://en.wikipedia.org/wiki/Vysochanskij%E2%80%93Petunin_inequality

[5] https://en.wikipedia.org/wiki/68%E2%80%9395%E2%80%9399.7_rule

- The disturbance is a reflection of a stronger signal that is emitted in the (relative) neighbourhood and is reflected by the tower and / or blade structure of the WTG.
- The noise floor is higher than the -35 dB limit value.
- Idiosyncratic behaviour of the LOFAR system: For example, due to nonlinear behaviour the receiver chain of LOFAR may create intermodulation (IM) products.

To a certain extent, the cause of exceeding the limit can be analysed as follows.

High Ambient Noise: In such a case, we find that the imaging algorithm doesn't create a "hotspot" of flux density at the location of the WTG, and / or we see that at other locations than the WTG-location in the voxel cube the flux is higher than at the WTG. An example of such a case is given in the following figure.

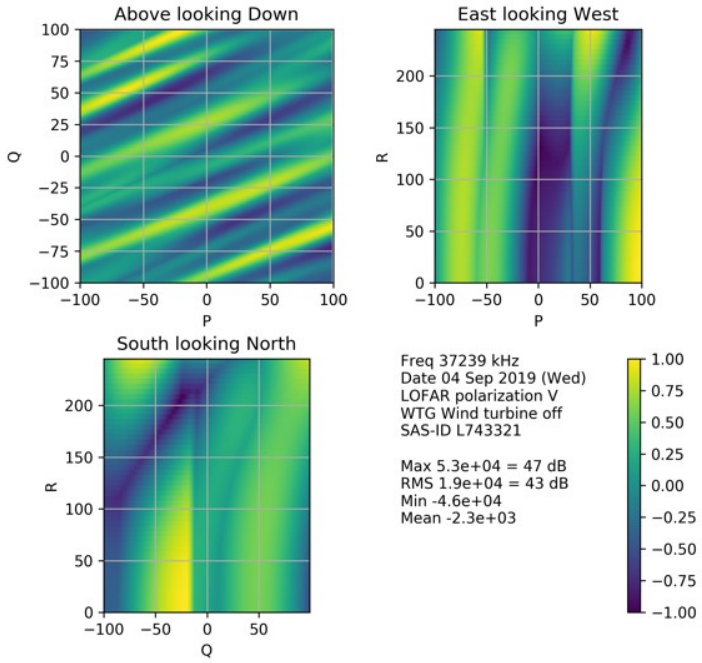

Figure 7: Noisy environment

Reflection: If the WTG acts as a reflector of a strong emitter then the signal can be reflected as a point source. This will be visible as a hot spot of flux in the voxel cube.

Often, we see also a rise in the noise level at the frequency where the disturbance takes place.

Reflections can also be identified by inspecting the ON and OFF (and SDM) modes of the WTG: If disturbances are visible in both the ON and OFF mode, it is very likely that the cause is a reflection.

We must remark, however, that the yaw direction of the nacelle may strongly affect the strength and the number of reflections. As the OFF and ON modes are measured at different dates (with different weather conditions), it may be that reflections in the OFF mode will not be visible during the ON mode (or vice versa).

Also, the spectral structure can provide a clue: For example, in the HBA-MID frequency region (and in the lower end of the HBA-HIGH) we see structures of approximately 1.5 MHz wide; an indication of DAB (i.e., outside the WTG). Furthermore, aviation and military communication overlap with LOFAR frequencies of interest.

Some examples of frequencies that are used by third parties:

- DAB uses a wide-bandwidth broadcast technology and typically spectra have been allocated for it in Band III (174–240 MHz) and L band (1.452–1.492 GHz)[6]. As we see, the Band III emissions overlap with the LOFAR frequencies of interest.
- The VHF airband uses the frequencies between 108 and 137 MHz.

Note that as the WTG is located close to the German border and the high structure of the WTG, we must consider both Dutch and German sources of EM emission.

Noise floor is higher than -35 dB: We see situations where the noise floor of the measurement system is higher than the -35 dB level. This is often the case of reflections of strong emissions, but can also be caused by other causes, either internally or externally, even possibly from celestial sources (it is likely that in the frequency range of < 40 MHz we primarily sense the noise from the milky way due to the fact that the sky is extremely bright at these lower frequencies, and in the range of 50 …60 MHz we see the effect of the antenna that has better gain pointing to the sky than pointing towards the horizon).

Intermodulation products: Nonlinear behaviour of a receiver chain may create intermodulation (IM) products resulting in a peak in the received spectrum. These IM-peaks are the product of mixing two or more signals which may originate outside the receiver chain and / or inside the chain. Such an IM-peak will most likely occur in both the ON and the OFF measurement, depending whether the signals that causes the IM-products is present in both the ON and OFF measurements.

Signal from the WTG: Similar to the reflection, the disturbance will be visible as a hotspot in the voxel cube.

- The signal must be visible in the ON mode, and not in the OFF mode (note that doesn't say it isn't a reflection, it can be that the direction of the nacelle is such that a reflection is visible during the ON measurements, but not during the OFF measurements).
- As further evidence: The spectral structure may be such that it roughly corresponds to one or more of the signals as found during EMC tests of individual components of the WTG in the lab. By interactions of the various components of the WTG may amplify the signal to a level much higher than the individual measurements show.
- Furthermore, if the spectral structure doesn't seem to match the structure of a known transmission source then it is likely the signal originates from the WTG.

4.2 Analysis reports

Automated in the processing pipeline, analysis reports are generated per measurement and per frequency band. Most of the reports have the latest format, described below. Some reports have not been updated and are listed below:

3. V-pol, 3-sep-2019, Normal operation, HBA_MID
7. V-pol, 4-sep-2019, Wind turbine off, HBA_MID
11. V-pol, 13-sep-2019, EMC Shutdown, HBA_MID
15. H-pol, 10-sep-2019, Wind turbine off, HBA_MID
19. H-pol, 11-sep-2019, Normal operation, HBA_MID
9. V-pol, 13-sep-2019, EMC Shutdown, LBA (including UPS)
21. H-pol, 12-sep-2019, EMC Shutdown, LBA (including UPS)

They have the following contents (the difference between new and old will be indicated)

- **General (new):**
  - Page header: Reference (report number updated), Version (text "Auto-generated")
  - Title page: Subtitle (Appendix number and contents line)
  - Update of Prepared, Checked and Approved table)
  - Section 1) Introduction text updated, depending on contents
- **Spectrum per band:**
  L-Plots over the frequency range of the specific frequency band in three forms:
  - No averaging,
  - Averaged over 1 MHz,
  - Averaged over 1 MHz zoomed in between -20 dB and – 50 dB.

[6] See: https://en.wikipedia.org/wiki/Digital_audio_broadcasting

- **Calibration "solutions" for the image:**
  - Spatial distribution of the flux maxima around the calibration source
    Not averaged and seen from three directions:
    - From above (new = in the direction of LOFAR, indicating the small cube around the reference source in orange)
    - New: facing LOFAR, Old: From the south side
    - New: perpendicular to facing LOFAR, Old: From the west side
  - Signal to noise ratio (SNR) of the Calibration Source
    Calculated per LOFAR dipole:
    - SNR using dipole DXX
    - SNR using dipole DYY
    - SNR using dipole SUM
  - Computed delays for each station to the main station
    Between specific LOFAR antennas
- **Reference source corrections:**
  Different corrections that been applied, based on calibration data
  - NPL calibration corrections, over the frequency range of the specific frequency band
  - Temperature corrections, over time
  - Voltage corrections, over time and frequency
  - With respect to the attenuator: All measurements have been conducted with a 0 dB reference source signal, and as such the attenuator hasn't been incorporated in the signal path. The attenuator has been disregarded in the source.
  - Total of all corrections
- **WTG data:**
  - Spatial distribution of the flux maxima around the WTG
    Showing cube maxima with different colours for maxima in the centre cube and those outside the centre cube, seen from three directions and with three different averaging (using 5 times MAD[7]) options.
    - Seen from above (New = in the direction of LOFAR, indicating the small cube around the WTG in orange)
      - averaged over 1 MHz
      - averaged over 240 kHz
      - not averaged
    - New: facing LOFAR, Old: Seen from the south side
      - averaged over 1 MHz
      - averaged over 240 kHz
      - not averaged
    - New: perpendicular to facing LOFAR, Old: Seen from the west side
      - averaged over 1 MHz
      - averaged over 240 kHz
      - not averaged
  - New: Frequency detail overviews. The number of frequencies, for which the details are shown, is based on linear distribution over the frequency range using steps of 2 MHz, which comes down to $(f_{max} - f_{min}) / 2$. Additionally, a number of specific frequencies of interest have been added. Table 7 lists the all the frequencies used per frequency range. Each analysis page consists of:
    - An ACM and flux plot with the reference source OFF and dipole SUM,
    - A limited L-Value plot around the specific frequency (Black dashed line: -35dB threshold, Red dashed line: the specific frequency being analysed here). *If there are few or no maxima to see in the plot, this is because these maxima exceed the scale of the plot.*
    - Improved 3D side views for 1 MHz frequency-averaged cubes around the WTG. The images show the location of the maxima (Blue circle: of the inner cube, Black circle: the total cube, White dot: location of WTG). Five vies are shown:
      - Top view, showing inner cube around the WTG (Orange) and axes towards and perpendicular to LOFAR

[7] https://en.wikipedia.org/wiki/Median_absolute_deviation

- East looking west
- South looking North
- Facing LOFAR
- Perpendicular to facing LOFAR

- Old:
  - ACM and flux plots, with the reference source OFF and dipole SUM and the frequencies linearly distributed over the frequency range.
  - 3D side views for 1 MHz frequency-averaged cubes, with frequencies linearly distributed over the frequency range, and including some specific frequencies of interest.

With 6 measurements and 4 frequency bands per measurement, the number of automated generated analysis reports is 24. They are appendices to this report and have been listed in Appendix 6.2.

Table 7: Frequencies in frequency detail overviews of new analysis reports

LBA		HBA_LOW		HBA_HIGH	
31.117	59.047	109.895	154.750	210.762	224.867
33.070	61.153	110.957	156.856	211.739	225.716
35.023	63.106	112.758	158.961	212.367	227.797
37.129	65.059	114.864	160.762	212.910	229.750
37.239	66.774	116.927	162.825	213.148	231.703
37.325	67.122	118.727	164.973	213.692	233.723
39.082	69.075	120.833	167.055	215.102	233.766
41.035	71.156	122.914	168.813	215.797	235.719
43.141	71.895	124.739	170.961	217.751	237.825
45.094	72.719	126.820	173.024	219.704	239.778
45.375	73.109	128.926	174.825	221.809	241.731
47.047	75.063	131.032	176.930	222.981	243.684
49.153	76.302	132.832	178.969	223.763	245.766
51.106	77.168	134.938	179.274	224.739	247.719
53.059	77.516	137.044	179.469		249.825
55.208	79.121	138.844	180.836		
57.094	80.141	140.950	182.942		
		143.031	185.023		
		144.856	186.696		
		146.938	186.848		
		148.763	188.930		
		150.844	189.388		
		152.950	189.516		
			189.864		

4.3 Overview of the results

For convenience, per polarisation direction (H and V) and for each of the frequency bands (LBA, HBA_LOW, HBA_MID and HBA_HIGH), we summarize the L-value plots for the three WTG-modes (ON, OFF, and SDM) in the following subsections, with a short description where the L-value plot warrants more discussion. This summary is followed by a more detailed analysis.

L-value plot legend:

- **Orange** Reference source level "0 dB" level (it deviates a bit from the 0 dB value because the narrow band signal characteristic of the source)
- **Light grey** Measured noise floor
- **Light green** 3-sigma line
- **Light blue** Measured maxima outside centre cube
- **Black** Measured maxima inside centre cube
- **Red** Window around frequency attention

4.3.1 V-polarization LBA

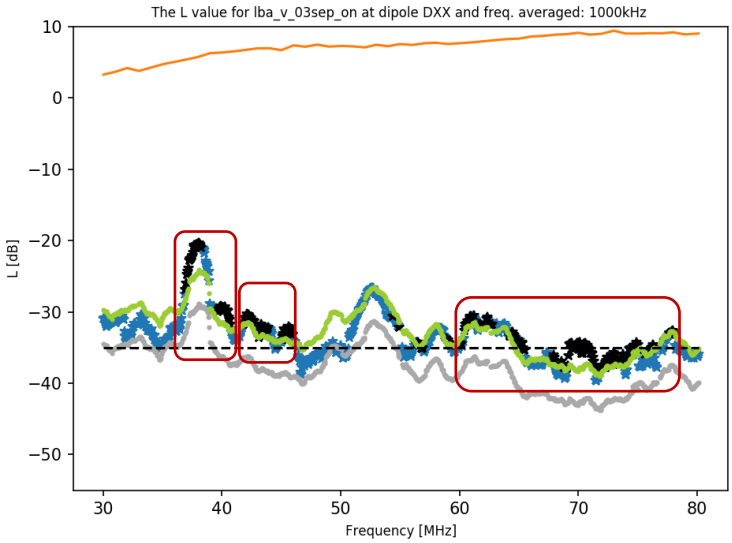

V-ON LBA (3-sept)

Frequency attention:
- 60 to 80 MHz
- 42 to 46 MHz
- 36 to 41 MHz

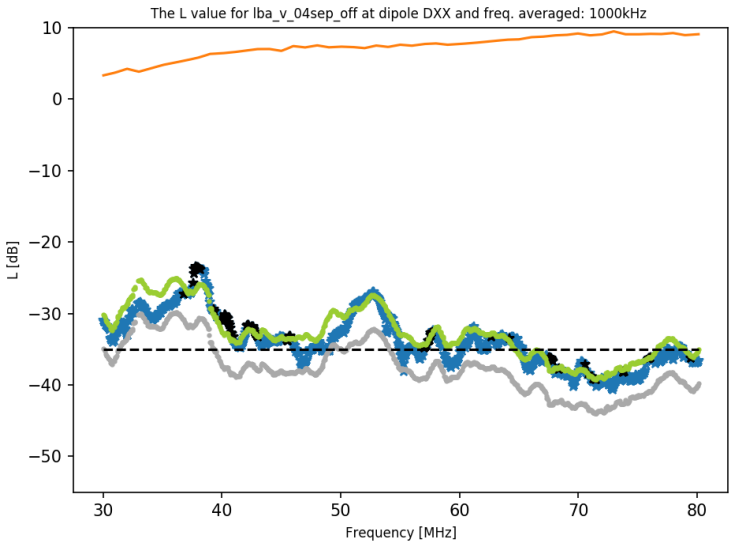

V-OFF LBA (4 sept)

-

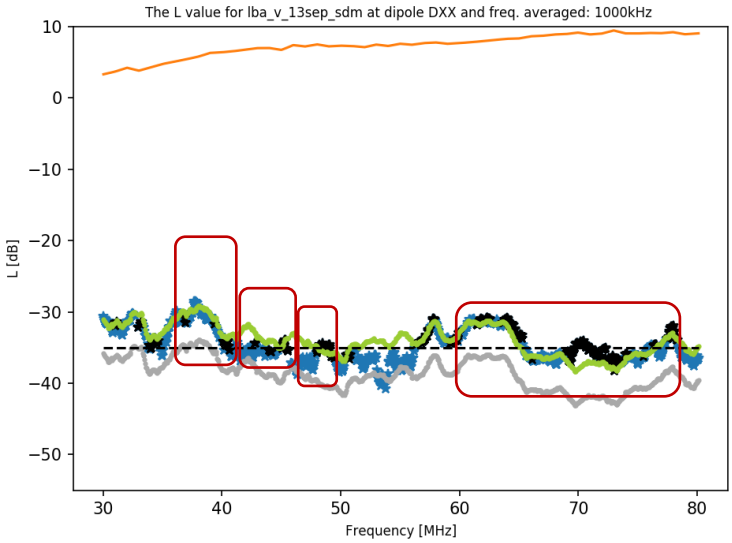

V-SDM LBA (13 sept)

Frequency attention:
- 60 to 80 MHz
- 46 to 48 MHz
- 42 to 46 MHz
- 36 to 41 MHz

For the V-POL data, we have seen the following areas warranting additional analysis:

- 36 to 41 MHz.
- 42 to 46 MHz.
- 60 to 80 MHz.

36 to 41 MHz: The spectral features, especially in the noise, that are visible during the ON measurements, we also find in the graph for the OFF measurements. This may indicate that the -35 dB exceedance is caused by excessive noise in the environment.

We have plotted for two frequencies the voxel cubes for the ON and for the OFF situation. The 37.2 MHz is a clear example of a noise contaminated frequency. The 40.6 MHz frequency does seem to contain a signal from the WTG, but the signal is visible in both the ON and the OFF situation, leading us to believe it is a reflection by the WTG rather than a source from the WTG.

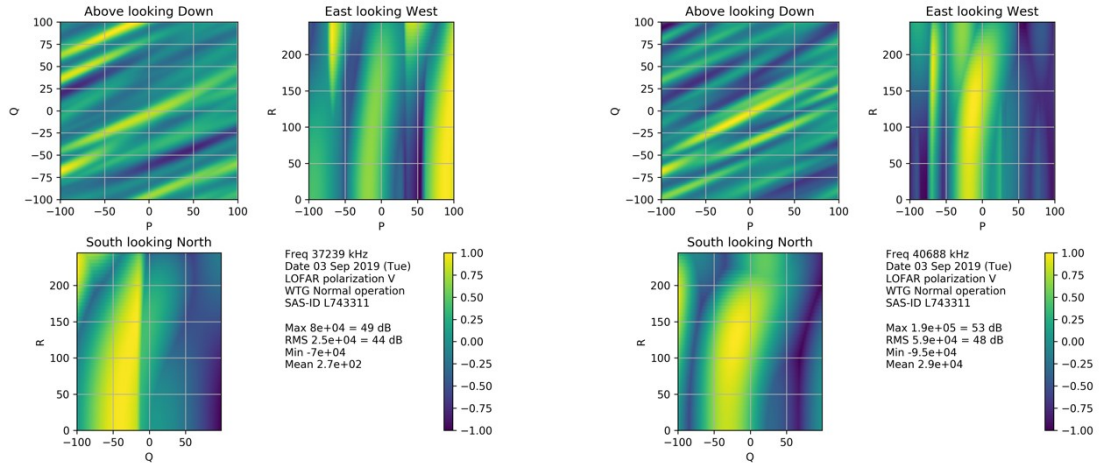

Figure 8: Voxel cubes for 37.2 and 40.7 MHz during the ON measurements.

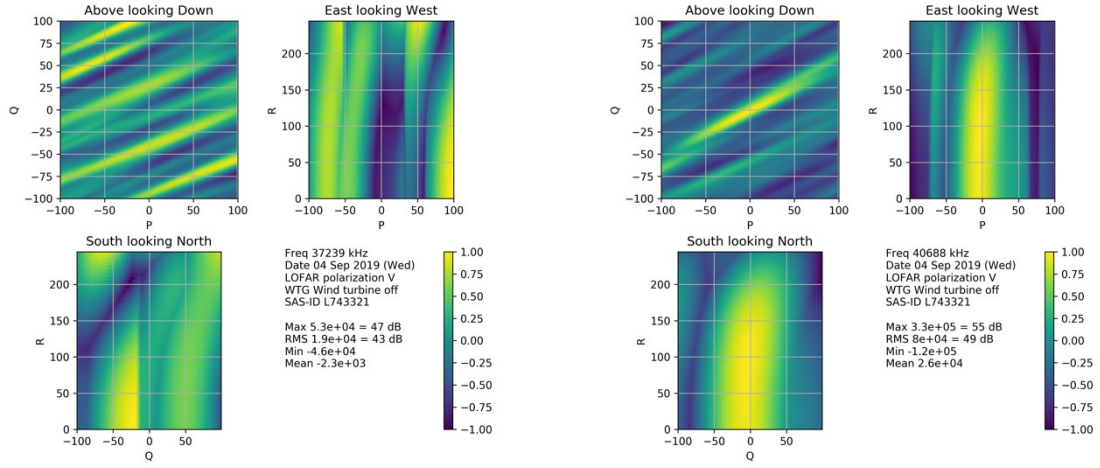

Figure 9: Voxel cubes for 37.2 and 40.7 MHz during the OFF measurements.

42 to 46 MHz: The noise structure in this region for the ON and OFF measurements have many similarities. It seems that these exceedances are caused by noise from the environment.

46..48MHz: We also investigated the 46 …48 MHz area, mainly because we see a possible signal in the V-pol results, but more prominently in the H-pol measurements (Section 4.3.5). We investigated the imaging

pictures in the range 46…48 MHz, and many of these images show a noisy pattern, but at 47.1 MHz we have some indication of a single source responsible for the main emission. In the figures below, we have plotted the resulting image of this frequency together with its neighbouring images.

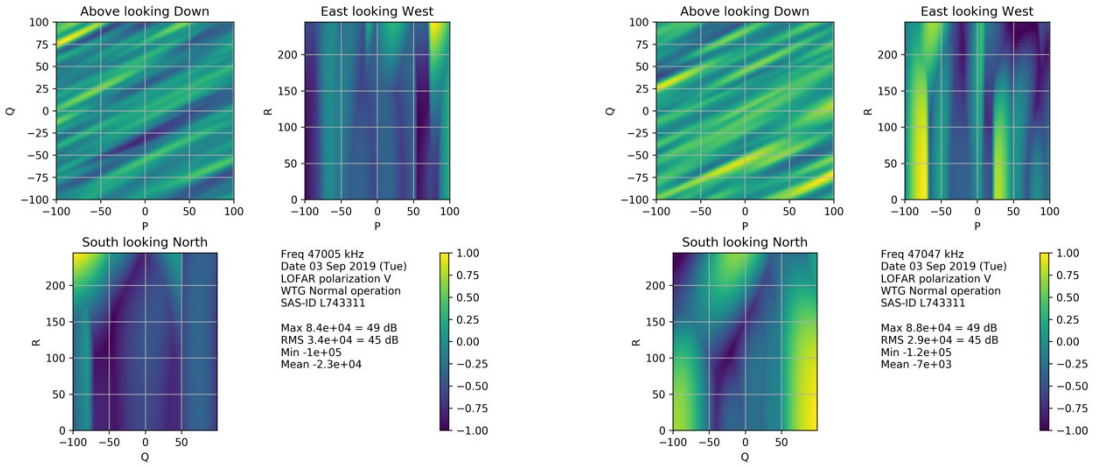

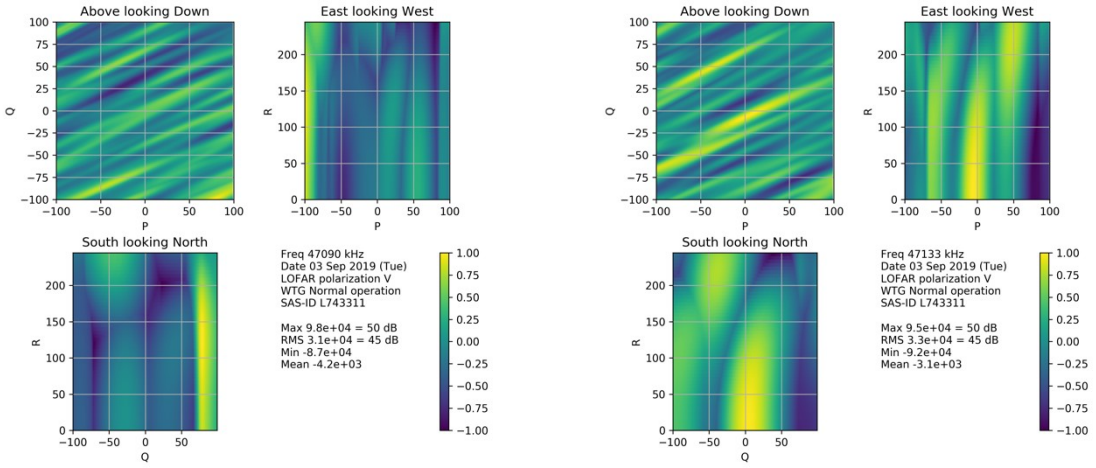

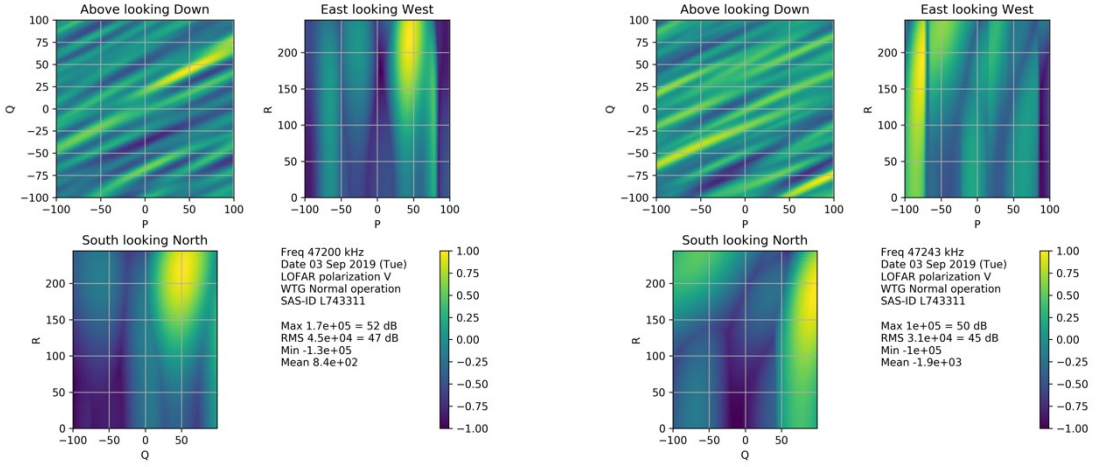

Figure 10 3D image around 47.1 MHz during the V-pol ON measurements.

We have analyzed the same frequencies for the OFF measurements as shown in the figures below. Again, the majority of the images are noisy, but similar to the ON measurements there is an indication of a single source at 47.1 MHz and also in the neighbouring frequencies. Thus, we see a similar signal, in the OFF modes as well as in the ON mode. So, we tend to believe that the disturbance is from a source outside the WTG.

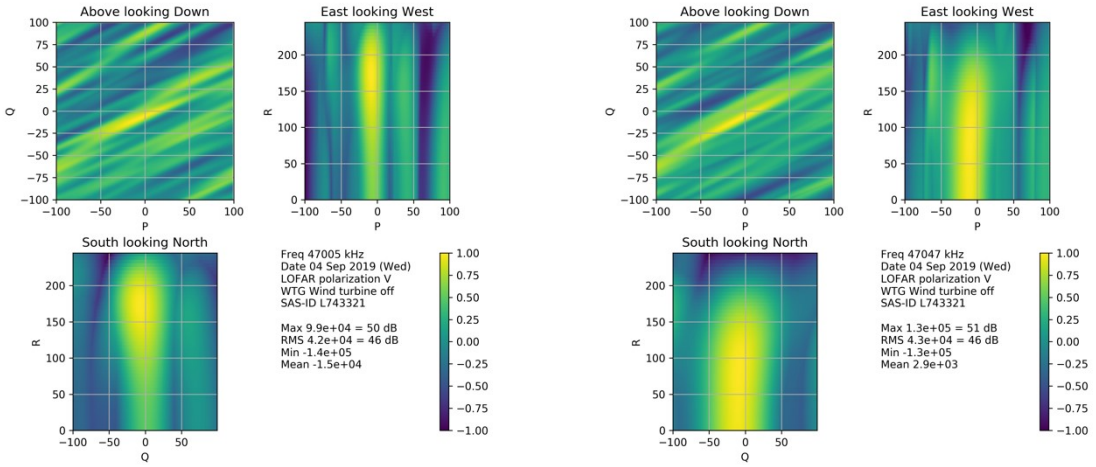

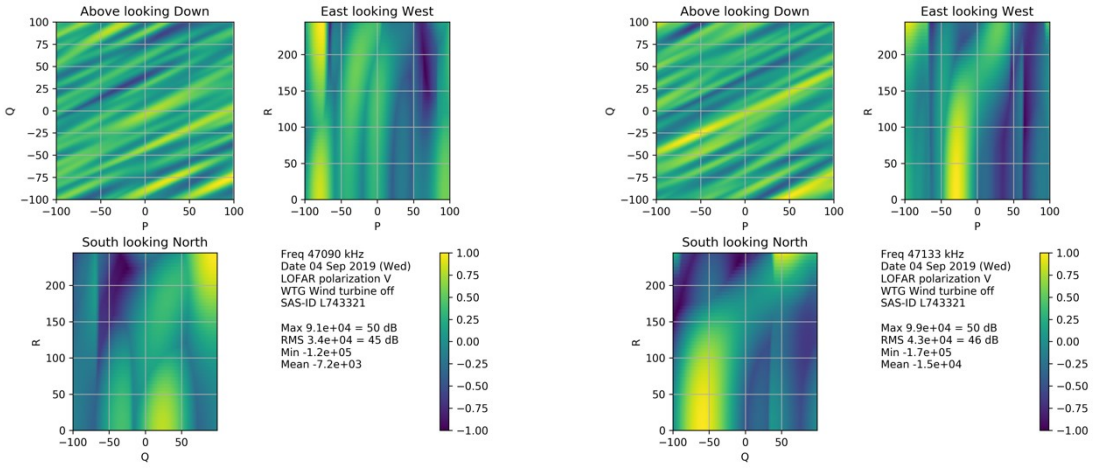

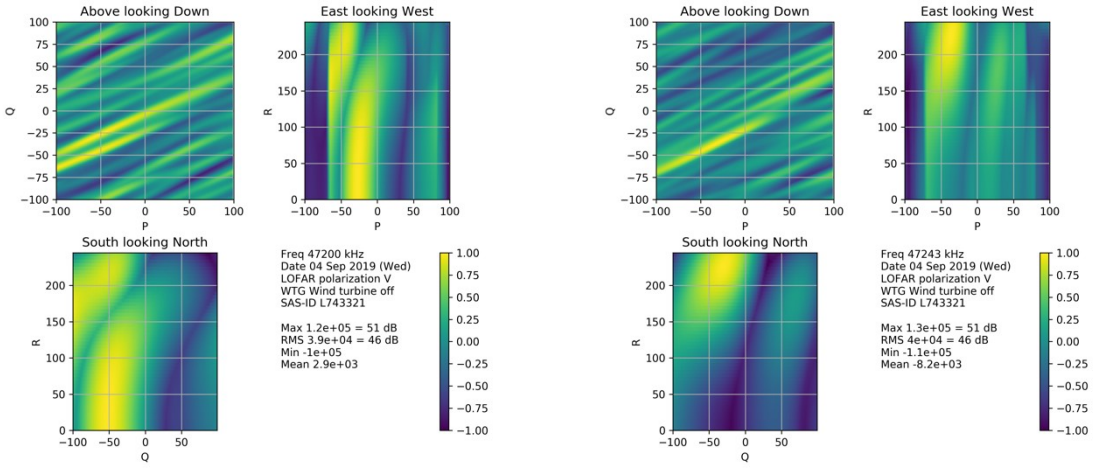

Figure 11 3D image around 47.1 MHz during the V-pol OFF measurements.

60 to 80 MHz: There is substantial difference between power values for the ON and OFF measurements, while on the SDM measurement we see a structure similar to the ON measurements. This either indicates that the signal is a reflection visible during only the ON and SDM mode, or from equipment that was switched on during both ON and SMD mode of the WTG. The fact that the signal seems to be rather broad banded (60 .. 80 MHz) and no external source with such spectral structure is yet known to the team, makes the hypothesis that a single source causes the reflection not very likely.

We see signals that seem to be originating from the WTG itself (such as 67.2 MHz and 73.5 MHz in the figure below), but the 72.7 MHz frequency seems to be dominated by noise. For the 75.9 MHz we might even see a reflection pattern that corresponds with the blades of the WTG.

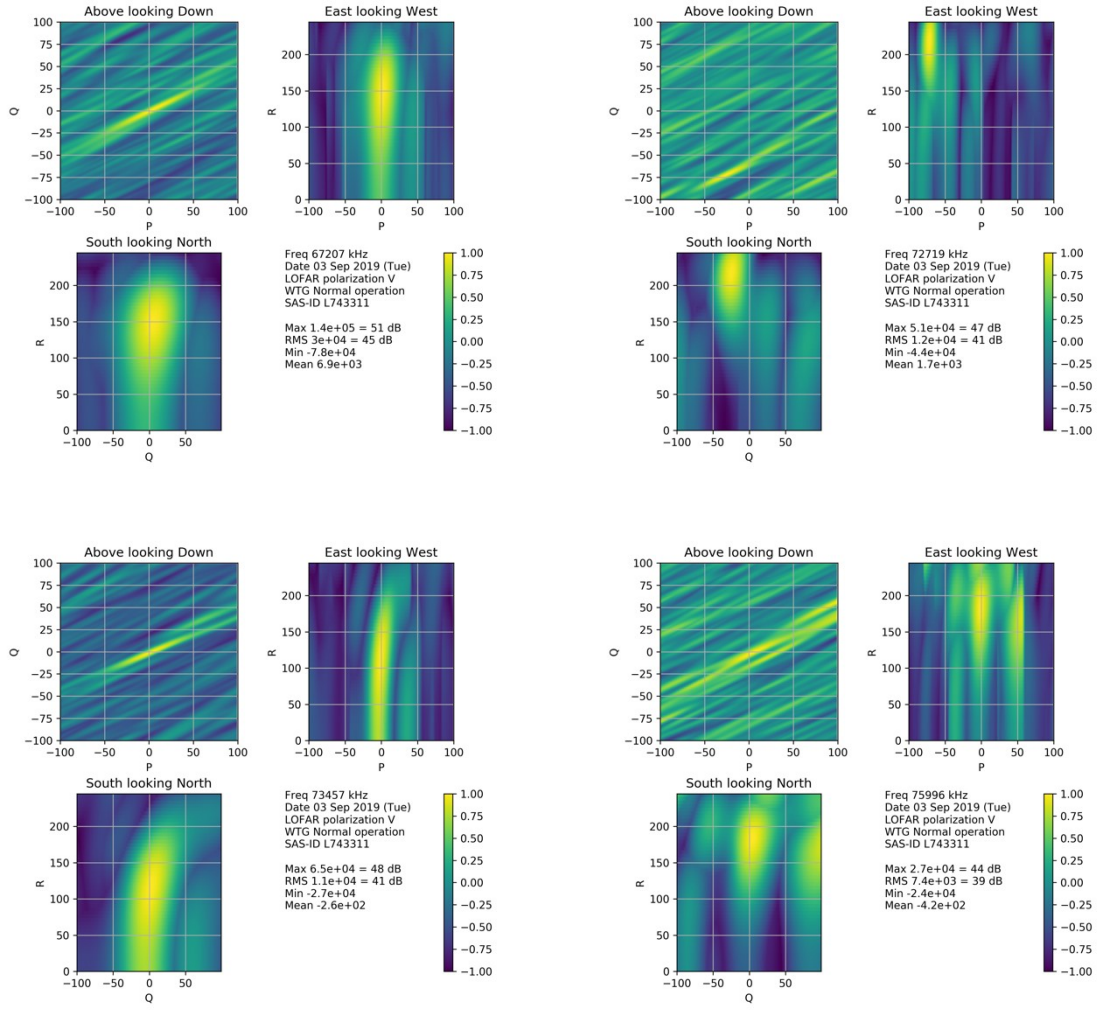

Figure 12: Some frequencies in the 60 ...80 MHz region during the ON day

There is also a peak visible at 67..68 MHz in the ON-mode measurements results and also in the OFF-mode measurements results. It also seems to be visible in the SDM-mode measurements. Although the voxel cube indicates a visible hotspot for the signal at the WTG-location, as this peak is also visible in the OFF-mode, we must assume that this peak results from a reflection outside the WTG. Similarly, at 78 MHz we see a peak during the same measurements as well.

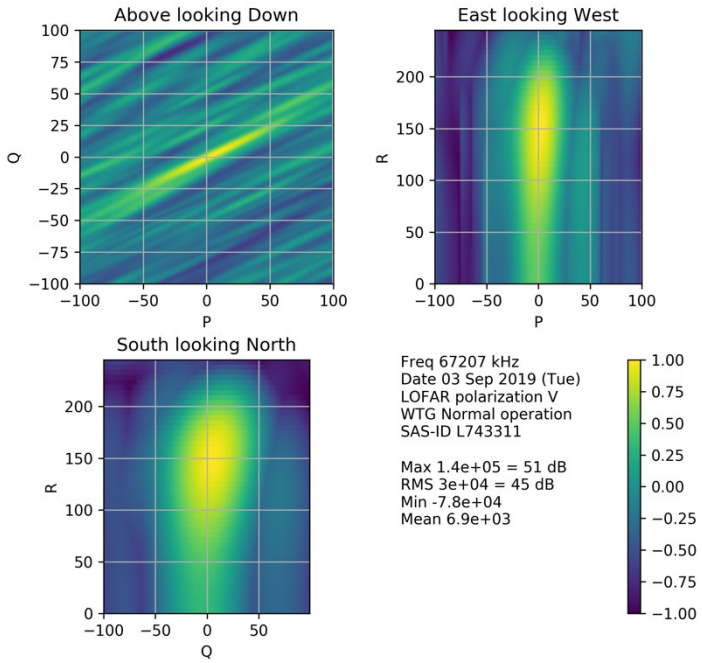

Figure 13: Voxel cube result for the 67.2 MHz frequency during the ON day

4.3.2 V-polarization HBA-LOW

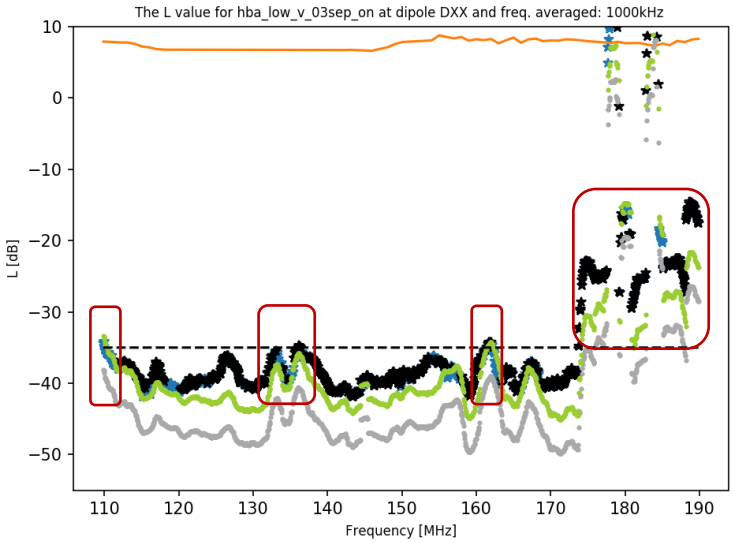

V-ON HBA_LOW (3 sept),

Frequency attention:
- 110 to 122 MHz
- 133 to 137 MHz
- 160 to 163 MHz
- 174 to 190 MHz (most likely reflections)

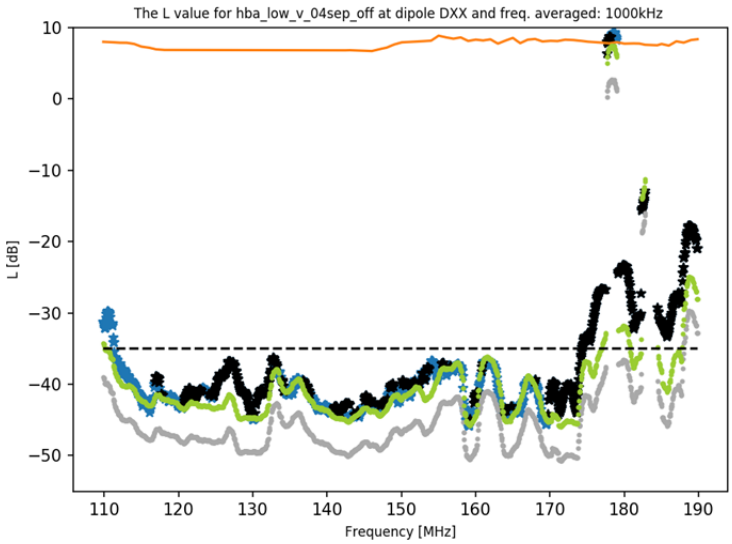

V-OFF HBA_LOW (4 sept)

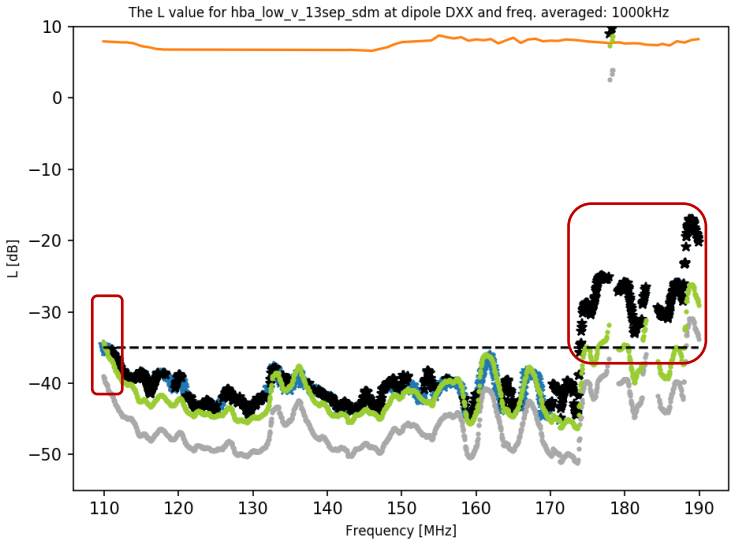

V-SDM HBA_LOW (13 sept)

Frequency attention:
- 110 to 112 MHz
- 174 to 190 MHz

110 – 112 MHz:

The spectral structure is visible in the ON, OFF, and SDM mode. In fact, the spectral structure is strongest in the OFF mode. This fact strengthens the belief that the source of the signal must be outside the WTG, or an IM-product caused by the nonlinear behaviour of the LOFAR receiver chain.

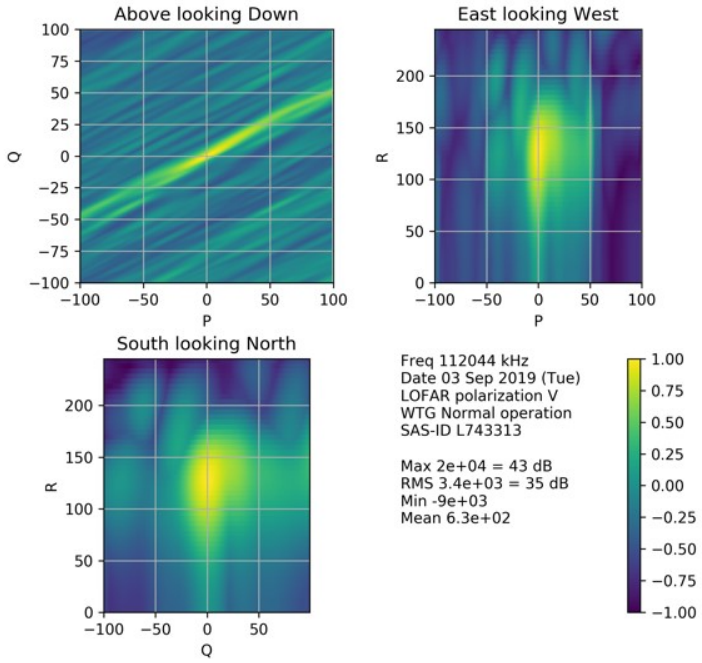

Figure 14: Voxel cube of the 112. MHz measurement during the ON day.

133 …137 MHz:

The 133 …137 MHz region is present in ON, OFF and SDM measurements, and as ASTRON has indicated in this area typically contaminated with spurious signals from intermodulation (IM) due to the nonlinear character of the LOFAR chain. For reasons of completeness we further analysed the area around 133 …137 MHz, and found many noisy voxel cubes. The figure below presents four neighbouring frequencies around 137.2 MHz, which are found to be the "sharpest" image. Given the fact that the spectrum for the OFF measurements does have strong reflections in this frequency as well, and only in a small frequency area a reasonable sharp image can be found, we must assume that the source is outside the WTG, and most likely due to the LOFAR receiver chain itself.

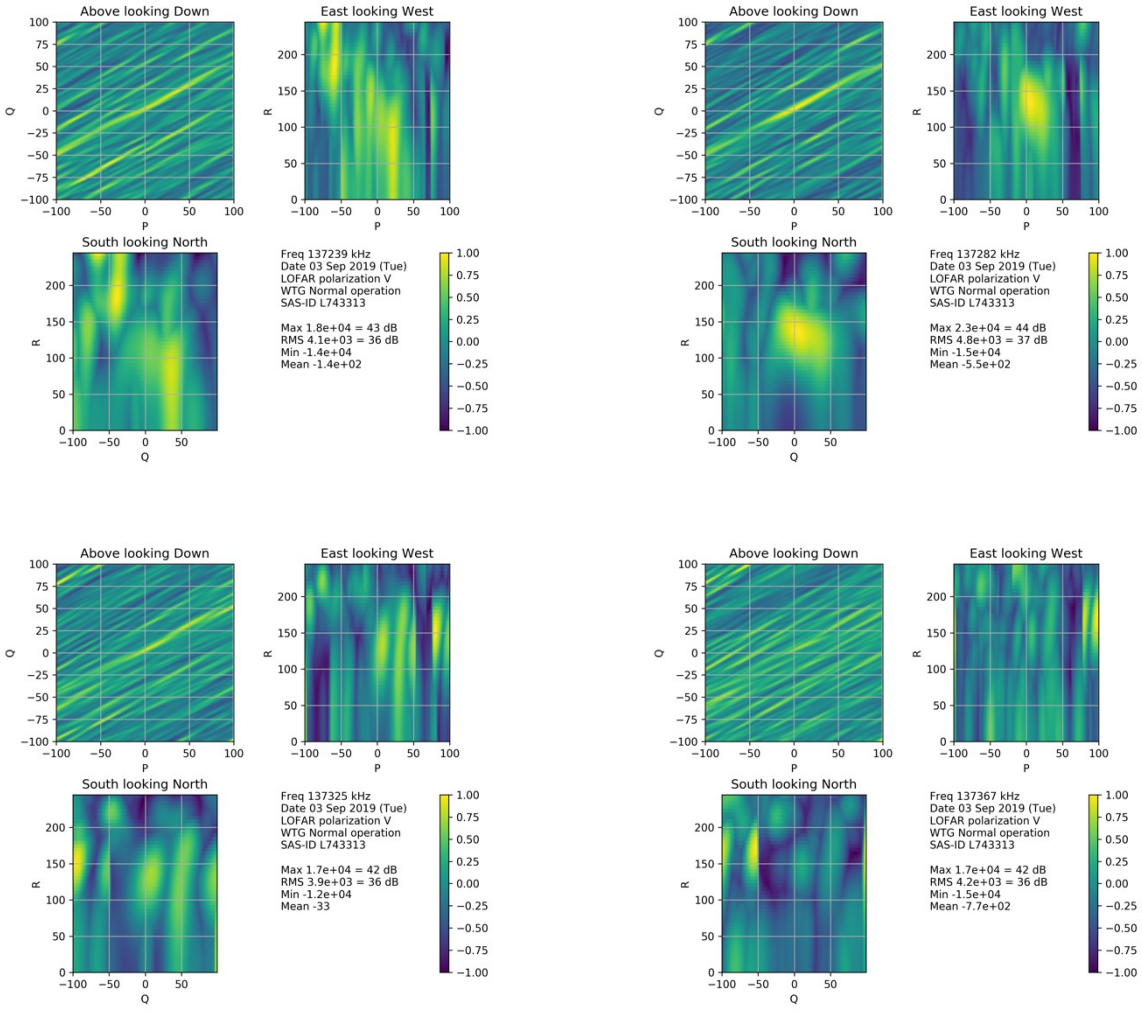

Figure 15: Voxel cubes of four neighbouring frequencies around 137.2 MHz during the ON day.

For the **160 … 163 MHz** region –present in ON, OFF and SDM measurement data – and as ASTRON has indicated this area is also (as 136…137 MHz area discussed above) known for contamination of spurious IM-products.

For completeness sake, we have analysed the resulting voxel cubes in this frequency area for the WTG in in ON-mode measurements, and most are dominated by noise, see Figure 16. There is a small bandwidth of approximately 100 kHz (160219 kHz … 160329 kHz) where a signal might be visible. The 3D voxel cube images for these frequencies seem to indicate signals also from the blades, which indicates that the signal originates from reflections from a source outside the WTG.

As there is a similar spectral feature for the measurements with the WTG in the OFF-mode, and the area is known for spurious IM products, it is likely that the signal comes from outside the WTG.

The **174 …190 MHz** region is known for DAB transmissions, and the signals that we find have the spectral structure that we expect from these transmissions. Thus, we assume that the signals that we find in this region are reflections of the DAB transmission.

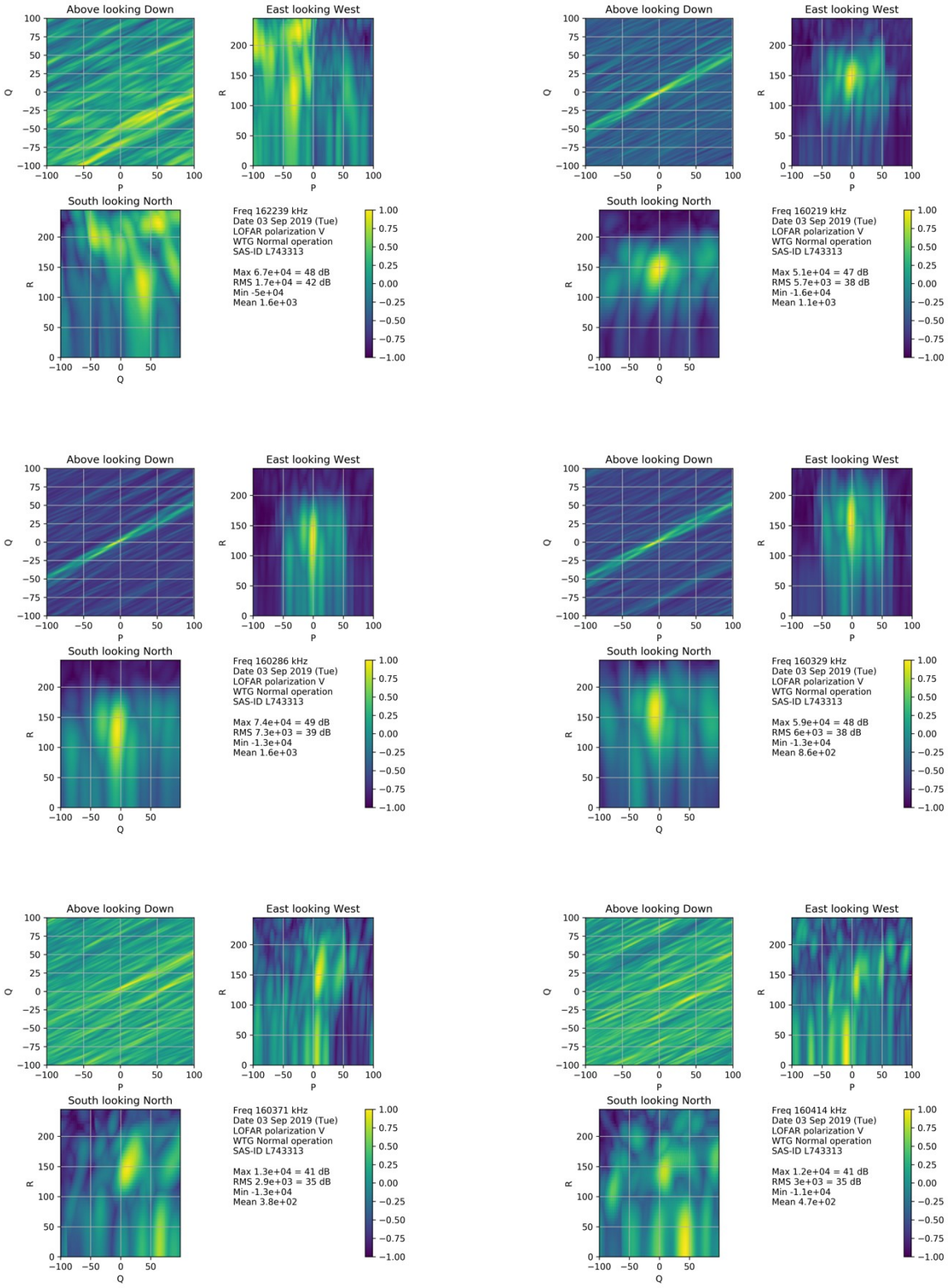

Figure 16 Voxel cubes 160 .. 161 MHz during the WTG =ON-mode measurement day

4.3.3 V-polarization HBA_MID

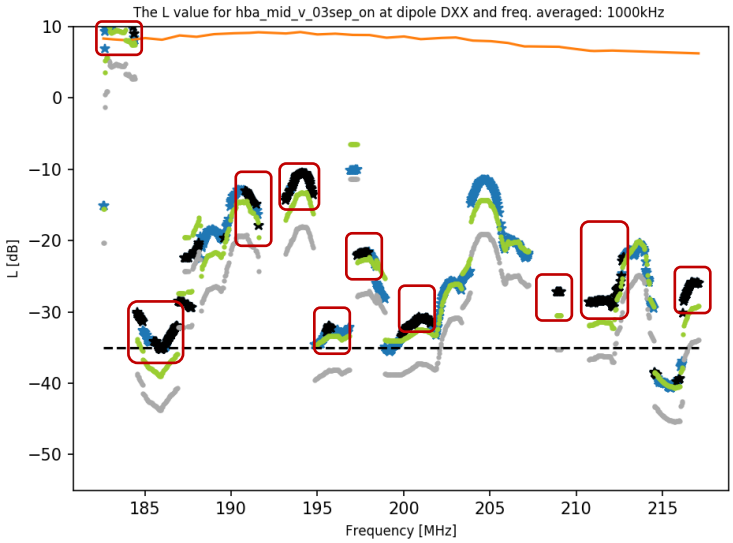

V-ON HBA_MID (3 sept)

Frequency attention:

- Large number of frequency ranges
- All most likely reflections, due to spectral structure, or because they are also present in the OFF image

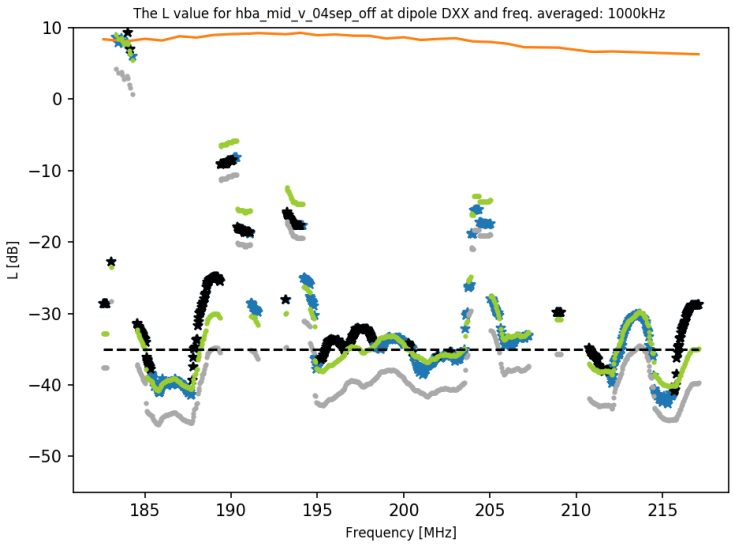

V-OFF HBA_MID (4 sept)

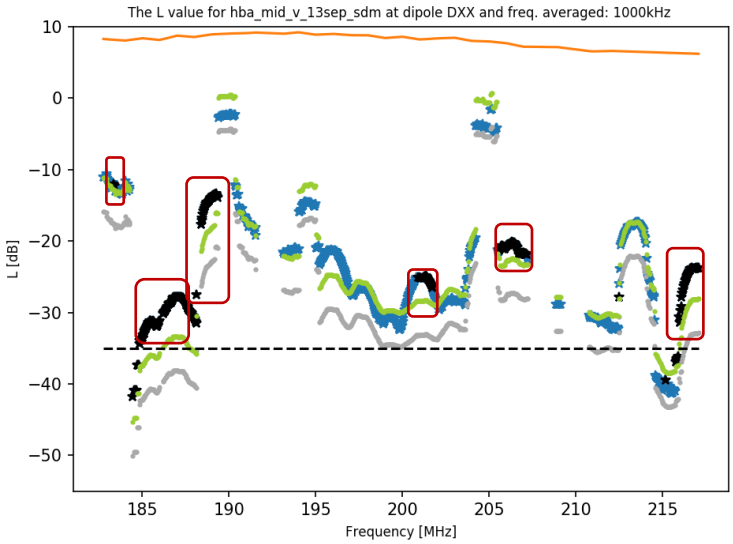

V-SDM HBA_MID (13 sept)

Frequency attention:

- Large number of frequency ranges
- All most likely reflections, due to spectral structure

All frequencies for which the power exceeds the -35 dB seems to be related to DBA or digital TV transmission reflections, because the spectral structure seem to correspond to transmissions of approximately 1.5 MHz wide. It is also known from ASTRON experience that DBA transmissions contaminate this frequency band.

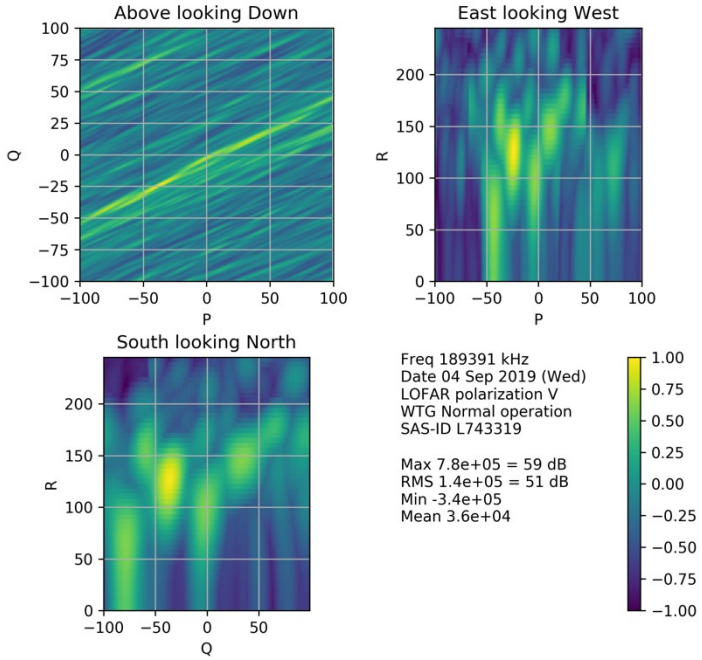

Figure 17 Voxel cubes 189.3 MHz during the WTG = ON measurements

4.3.4 V-polarisation HBA_HIGH

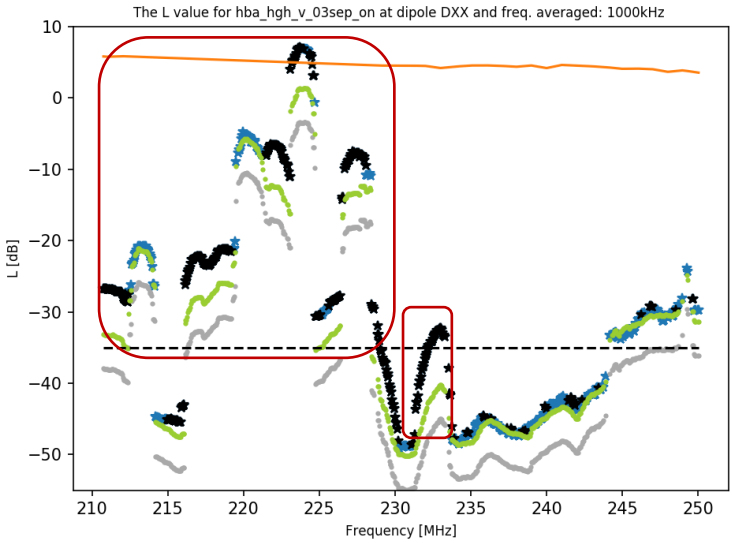

V-ON HBA_HIGH (3 sept)

Frequency attention:
- 210 to 230 MHz
- 232 to 234 MHz

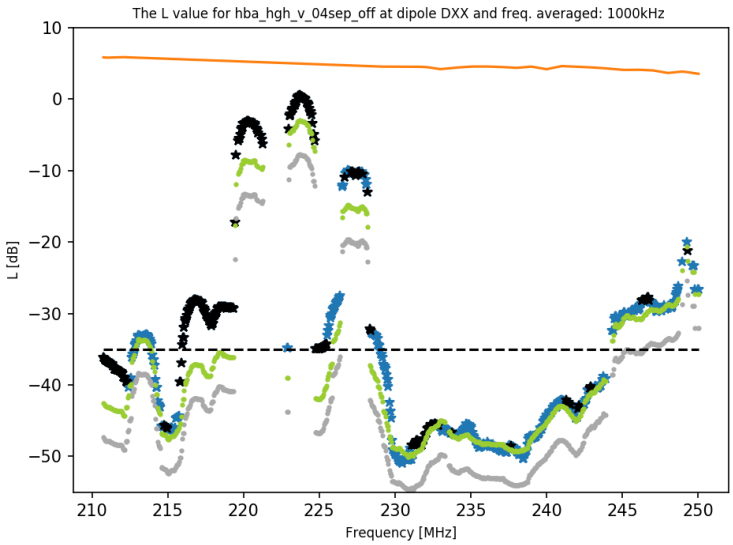

V-OFF HBA_HIGH (4 sept)

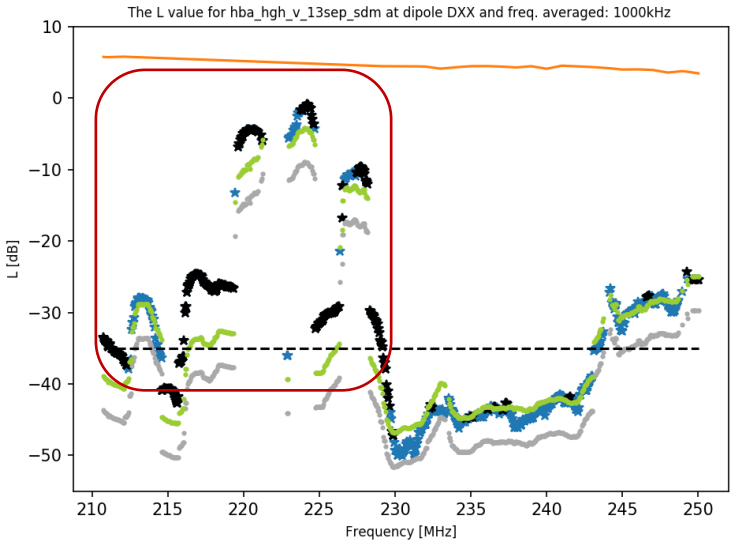

V-SDM HBA_HIGH (13 sept)

Frequency attention:
- 210 to 230 MHz

For the region **210 .. 230 MHz**, we find the various -35 dB exceedances, for which we either find:

- The spectral structure is 1.5 Mhz wide, indicating a DAB transmission
- And the exceedances can also be found in the OFF mode and SDM mode.

Thus, we must assume that the found exceedances cannot be blamed to sources inside the WTG.

For the ON measurement we find a signal between **232 … 234 MHz**. The signal does have a spectral structure that is similar to the DAB transmission as given above (indicating reflection), and can also been seen in the OFF and SDM measurements, although not so strong. In the Netherlands and Germany, DAB transmissions are allocated up to 230 MHz, and therefore, we must assume that this signal doesn't originate from a DAB transmitter in the Netherlands or Germany. In Denmark and Norway, however, DAB transmissions are allocated up to 235 MHz, which might reach the WTG location under ideal atmospheric conditions.

One explanation could be that due to different yaw directions the signal reflection properties of the WTG are different for these days. We have investigated the voxel cubes of the OFF measurements and did find a reflected signal (see figure below).

This all may indicate that the signal that we find in the ON measurements doesn't necessarily originates from the WTG itself, and maybe more likely a reflection form a DAB transmitter in, e.g., Denmark.

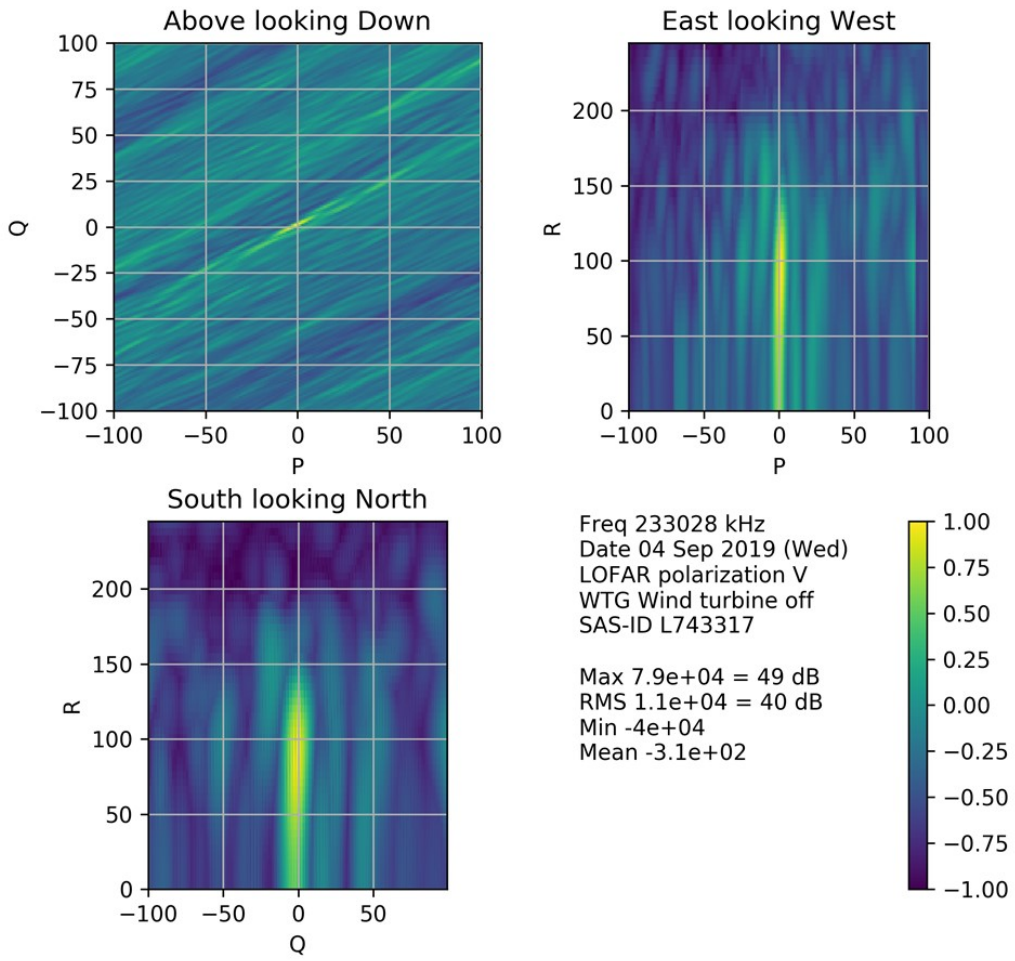

Figure 18: Voxel cubes 233 MHz during the WTG = OFF measurements

4.3.5 H-polarization LBA

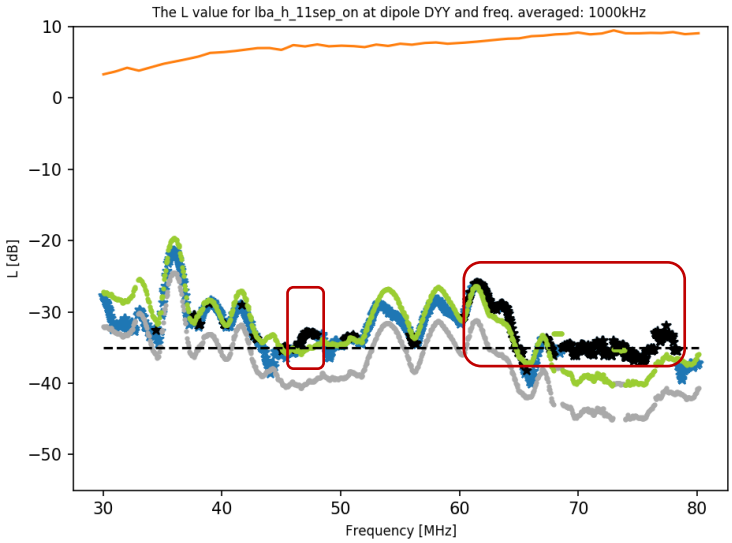

H-ON LBA (11-sept)

Frequency attention:
- 60 to 80 MHz
- 46 to 48 MHz

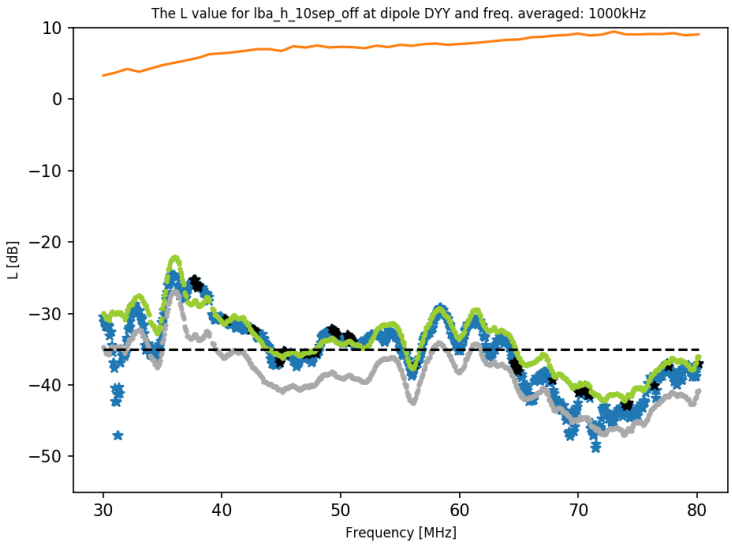

H-OFF LBA (10 sept)

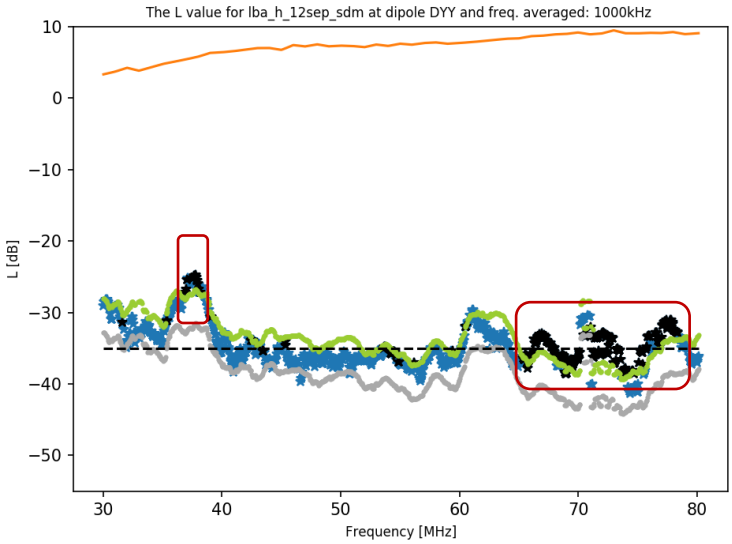

H-SDM LBA (12 sept)

Frequency attention:
- 60 to 80 MHz
- 38 to 40 MHz

46..48MHz: In 47 MHz range for the H-polarization there also seems to be some signal present. Again, we investigated the imaging pictures in the range 46…48 MHz, and many of these images show a noisy pattern, but at 47.047 we have the sharpest image. In the figures below, we have plotted the resulting image of this frequency together with its neighbouring images.

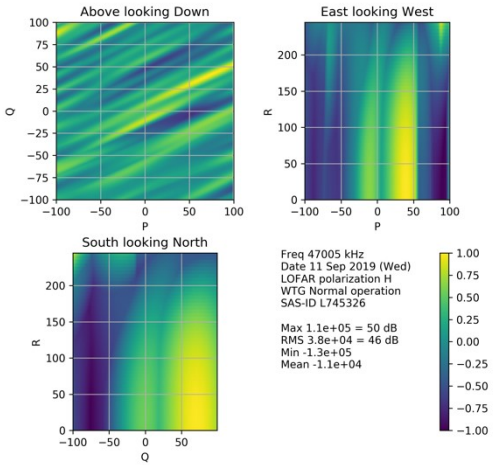

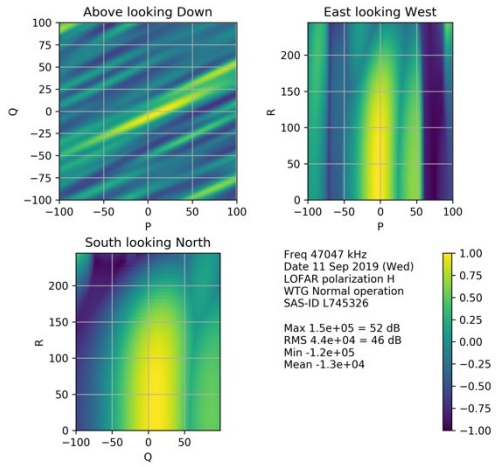

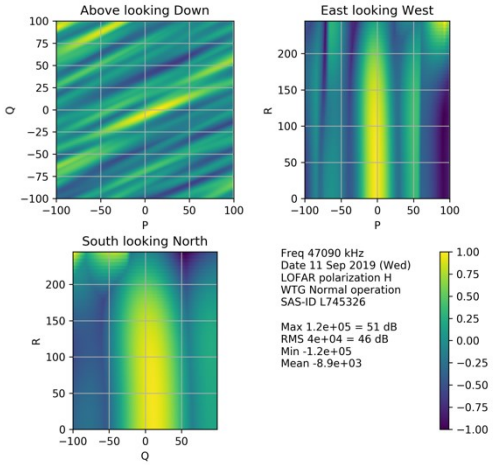

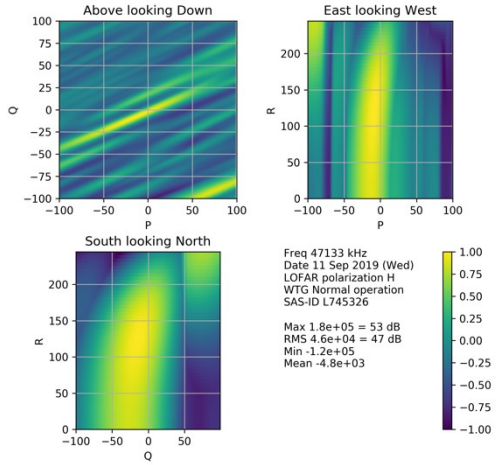

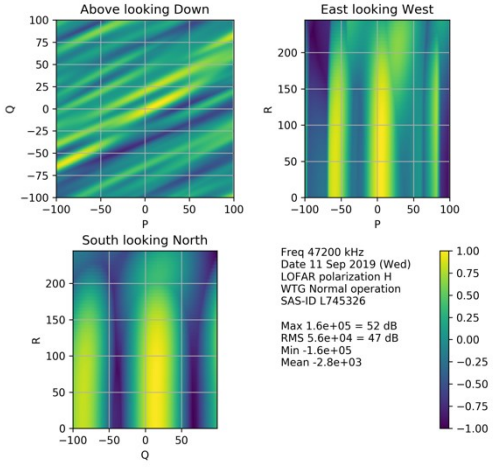

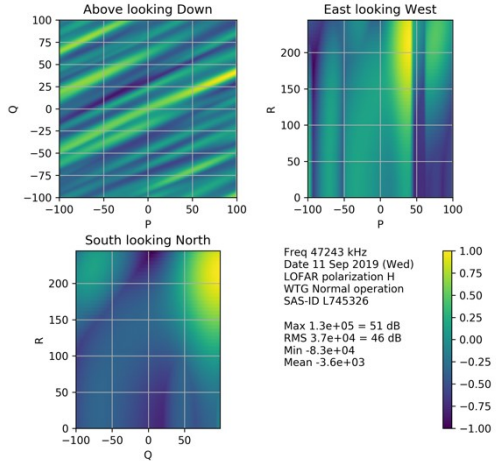

Figure 19 3D image around 47.1 MHz during the H-pol ON measurements.

We have analysed the same frequencies for the H-pol with the WTG in the OFF mode, which we show below. It is hard to tell whether we do or don't see the same pattern as in the case that the WTG is in the ON mode (as depicted above). Of course, if the signals, as presented in the WTG in the ON mode are reflected signals from the WTG, the yaw direction of the nacelle may affect the strength of the reflection. Unfortunately, as no log has been maintained during the OFF-measurements (all equipment was switched off), there is no way to tell whether the nacelle was exactly in the same direction as during the ON measurements.

However, we have also seen that many disturbances are often unpolarized. Thus, in such an unpolarized case, a signal should be visible in both the H-pol and V-pol measurements. We have given in Figure 11 the images for the same frequencies for the V-pol measurements where the WTG is in the OFF mode. As remarked for the V-measurements, these images do give the impression of a signal in the same frequency range.

Thus, we see a similar signal, as measured during the H-pol measurements when the WTG was in the ON mode, also during the measurements when the WTG is in the OFF mode, albeit during the V-pol measurements. Assuming the disturbance is unpolarized, we may be tempted to conclude that the disturbance is from a source outside the WTG.

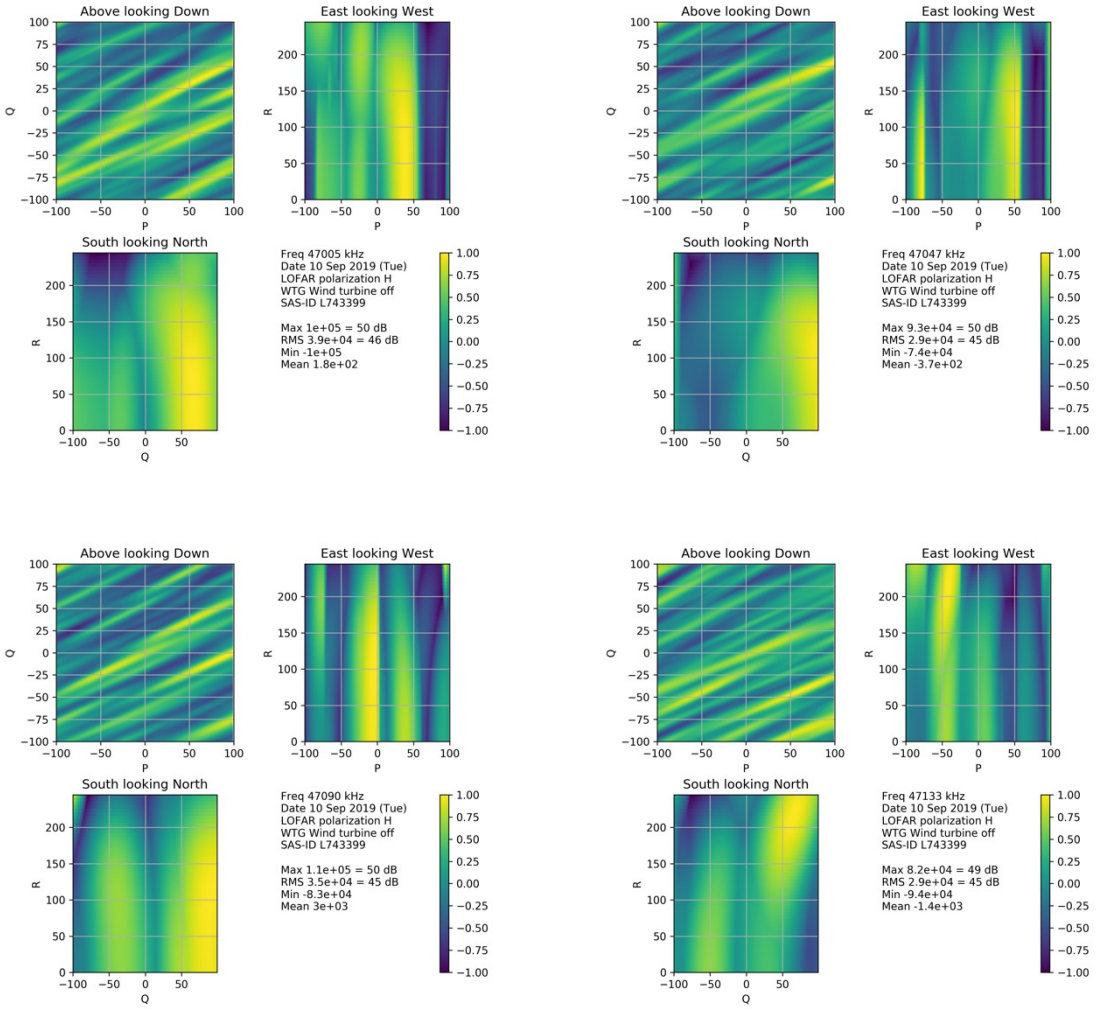

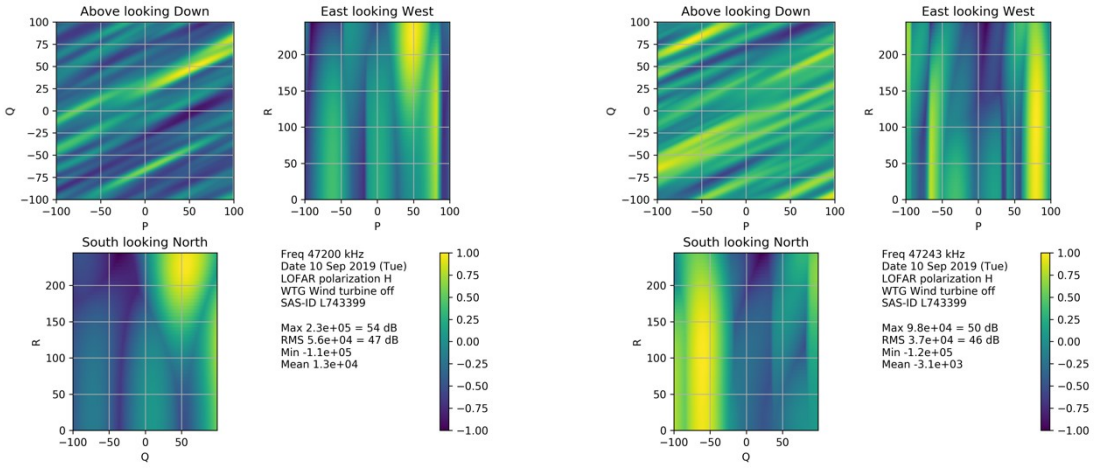

Figure 20 3D image around 47.1 MHz during the H-pol OFF measurements.

In the H-pol measurements with the WTG switched ON, we may have also found a possible signal at 47.8 MHz (although the side views are not so clearly focused), see figure below. Again, at the same frequency for the V-pol measurements with the WTG switched OFF, we see a similar signal to be present (with even the side views showing a better focused image), see Figure 22 after the previous picture.

Again, this information leads us not to suspect the WTG as source of disturbance in the first place.

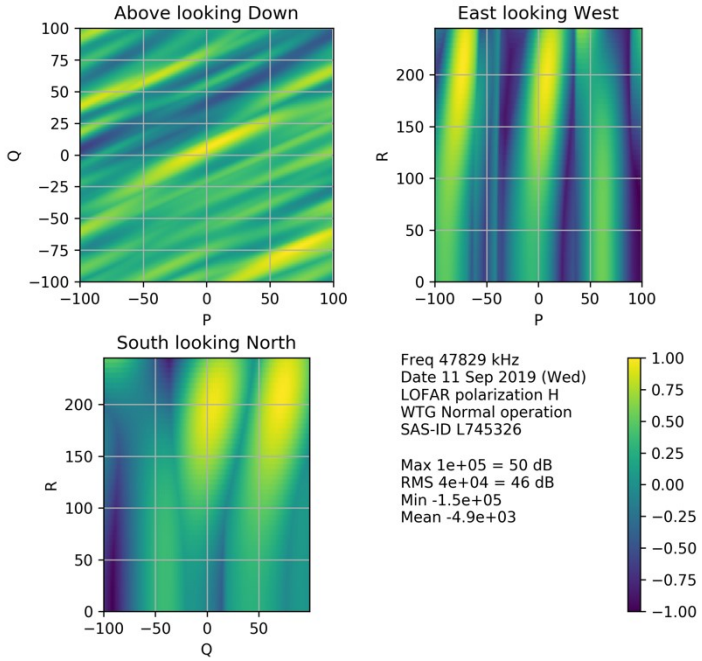

Figure 21 3D image around 47.8 MHz during the H-pol ON measurements.

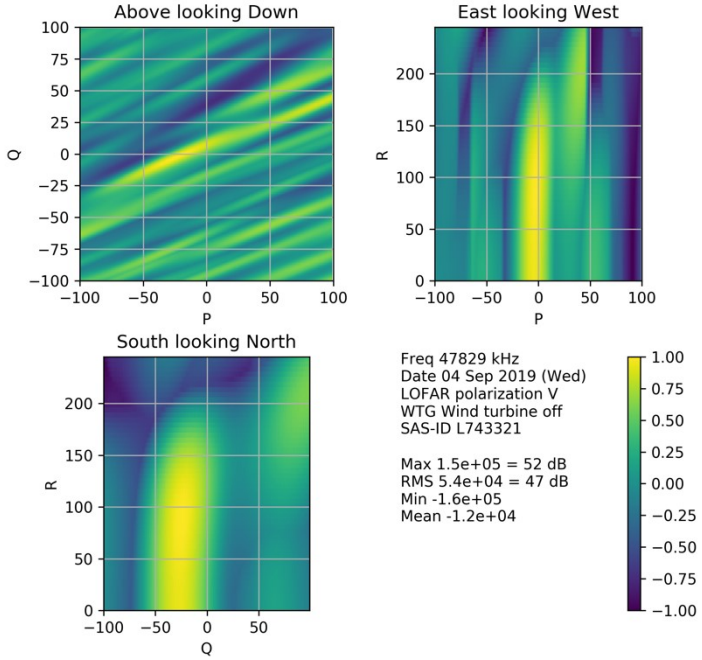

Figure 22 3D image around 47.8 MHz during the V-pol OFF measurements.

60 to 80 MHz: This, again, seems similar to the V-polarized signals, where the same deviation in the signal strength is seen. In the following figure, we present some examples of the voxel cubes. We see a number of signals that seem to originate from the WTG, but there are also some examples that seem to indicate a disturbance (see the 66.7 MHz example).

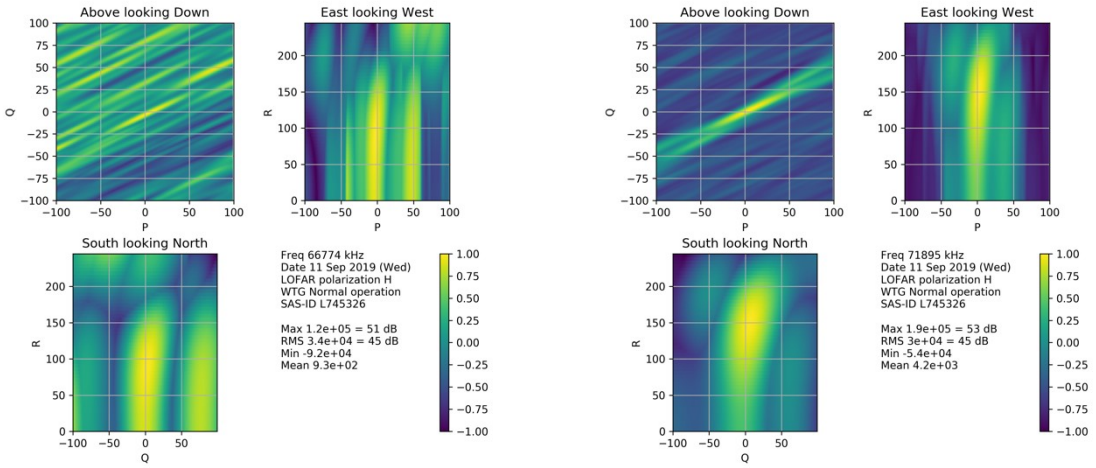

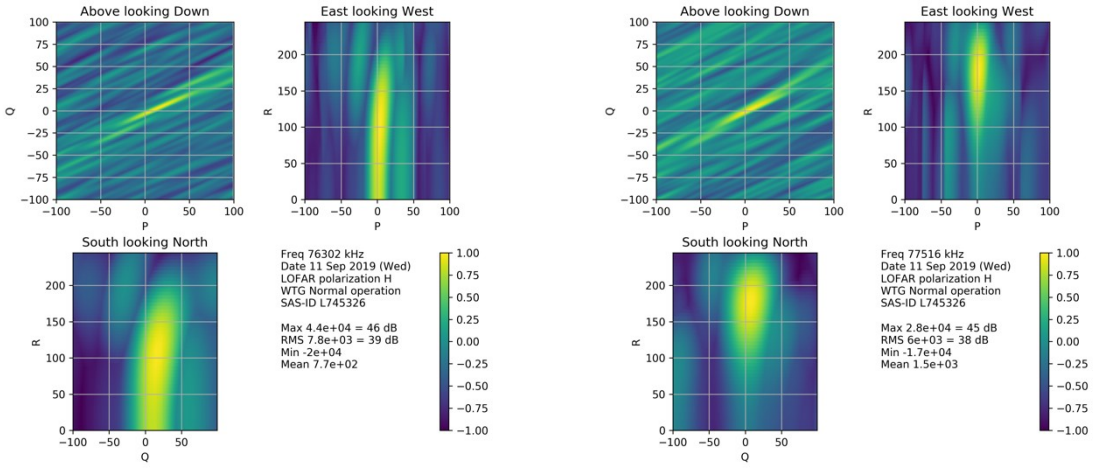

Figure 23: Voxel cube of frequencies in the 60 .. 80 MHz range. Measurements during the ON day

The suspected frequencies for the OFF situation (37 .. 38 MHz and 51 …53 MHz) must originate from disturbance outside. As an example, the 37.7 MHz is shown below. The imaging seems to indicate a reflection (note the resolution in the height direction is particular poor for these low frequencies.

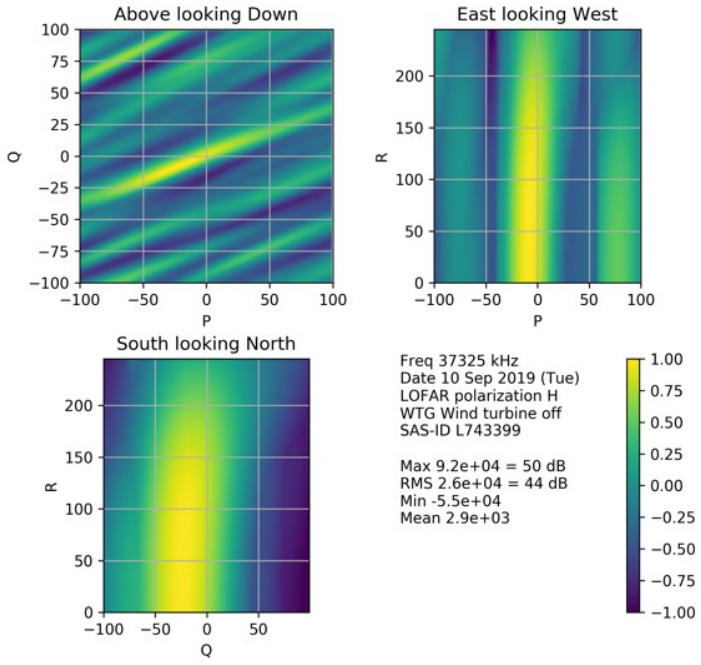

Figure 24: Voxel cube of 37.7 MHz range. Measurements during the OFF day

For the V-measurement results we highlighted also the 67..68 MHz peak and concluded that this peak is most likely is the result of a reflection from a source outside the WTG. In the results for the H-measurements, this same peak is visible as well.

The peak at 78 MHz that we found for the V-measurements can also been seen for the H-measurements for the ON-mode and the SDM-mode. For the H-measurements, the peak is less clear, although we see the noise level rise in a similar way to the ON and SDM-modes. We have already seen earlier that the yaw angle of the nacelle can affect the strength of a reflection. Unfortunately, the WTG can't produce a log of its state variables when it is in the OFF-mode.

4.3.6 H-polarization HBA_LOW

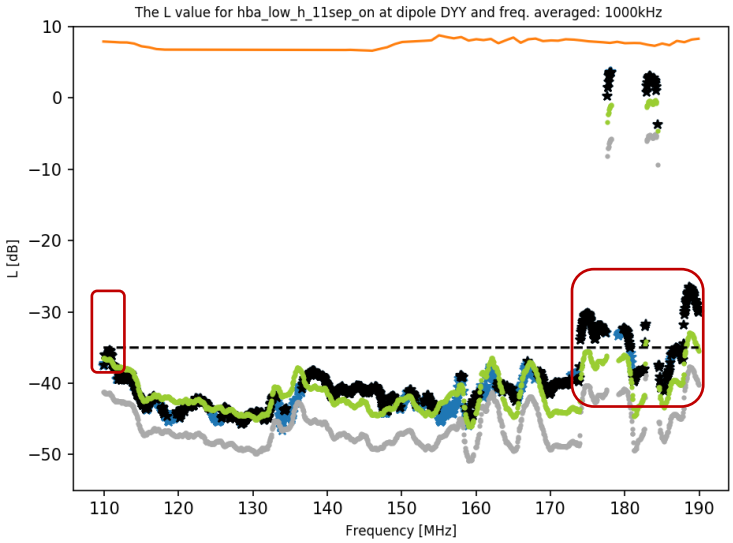

H-ON HBA_LOW (11 sept)

Cleaned

Frequency attention:

- 110 to 112 MHz
- 174 to 190 MHz

All most likely reflections, as they are determined from a noisy voxel cube (blue dots).

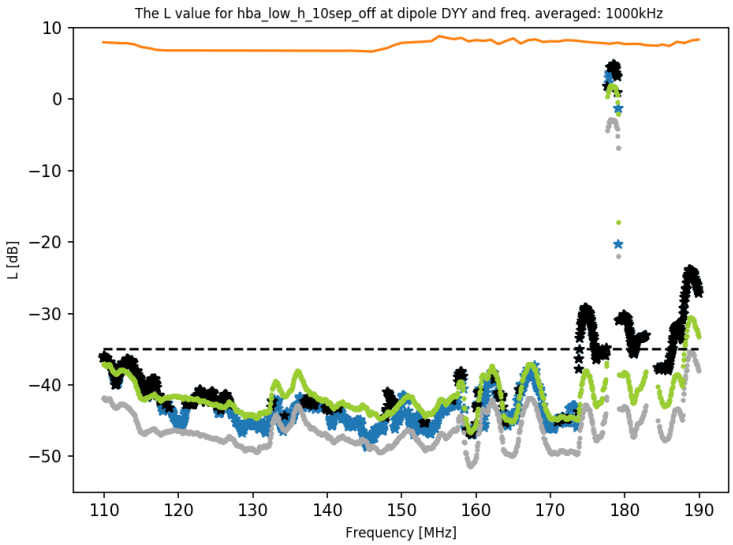

H-OFF HBA_LOW (10 sept)

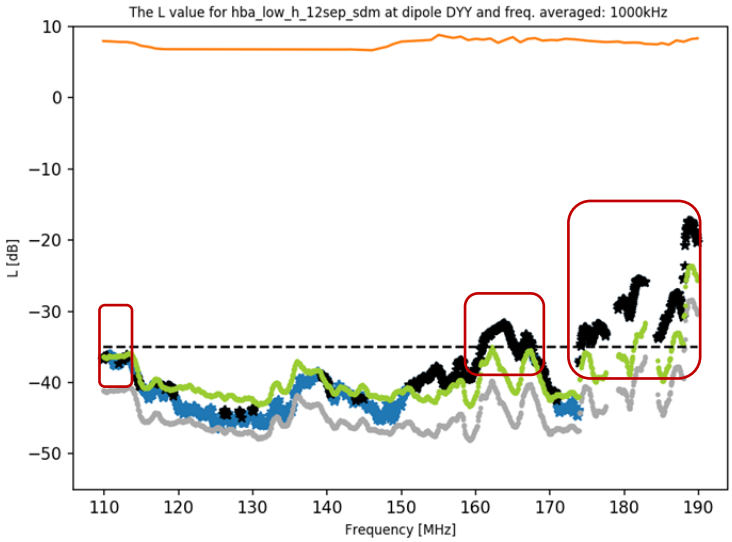

H-SDM HBA_LOW (12 sept)

Cleaned

Frequency attention:

- 110 to 112 MHz
- 160 to 170 MHz
- 174 to 190 MHz

All most likely reflections, as they are determined from a noisy voxel cube (blue dots).

For the region of **110 … 170** MHz we see a number of spectral features in the ON, OFF and SDM modes that we also have seen the V-pol measurements. We refer to that discussion in section 4.3.2. From that discussion these spectral features are not likely to be caused inside the WTG, but are either reflections, or –more likely-- IM-products caused by the nonlinearity of the LOFAR receiver chain.

Concerning the additional signal structure (on top of the "IM product") in the **160 … 170 MHz** range, we have analysed the 3D imaging pictures. Many of these pictures have a noisy character[8]. We do find signals with their place of origin corresponding to the WTG position. An example of such a signal is found at 161.1 MHz. This signal is either a reflection from a distant source, or a signal originating from the WTG itself. Remark that the height where the signal seems to be originating is approximately at 100m. This is lower in height than we usually find, which is usually around 145m.

In the following figure, we provide an overview of the imaging-figures for the 161.1 MHz and for the neighbouring frequencies.

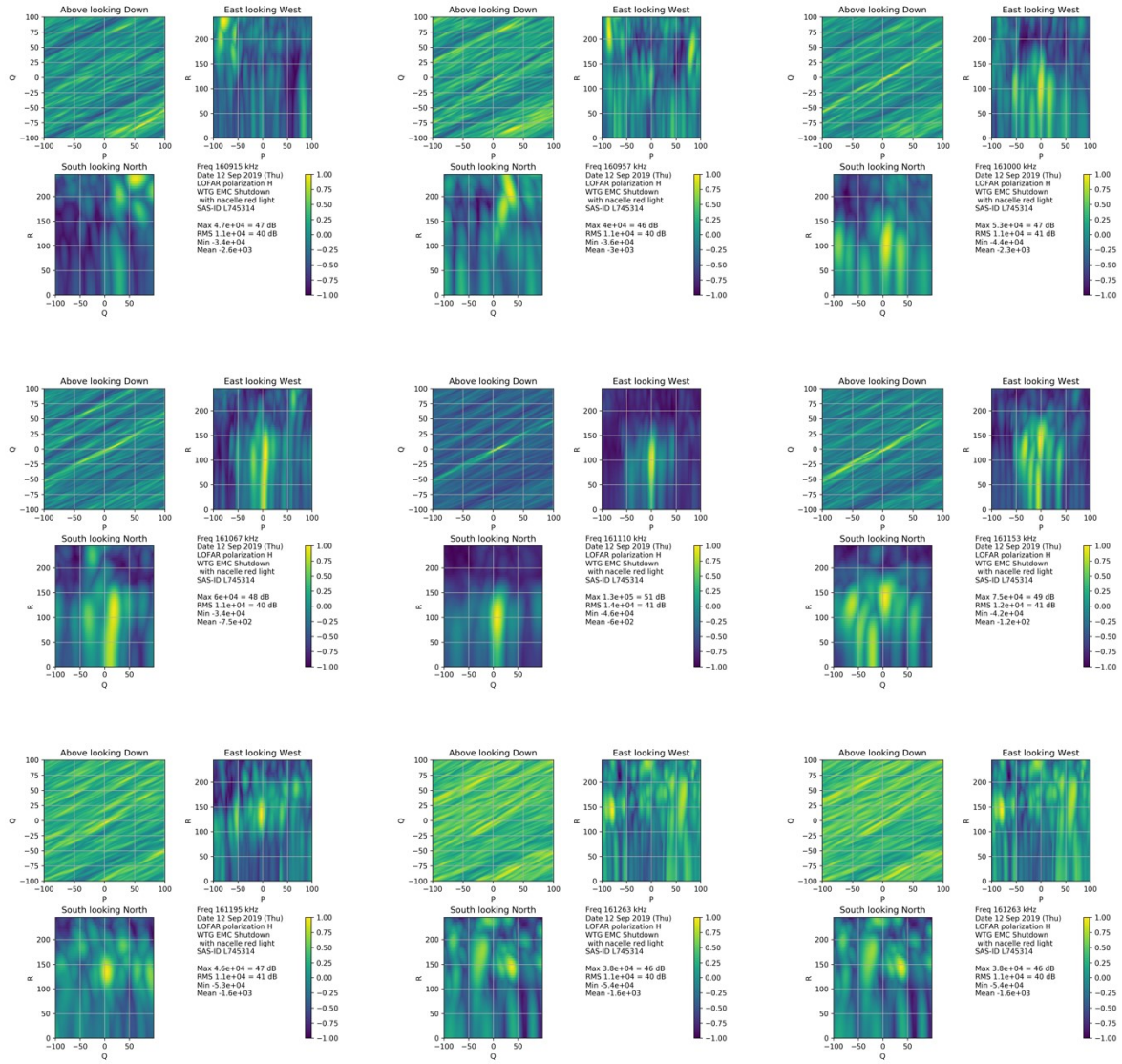

[8] Note, due to the aviation light was still flashing during the measurement, only one third of the samples have been used for the averaging per frequency, instead of the normal full 2 hours.

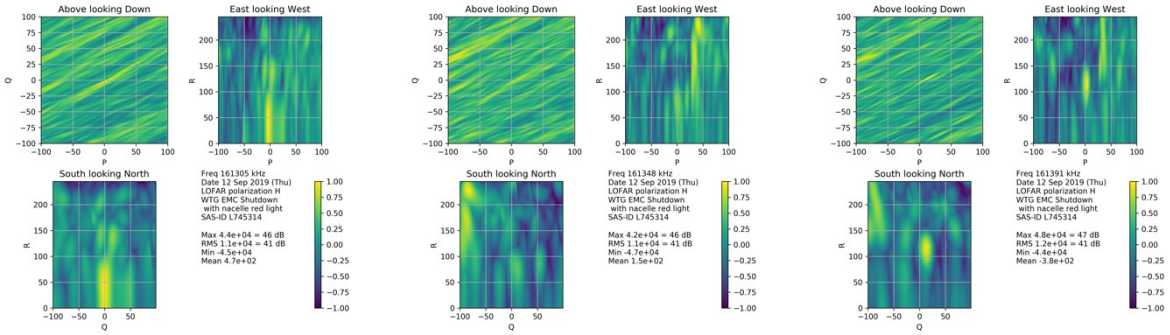

Figure 25 3D images from the range 160.9 …161.4 MHz during the H-POL SDM measurement

In order to assess whether the 161.1 signal is a reflection or is due to an emission from the WTG, we also inspected this frequency range for the OFF measurements. During these OFF measurements, at this particular frequency, we do find, albeit fainter, a signal at the location of the WTG as well, as is shown in the following figure. As the WTG is switched off, we tend to conclude that the signal, causing the -35 dB exceedance during the SDM measurements, is caused by a reflection.

Now, the lower height at which the signal is reflected is interesting. Distant sources would likely to reflect from the nacelle or blades. A lower height may indicate a source emitting at approximately at 161 MHz with a location closer by the WTG. Although the location of the crane is more than 200 m away from the WTG, it may be the location of the source of this disturbance.

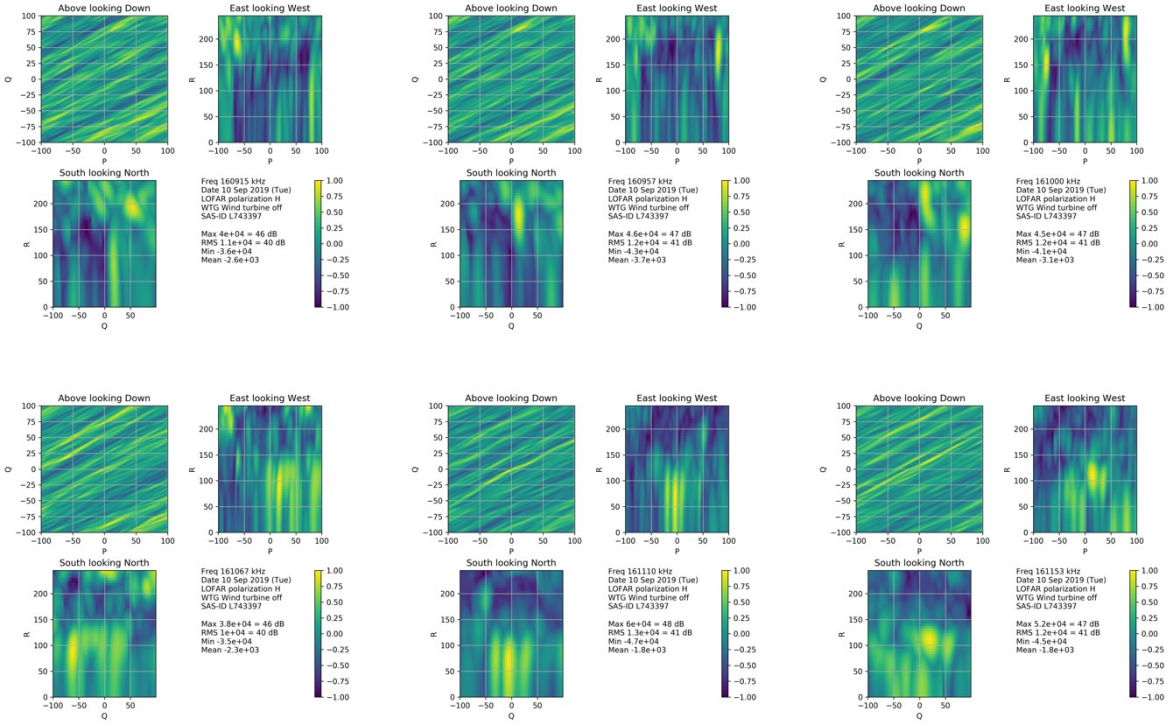

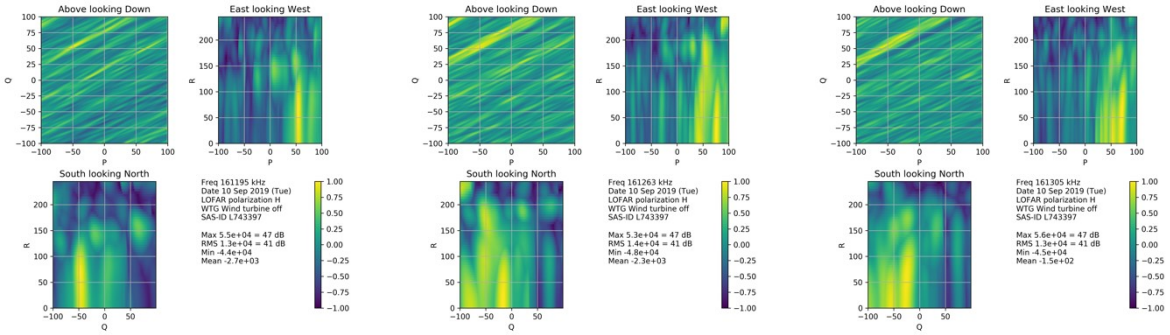

Figure 26 3D images from the round the 161,1 MHz during the H-POL OFF measurement

In the region **174…190** MHz, known for DAB transmissions, we see a number of exceedances during the ON mode. We see, however, a similar structure during the OFF measurements as well. Given the spectral structure in the L-graphs, as given above, these are most likely DAB disturbances. Below we have given an example voxel cube where the disturbance is rather clearly visible.

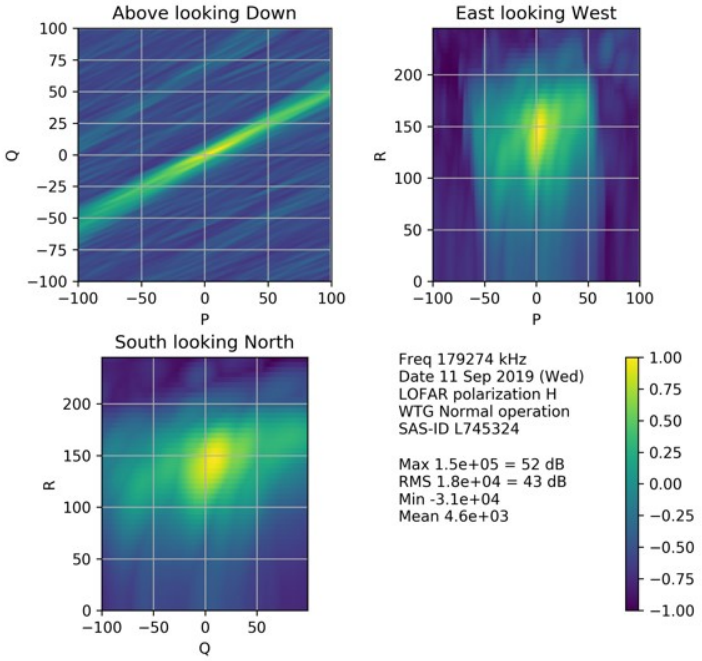

Figure 27: Voxel cube of frequencies in the 174 .. 190 MHz range. Measurements during the ON day.

4.3.7 H-polarization HBA_MID

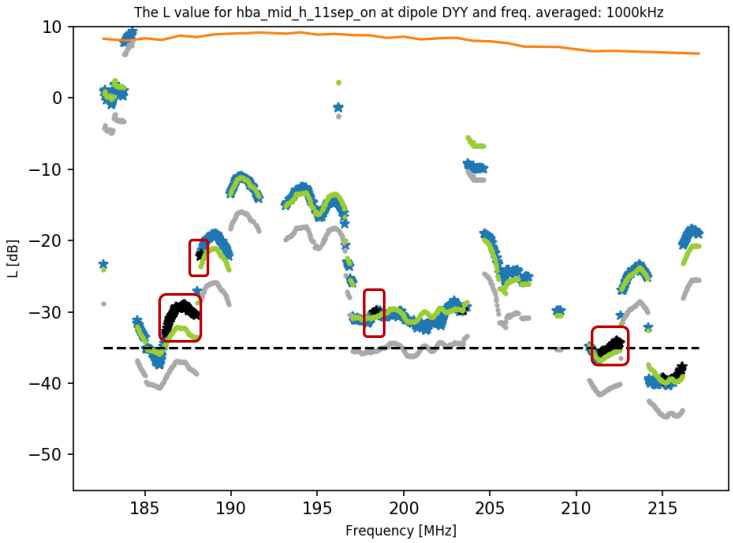

H-ON HBA_MID (11 sept)

Frequency attention:

- Large number of frequency ranges

All most likely reflections, due to spectral structure, and / or the reflections are also visible in the OFF-mode measurements.

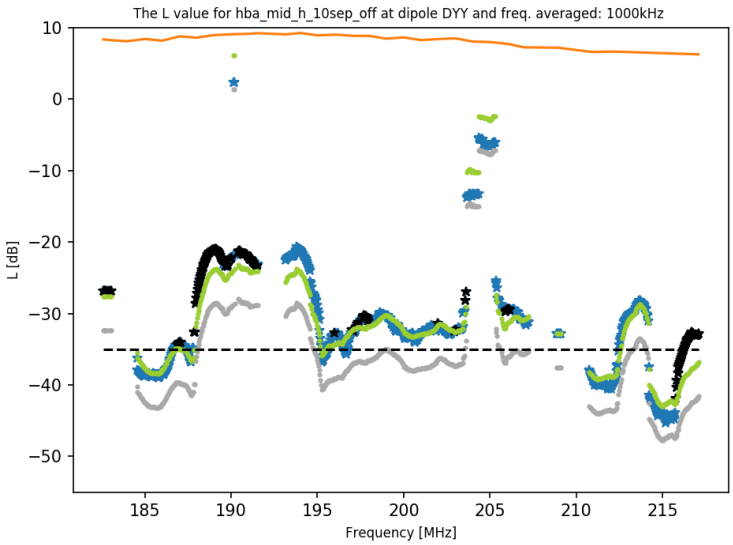

H-OFF (HBA_MID 10 sept)

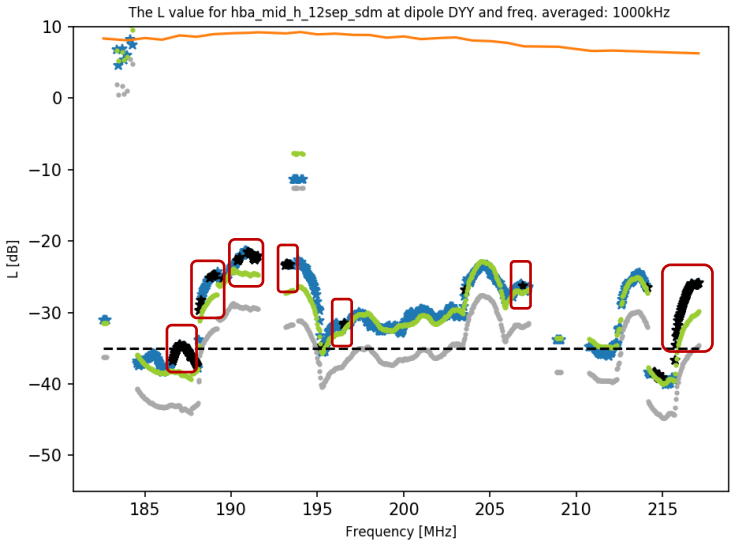

H-SDM HBA_MID (12 sept)

Frequency attention:

All most likely reflections, due to their spectral structure and as they are determined from a noisy voxel cube (blue dots), or similar structure as found during the OFF measurements

Similar to the V-polarizations, we see a number of signal exceedances, that all –given their spectral structure (approx. 4 MHz wide)—seem to be related to Digital TV or DAB broadcasts. For the Shutdown mode, the following figure shows the voxel cube for the 204.7 MHz. This seems to be noise dominated.

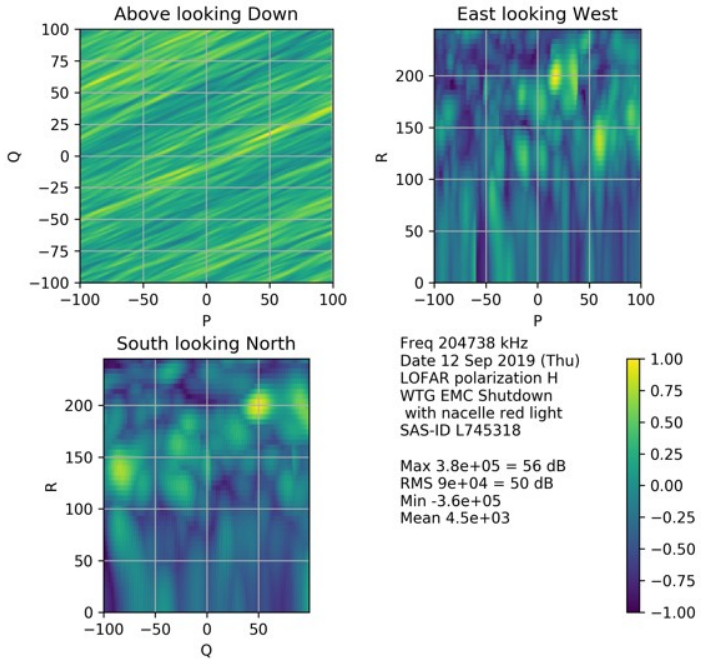

Figure 28: Voxel cube of the 204.8 MHz frequency. Measurement during the Shutdown mode day.

We furthermore have an example of 189 MHz and 190 MHz range. Again, these figures seem to be noisy.

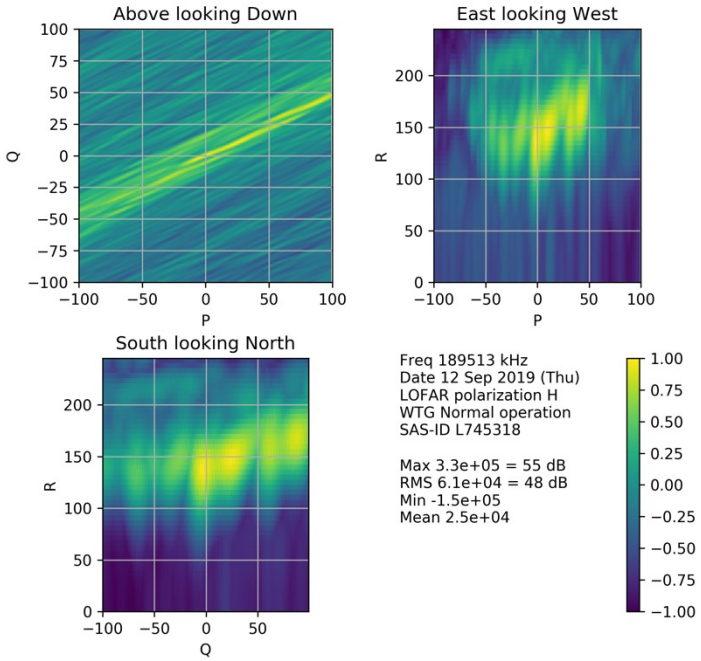

Figure 29: Voxel cube of the 189.5 MHz frequency. Measurement during the ON mode day.

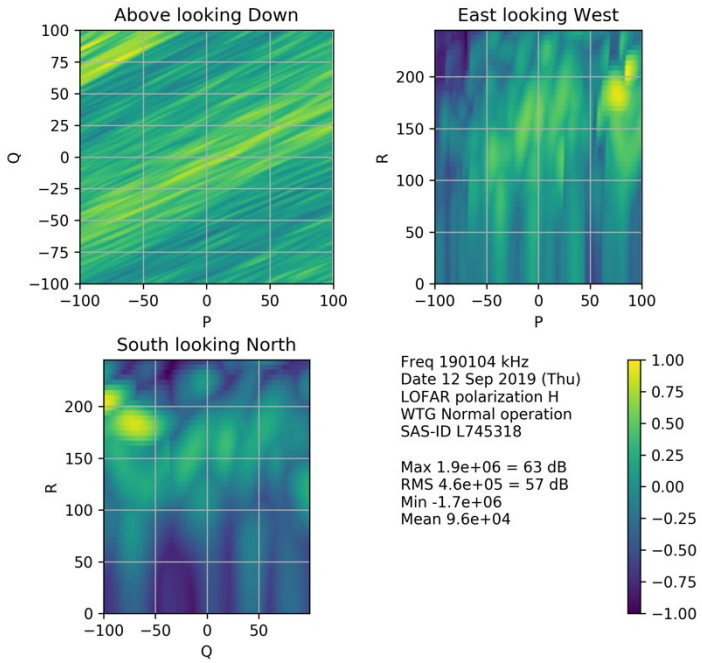

Figure 30: Voxel cube of the 190.1 MHz frequency. Measurement during the ON mode day.

4.3.8 H-polarization HBA_HIGH

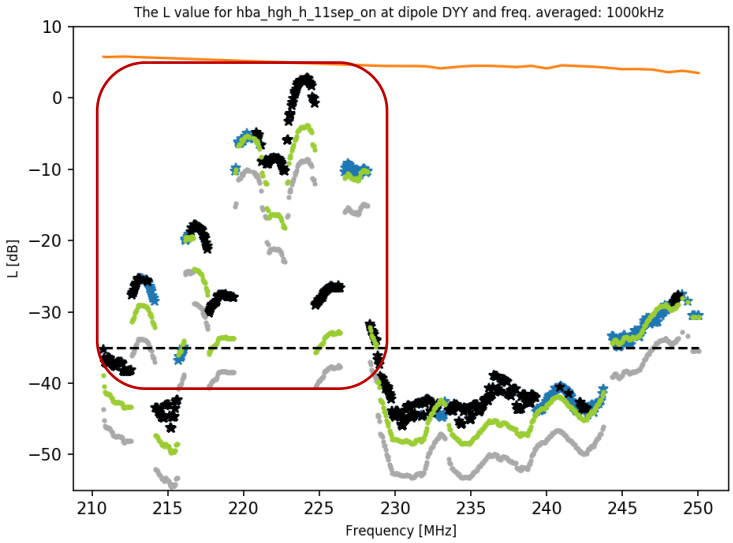

H-ON HBA_HIGH (11 sept)

Cleaned

Frequency attention:

- Large number of frequency ranges

All most likely reflections, due to the spectral structure

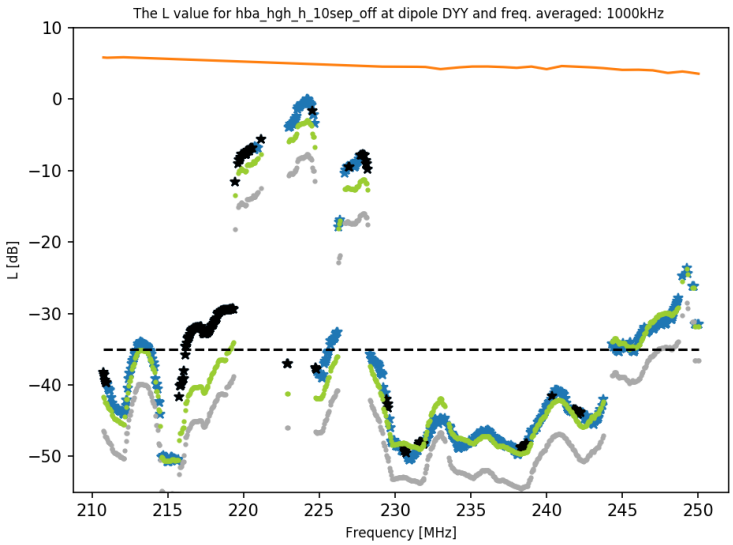

H-OFF HBA_HIGH (10 sept)

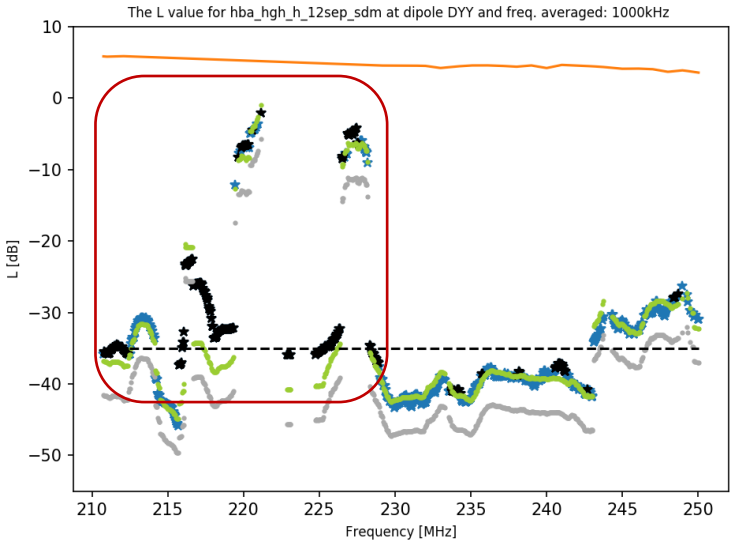

H-SDM HBA_HIGH (12 sept)

Frequency attention:

Large number of frequency ranges

All most likely reflections due to spectral structure, and the similarity with the OFF mode.

For the region **210 … 230** MHz, again, the type of exceedances that are measured during the ON mode, are also mostly present during the OFF mode and during the SDM mode, or seem to have a spectral structure that indicates a DAB.

For the H-POL ON measurements, we see a signal (lower than -35 dB) at the frequencies **230 MHz and higher** while in the SDM measurements this signal isn't visible, but may be hidden in noise (note, the noise level in this measurement is a little higher than for the ON and OFF measurements as only 1/3 of the data could be used). The following figure shows both the ON and SDM results.

Note also for the ON measurements, the WTG doesn't exceed the -35 dB level. We investigate this behaviour to see (a) if a signal in the 3D-imaging pictures is visible in the ON mode, and (b) to see if a trace of the signal is visible during the SDM measurements as well (a possible indication that the signal is caused by one of the components that is switched on during the SDM).

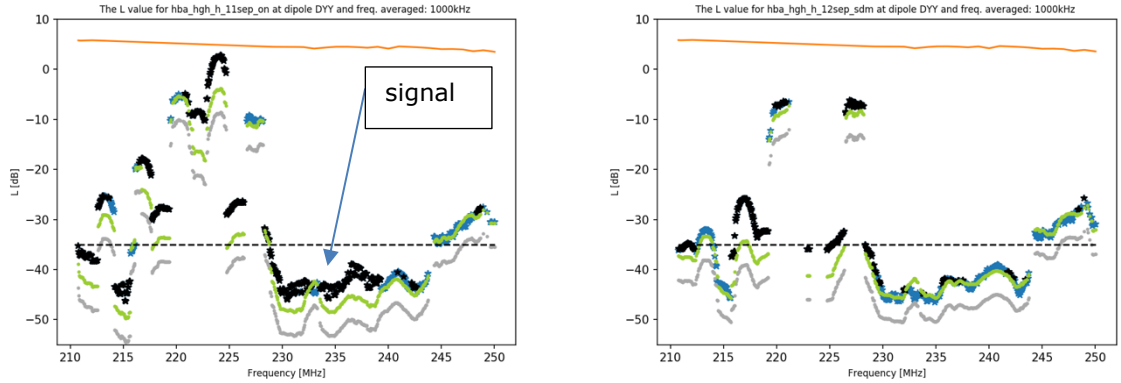

Figure 31 PSD of the ON measurement (left) and SDM measurement (right)

For the ON measurement, we found a number of signals, as is shown in the following figure. These signals seem to be originating from approximately the nacelle position of the WTG.

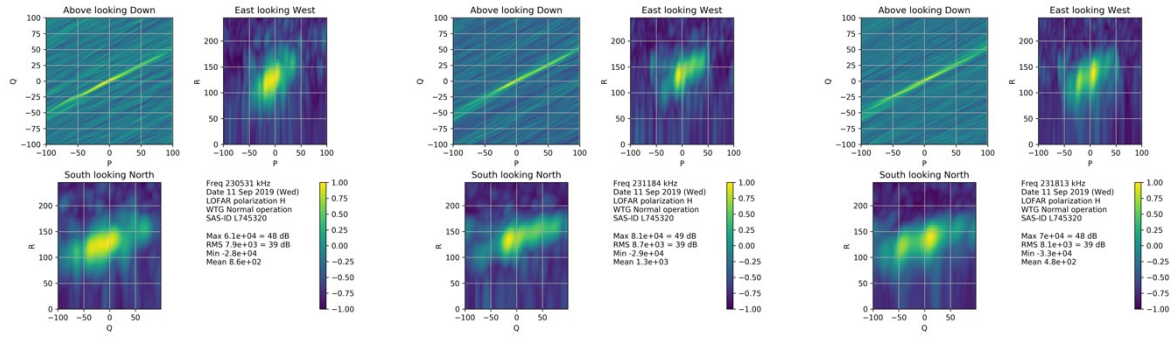

Figure 32 Example signals as found during the H-POL ON measurements

The 3D images of the corresponding frequencies (or any other 3D image that we inspected in the range 230 … 234 MHz) during the SDM measurement don't show any clear signals, as is shown below. The maximum values as found during the SDM measurements are a few dB lower than those in ON, although the noise is a bit higher.

Thus, the signal in the H-POL ON measurements in the frequency range 230 MHz and higher can't be found in the H-POL SDM measurements, and most likely the signal that is visible during the ON measurements is not caused by equipment switched-on during the SDM.

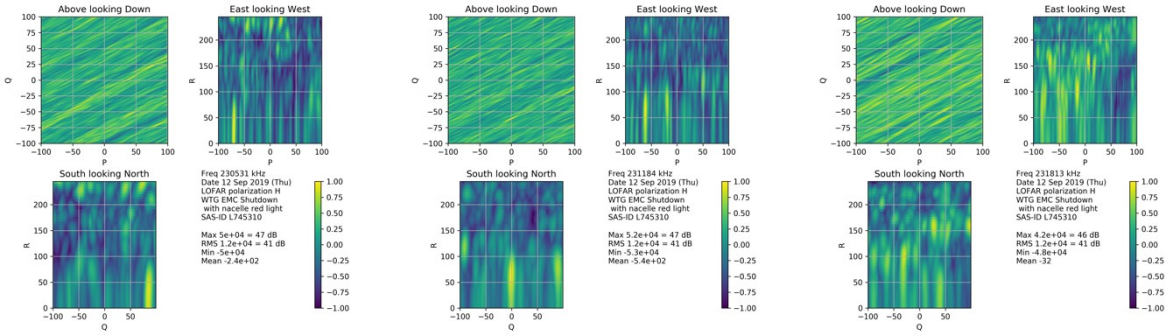

Figure 33 Corresponding (to the signal found during the ON measurements; see figure above) 3D images for the H-POL SDM measurements.

4.3.9 Summary of the H-polarized and V-polarized data results

To summarize, the observations include:

- We find a fairly large number of cases where we suspect to see a strong reflection in the power spectrum, for both the V-polarized and H-polarized data.
- Around 70 MHz we find a broad-banded disturbance in both the V-polarized data as well as the H-polarized data.
- In general, the structure of H-polarized measurement results is similar to the V-polarized measurement results.

4.3.10 Further analysis around 70 MHz (LBA)

Research, by Nordex and AT, into a possible source of interference around the 70 MHz has led to the suspicion of an UPS being able to radiate around that frequency. This UPS is meant to supply power to the tower light in case of power failure. The official duration of power supply is listed as 45 minutes. It may be that it lasts way longer.

The measurement for the Wind turbine off modes, V-OFF LBA 4 sept and H-OFF LBA 10 sept (refer to sections 4.3.1 and 4.3.5) show no peak at 70 MHz above the -35 dB level. The measurements for the EMC Shutdown modes, V-SDM LBA 13 sept and H-SDM LBA 12 sept (refer to sections 4.3.1 and 4.3.5), show peaks at 70 MHz at or above the -35 dB level.

Table 8 shows the time (yellow highlighted) that WTG power was shutdown. A theory is now that the UPS takes longer to unload, since no peaks are seen above the -35 dB on the Wind turbine off modes and the UPS has had time to unload (1 hour and 52 minutes and 1 hour and 28 minutes respectively).

Table 8: WTG Power shutdown times

Date		Remark	Pol.	NC2: WTG switch OFF time	Test Time over night	Delay WTG OFF / Test start	WTG mode
02./03.09.	Mon/Tue	tower-aviation light fault	V		Start 21:00	-	WTG NOM OPERATION
					End 06:40	-	
03./04.09.	Tue/Wed	-	V		Start 20:56	-	WTG NOM OPERATION
					End 06:36	-	
04./05.09.	Wed/Thu	-	V	from 19:00 OFF	Start 20:52	01:52 h	WTG OFF
				to 07:30 ON	End 06:32	-	
05./06.09.	Thu/Fri	-	V		Start 20:48	-	WTG STDBY (DWNTM) PLUS
					End 06:28	-	
06./07.09.	Fri/Sat	-	V		Start 20:44	-	WTG STDBY (DWNTM)
					End 06:24	-	
07./08.09.	Sat/Sun	faulty reference source	H		Start 20:40	-	WTG NOM OPERATION
					End 06:20	-	
08./09.09.	Sun/Mon	-	H		Start 20:36	-	WTG STDBY (DWNTM)
					End 06:16	-	
09./10.09.	Mon/Tue	-	H		Start 20:32	-	WTG STDBY (DWNTM) PLUS
					End 06:12	-	
10./11.09.	Tue/Wed	-	H	from 19:00 OFF	Start 20:28	01:28 h	WTG OFF
				to 07:30 ON	End 06:08	-	
11./12.09.	Wed/Thu	-	H		Start 20:24	-	WTG NOM OPERATION
					End 06:21	-	
12./13.09.	Thu/Fri	AOL "Software-Bug"	H	from 20:10 OFF	Start 20:20	00:10 h	WTG EMC SHUTDOWN
				to 08:00 ON	End 06:00	-	
13./14.09.	Fri/Sat	-	V	from 19:10 OFF	Start 20:16	01:06 h	WTG EMC SHUTDOWN

To test this theory, the LBA measurement data of 12 and 13 September has been reprocessed, but now excluding some time that the UPS may been generating signal.

The assumption that has been made here is that the UPS lasts for 1 hour and 30 minutes. This means that UPS was "dead" on:

- 12 September on CEST (20:20:40-00:10+01:30 = 21:40:40), UTC (19:40:40)
- 13 September on CEST (20:16:44-01:06+01:30 = 20:40:44), UTC (18:40:44)

Written down in the processing format yyyy-mm-ddThh:mm:ss, this gives the following time exclusions:

12 Sept	**CEST**	**UTC**
Start	2019-09-12T20:20:40	2019-09-12T18:20:40
End	2019-09-12T21:40:40	**2019-09-12T19:40:40**

13 Sept	**CEST**	**UTC**
Start	2019-09-13T20:16:44	2019-09-13T18:16:44
UPS end	2019-09-13T20:40:44	**2019-09-13T18:40:44**

Therefore, the following exclusions of measurement data were made during reprocessing of the measurement data of 12 and 13 September:

Exclusion time(s) 12 September**	**Explanation**
2019-09-12T18:20:40 - 2019-09-12T19:40:40	UPS exclusion
2019-09-12T19:45:24 - 2019-09-12T19:56:26	Remaining aviation light off exclusions*
2019-09-12T20:01:59 - 2019-09-12T20:13:02	
2019-09-12T20:18:34 - 2019-09-12T20:29:36	

*: For the processing of 12 September, already exclusions of measurement data were made, since during the measurement the aviation light was switched on and off in a regular pattern, due to a software bug.

**: This will leave about 15 minutes of data for processing

Exclusion time(s)* 13 September	**Explanation**
2019-09-13T18:16:44 - 2019-09-13T18:40:44	UPS exclusion

*: This will leave about 1 hour and 36 minutes of data for processing

4.3.10.1 Results 12 September (LBA reduced data set)

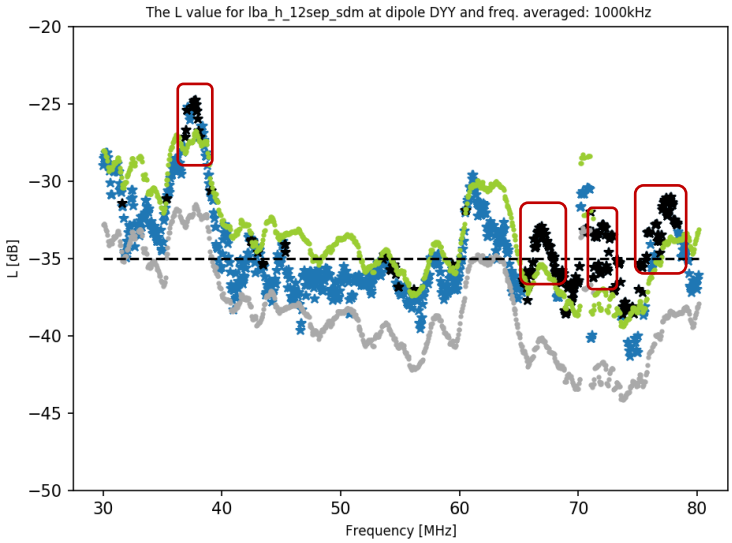

H-SDM LBA (12 sept), zoomed in
All data, cleaned version is pending

Frequency attention:
Around 38 MHz
66 to 70 MHz
72 to 73 MHz
76 to 78 MHz

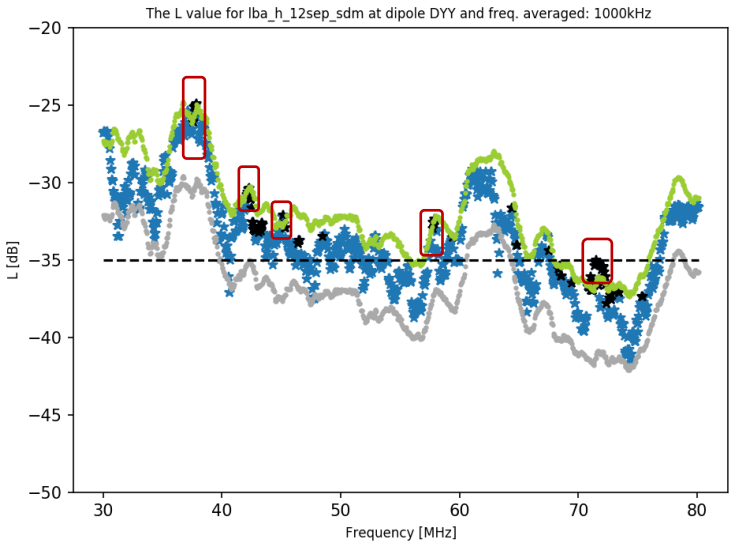

H-SDM LBA (12 sept), zoomed-in
UPS reduced data

Frequency attention:
Around 38 MHz
Around 43 MHz
Around 45 MHz
Around 58 MHz
Around 73 MHz

For the date of 12 September, the reduced data set results in significantly lower signal in the region of 66 to 78 MHz, while the remaining frequency range does not change significantly. Only one peak remains around 72 to 73 MHz.

The result indicates that the suspected UPS contributes significantly to the measured interference.

4.3.10.2 Results 13 September (LBA reduced dataset)

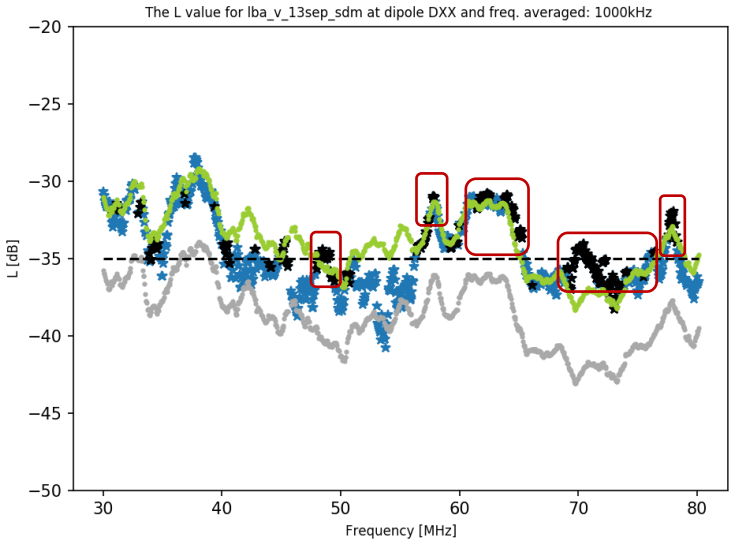

V-SDM LBA (13 sept), zoomed-in
All data

Frequency attention:
48 to 49 MHz
58 MHz
61 to 66 MHz
70 to 78 MHz
78 to 79 MHz

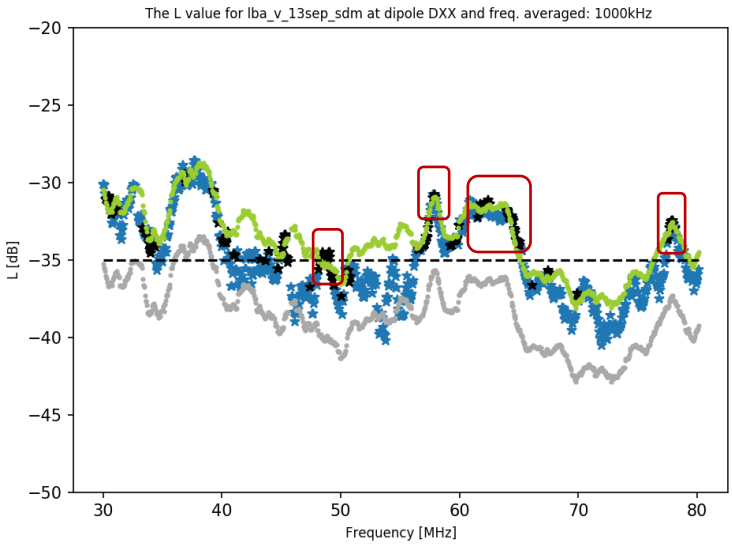

V-SDM LBA (13 sept), zoomed-in
UPS reduced data

Frequency attention:
48 to 49 MHz
58 MHz
61 to 66 MHz
78 to 79 MHz

For the date of 13 September, the reduced data set results clearly in significantly lower signal in the region of 66 to 78 MHz, while the remaining frequency range does not change significantly.

The result clearly indicates that the suspected UPS contributes significantly to the measured interference.

4.3.11 H+V

In the following subsection the additions of H+V have only been given for the frequency band LBA, given the time constraints and current necessity. HBA_LOW and HBA_HIGH appear to contain no apparent WTG signal in the neighbourhood of -35 dB. HBA_MID has been left out here as it appears to be a no-go frequency range anyway for LOFAR.

The tables are setup as one page each with three L-value plots for:

- OFF (H+V), with the original H and V given for comparison
- ON (H+V), with the original H and V given for comparison
- SDM (H+V), with the original H and V given for comparison
- H (ON - OFF), V (ON - OF) and ON (H+V) minus OFF (H+V)
- H (SDM - OFF), V (SDM - OF) and SDM (H+V) minus OFF (H+V)

Where:

- OFF is: Wind turbine off mode
- ON is: Normal operation mode
- SDM is: EMC Shutdown mode

All results have been processed with the latest version of the pipeline processing software, including the ACM-filter to clean the ACM form excessive values.

The additions and subtractions have been performed using the actual voxel cubes for H and V, as well as the resulting voxel cubes of H+V.

The order in the calculations was:

1. First apply L-formula to the whole flux cubes per frequency.
2. For averaged plots, all cubes in the frequency range are averaged, with exception of cubes that are considered outliers according to the MAD filter (refer to section 4.2, WTG Data).
3. Add or subtract the cubes per voxel value.
4. Then calculate the statistics, like the maximum, minimum, RMS etc.

The summation results show no other -35 dB level exceedances than those analysed in the individual H-pol and V-pol results.

4.3.11.1 LBA

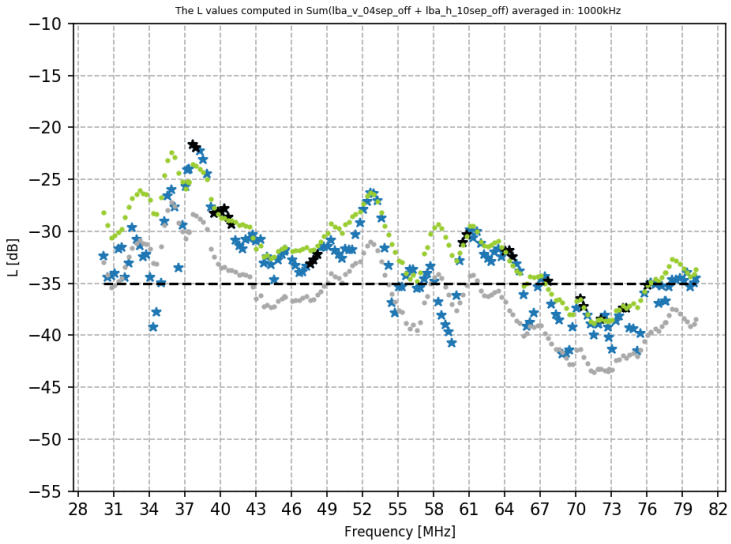

LBA OFF (H+V)
4+10 September

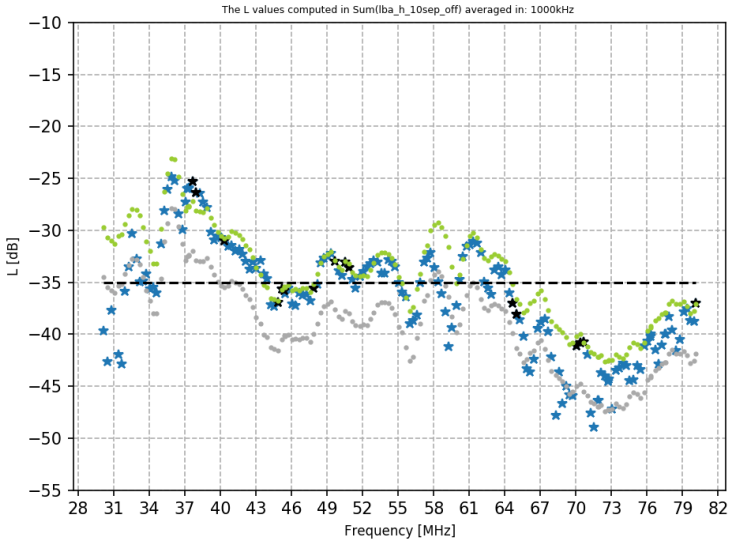

LBA OFF (H),
10 September

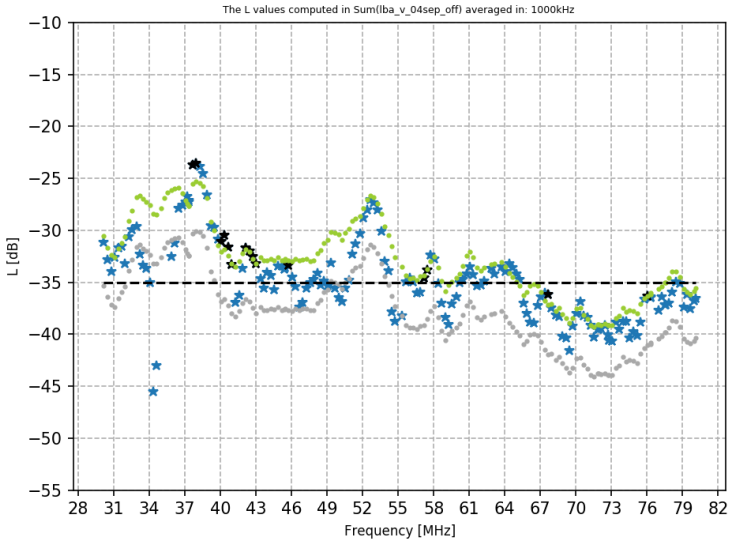

LBA OFF (V)
4 September

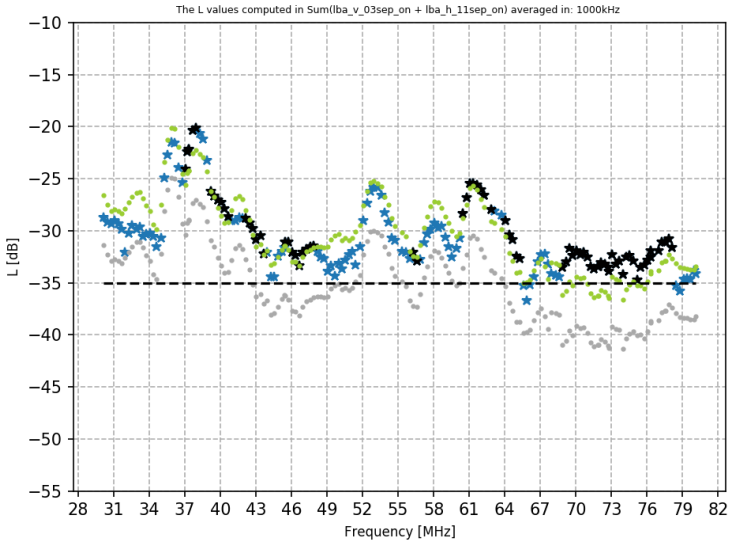

LBA ON (H+V)
3+11 September

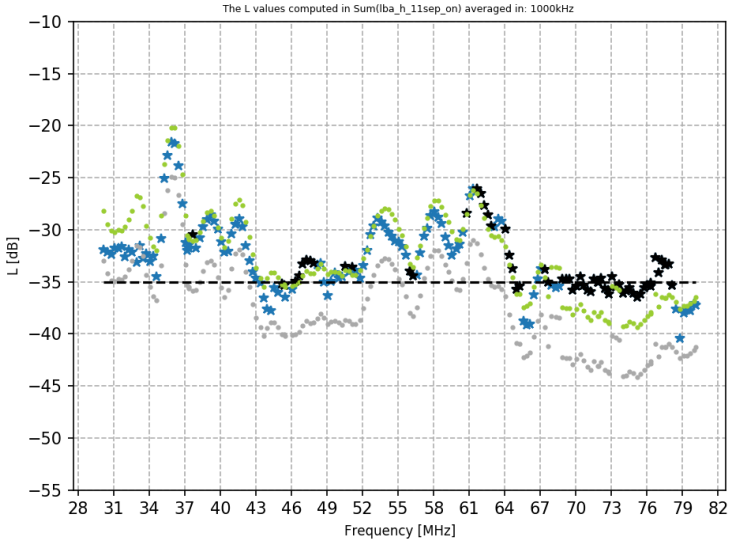

LBA ON (H)
11 September

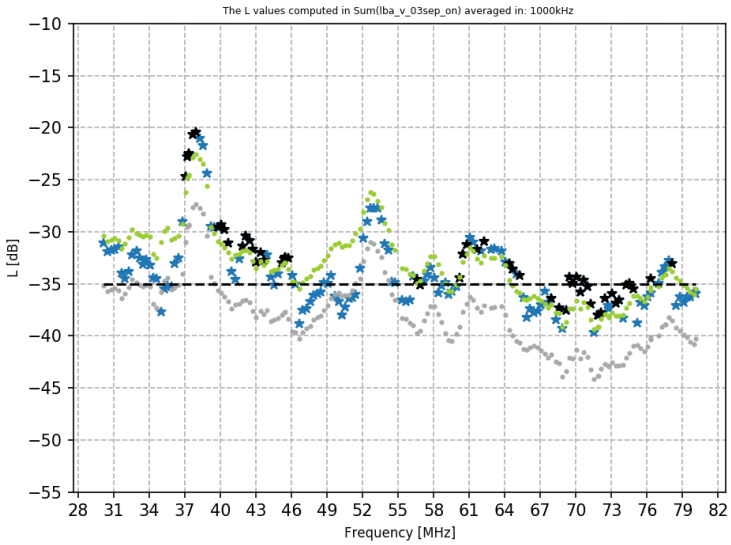

LBA ON (V)
3 September

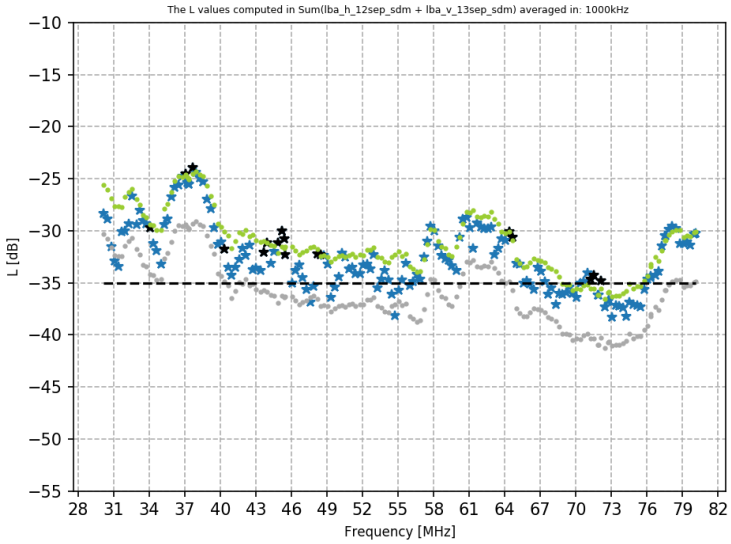

LBA SDM (H+V)
12+13 September
- UPS filtered

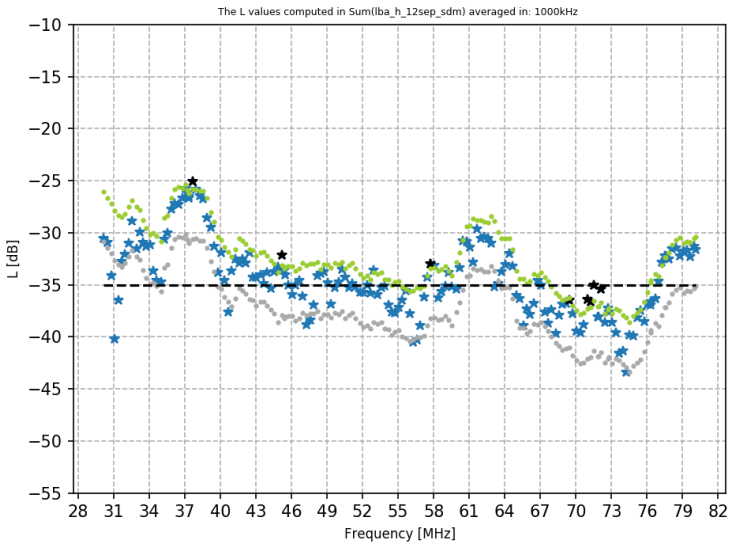

LBA SDM (H)
12 September
- UPS filtered

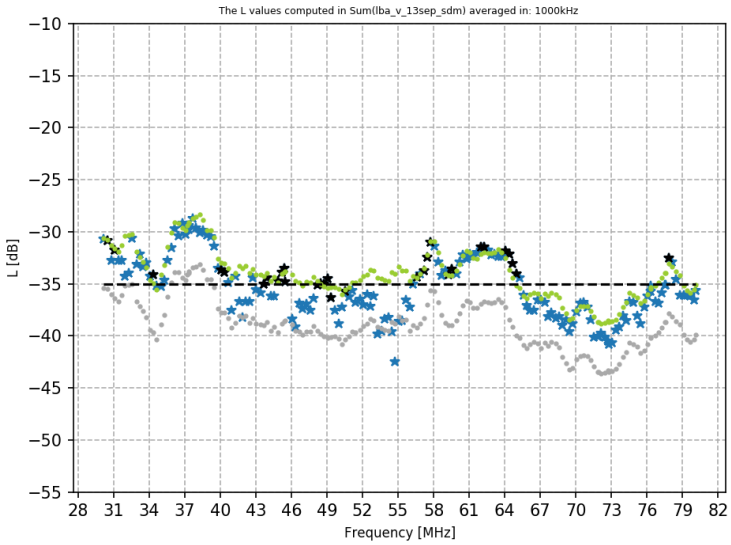

LBA SDM (V)
13 September
- UPS filtered

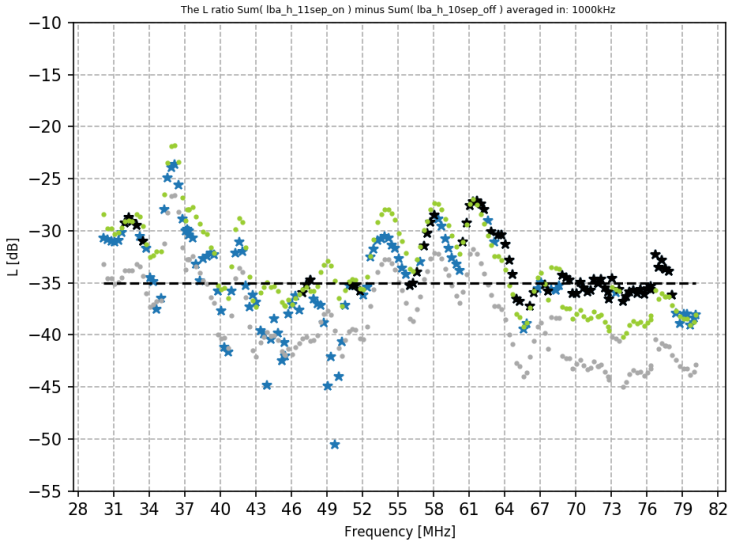

LBA H (ON - OFF)
11 -10 September

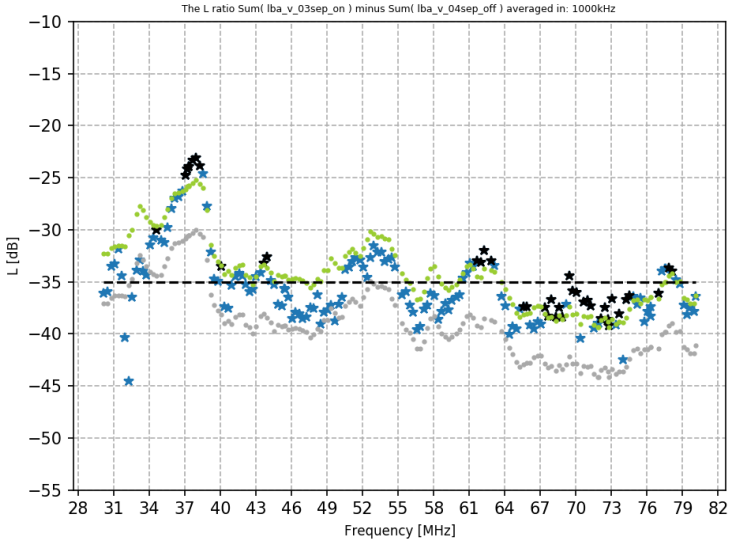

LBA V (ON - OFF)
3 - 4 September

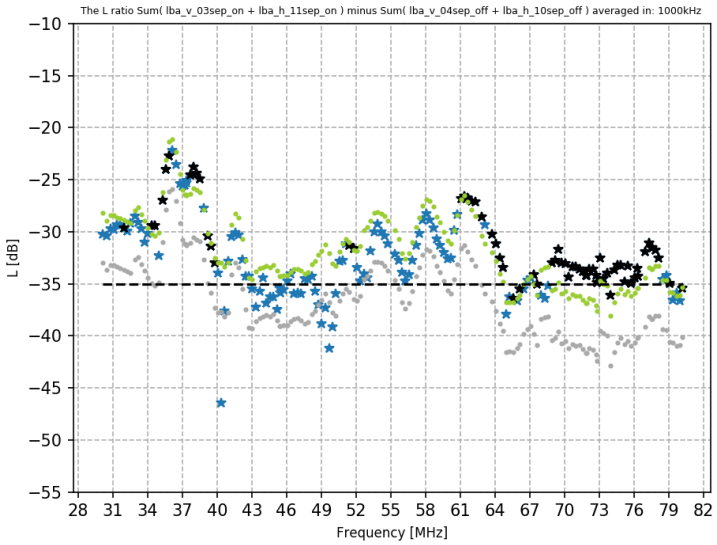

LBA ON (H+V) – LBA OFF (H+V)
(3+11) – (4+10) September

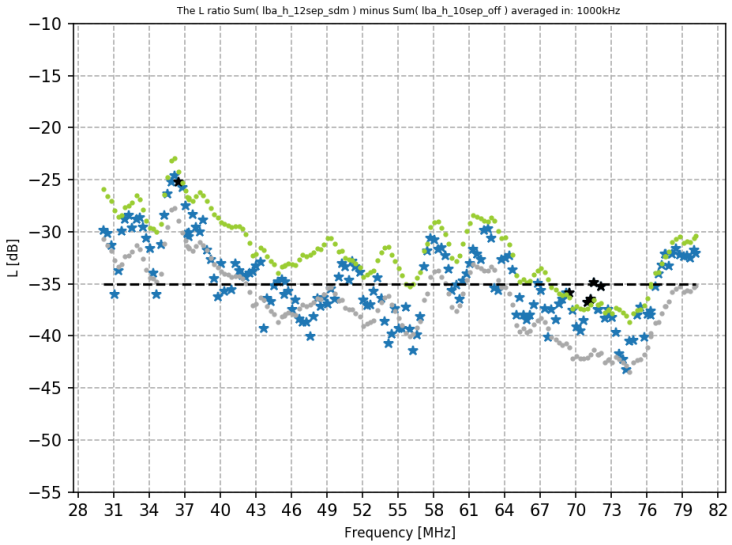

LBA H (SDM - OFF)
12 -10 September
- UPS filtered

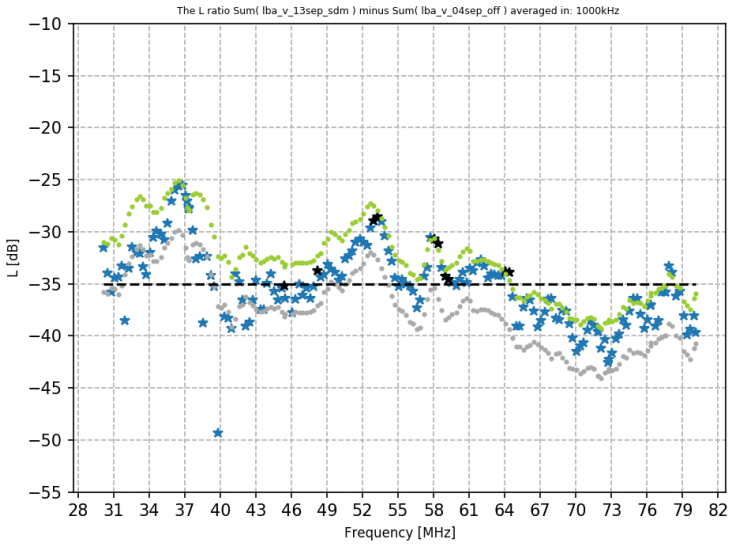

LBA V (SDM - OFF)
13 - 4 September
- UPS filtered

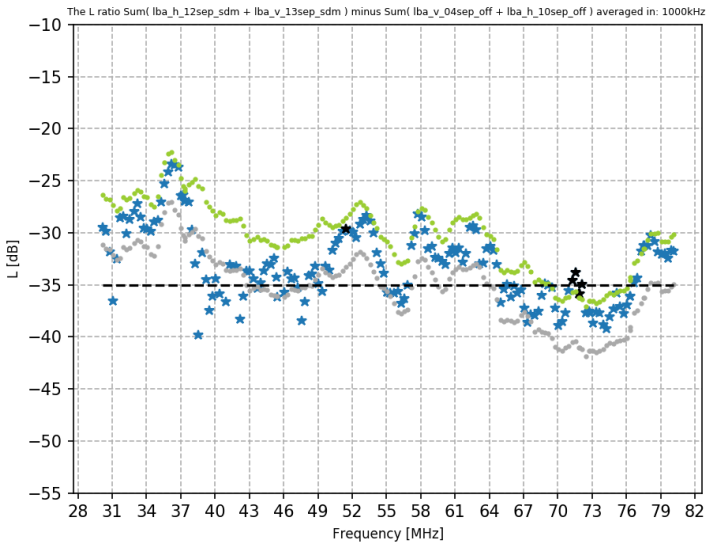

LBA SDM (H+V) – LBA OFF (H+V)
(12+13) - (4+10) September
- UPS filtered

4.3.11.2 HBA_LOW

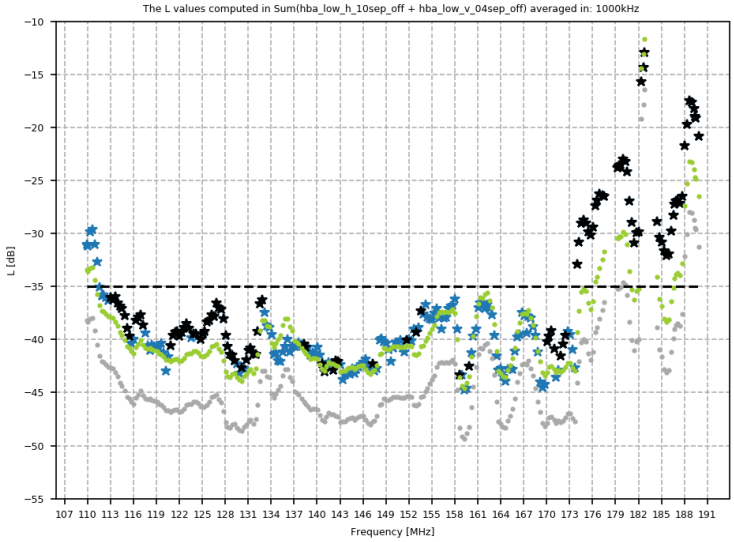

HBA_LOW OFF (H+V)
4+10 September

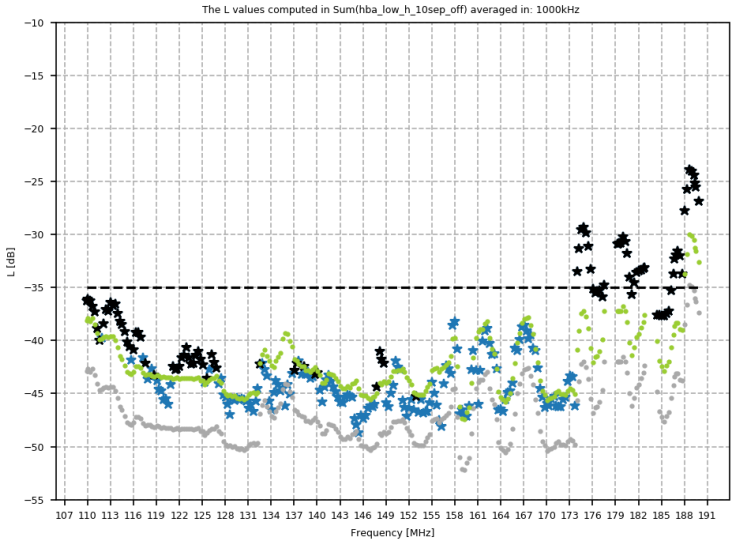

HBA_LOW OFF (H),
10 September

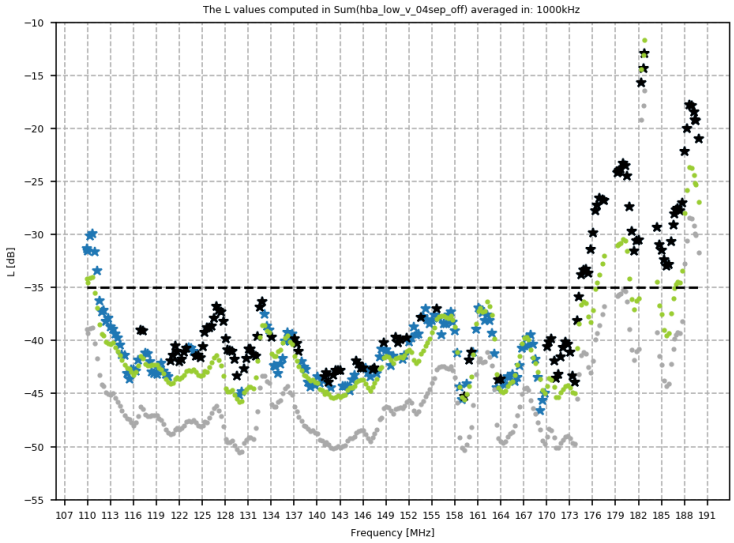

HBA_LOW OFF (V)
4 September

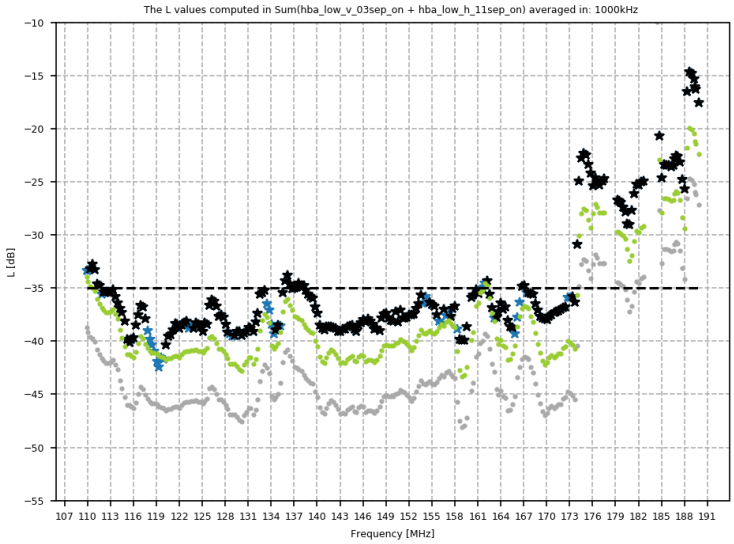

HBA_LOW ON (H+V)
3+11 September

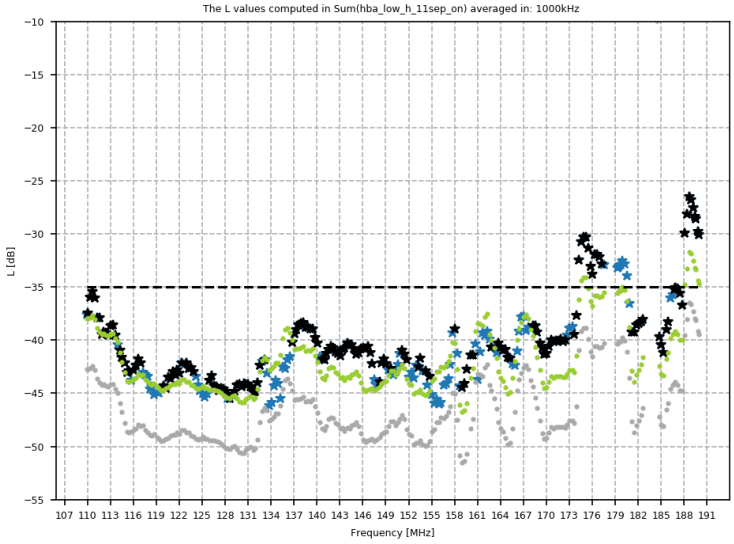

HBA_LOW ON (H)
11 September

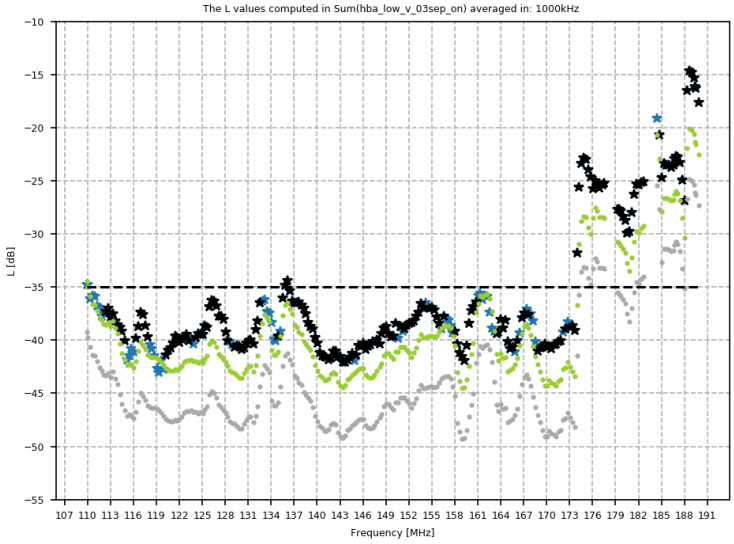

HBA_LOW ON (V)
3 September

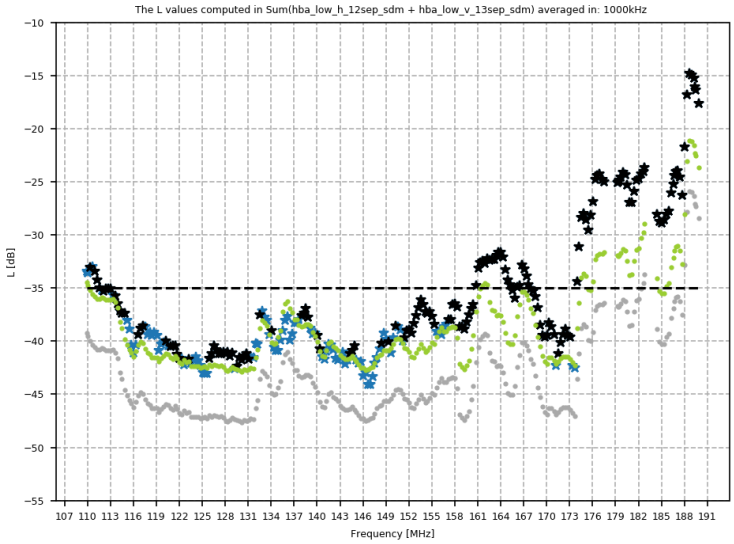

HBA_LOW SDM (H+V)
12+13 September

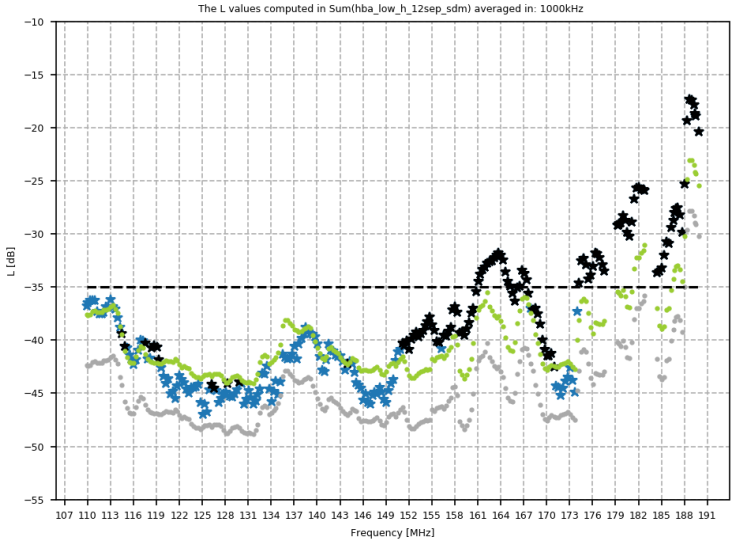

HBA_LOW SDM (H)
12 September

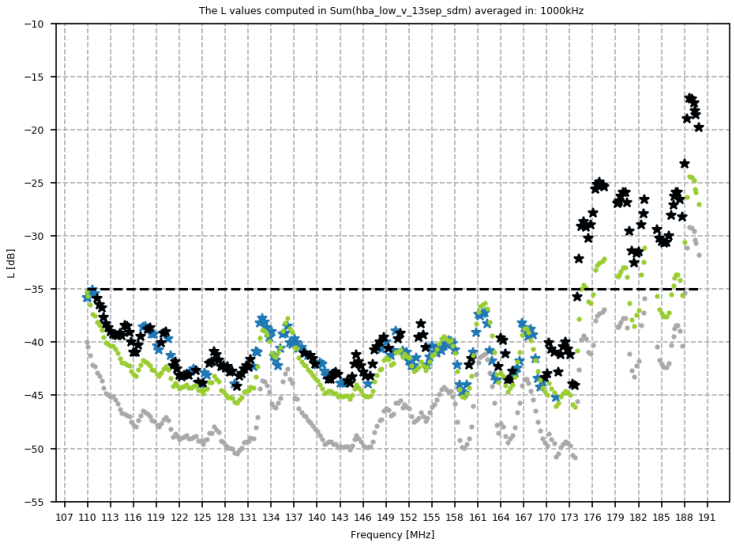

HBA_LOW SDM (V)
13 September

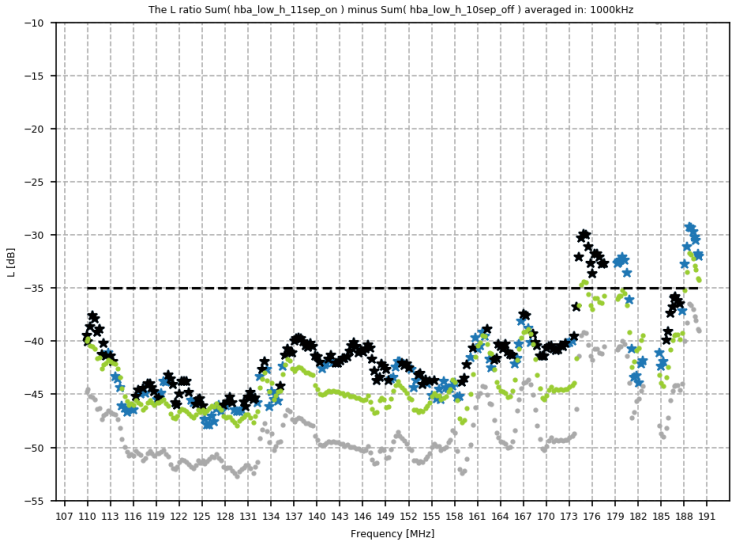

HBA_LOW H (ON - OFF)
11 -10 September

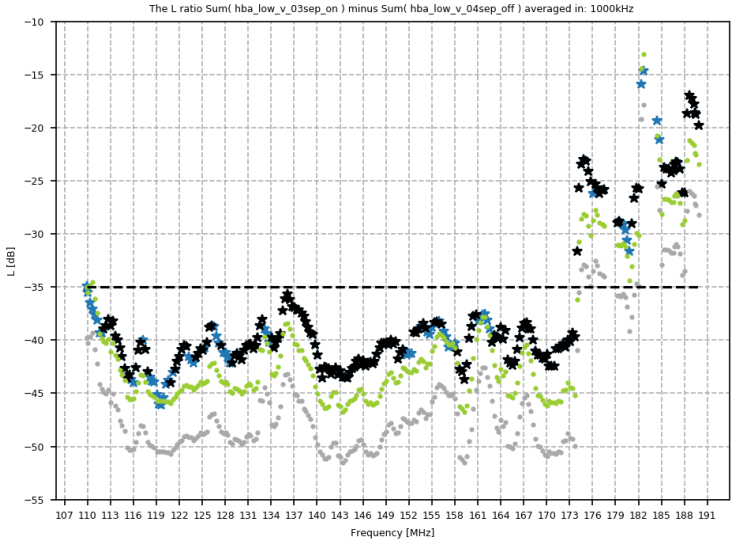

HBA_LOW V (ON - OFF)
3 - 4 September

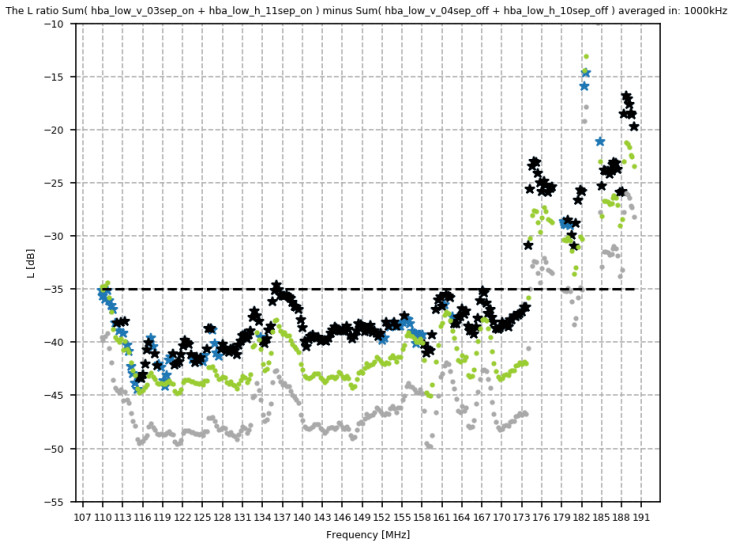

HBA_LOW ON (H+V) – HBA_LOW OFF (H+V)
(3+11) – (4+10) September

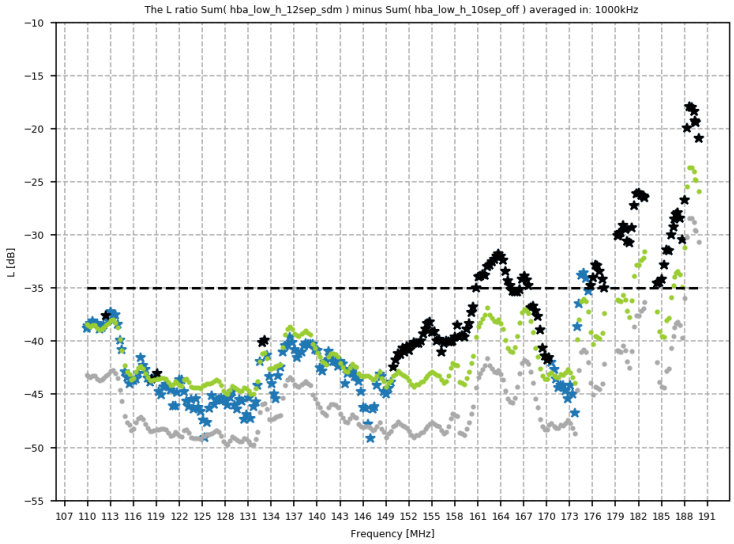

HBA_LOW H (SDM - OFF)
12 -10 September

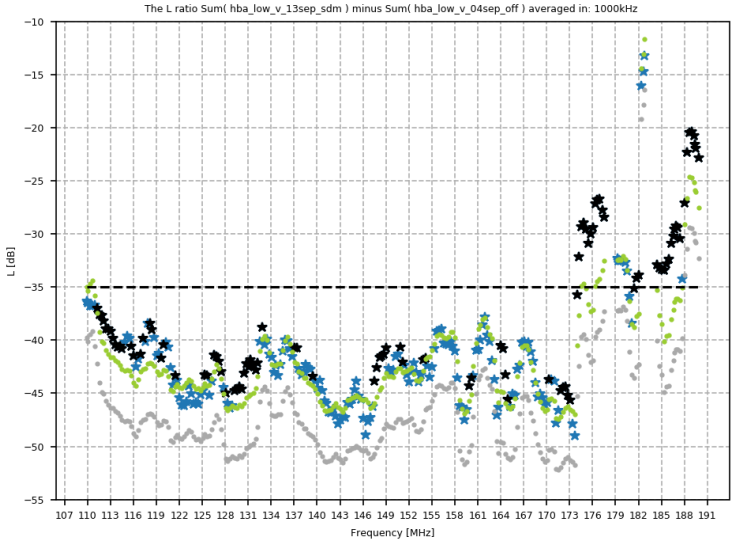

HBA_LOW V (SDM - OFF)
13 - 4 September

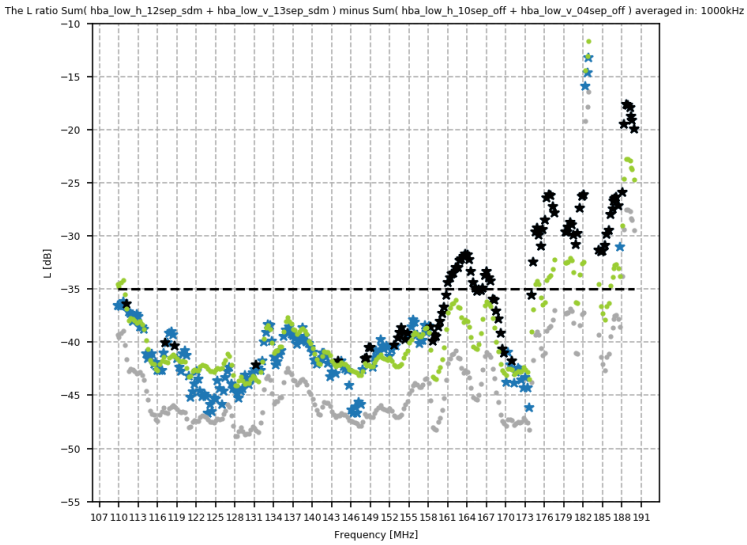

HBA_LOW SDM (H+V) – HBA_LOW OFF (H+V)
(12+13) - (4+10) September

4.3.11.3 HBA_HIGH

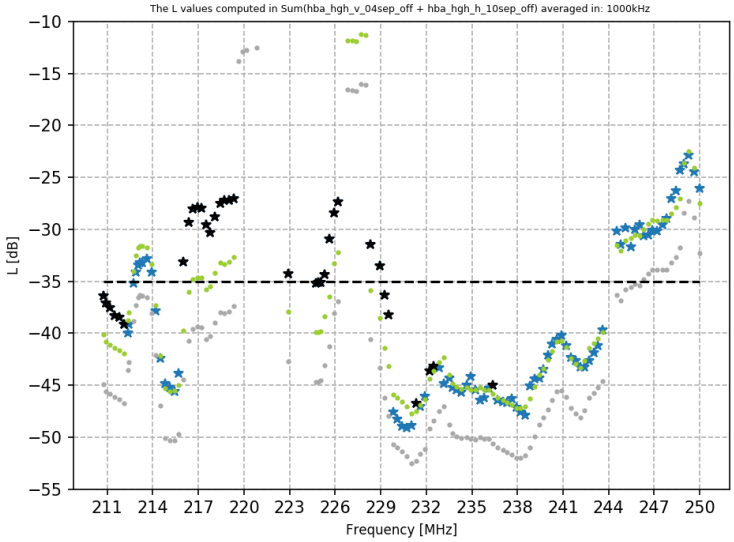

HBA_HIGH OFF (H+V)
4+10 September

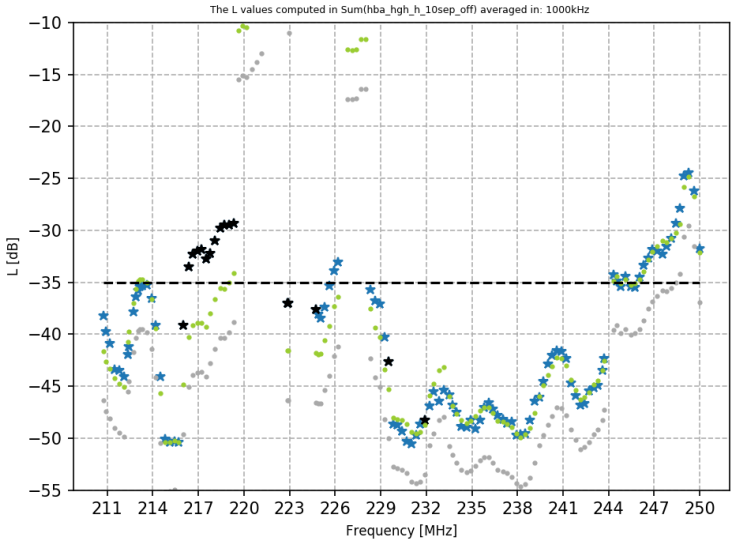

HBA_HIGH OFF (H),
10 September

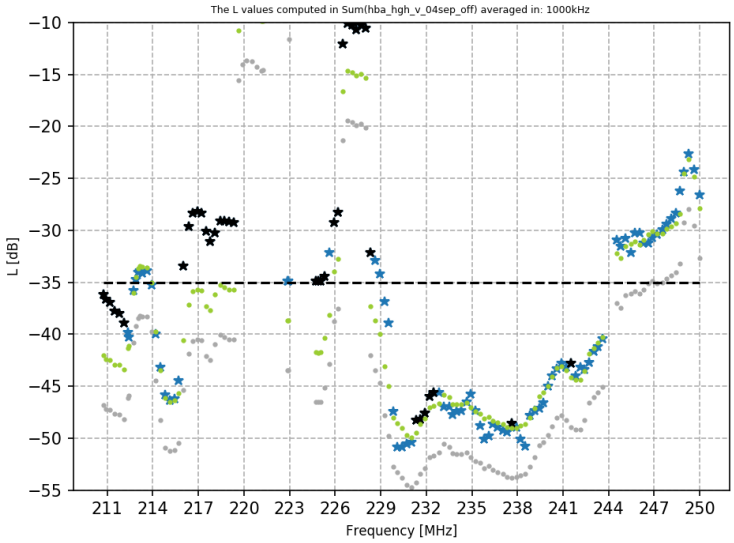

HBA_HIGH OFF (V)
4 September

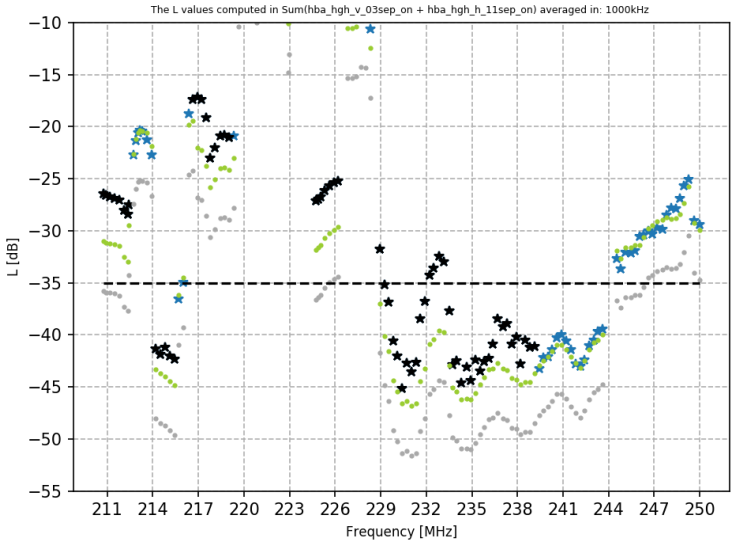

HBA_HIGH ON (H+V)
3+11 September

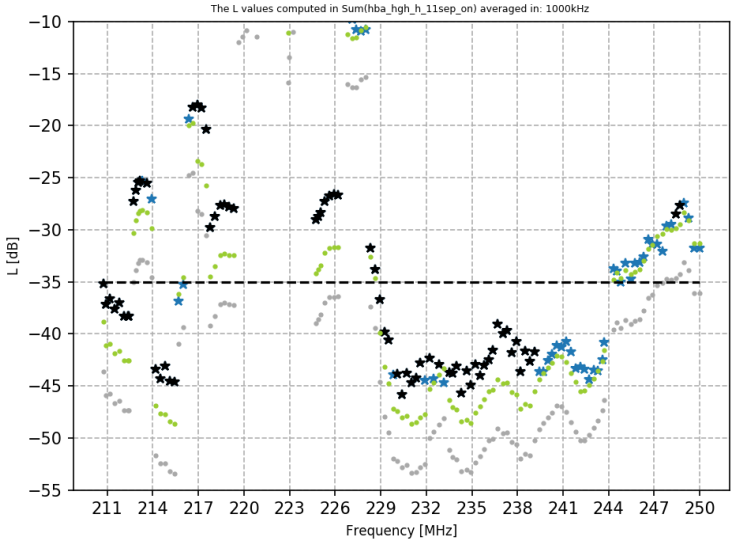

HBA_HIGH ON (H)
11 September

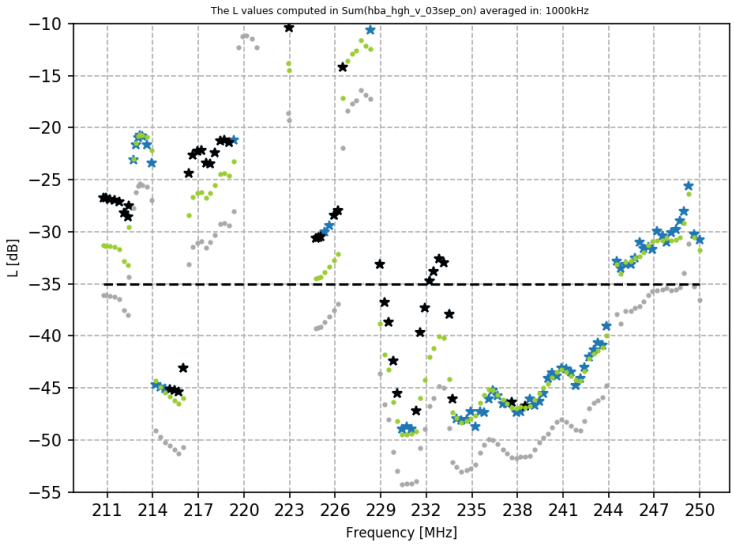

HBA_HIGH ON (V)
3 September

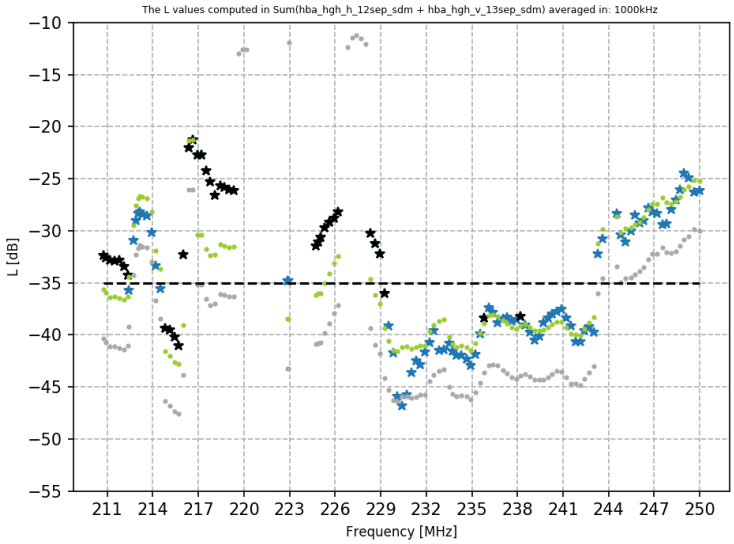

HBA_HIGH SDM (H+V)
12+13 September

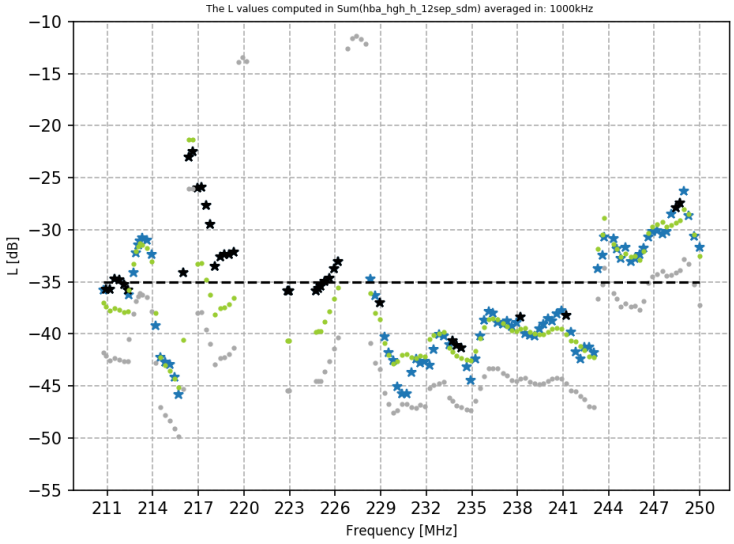

HBA_HIGH SDM (H)
12 September

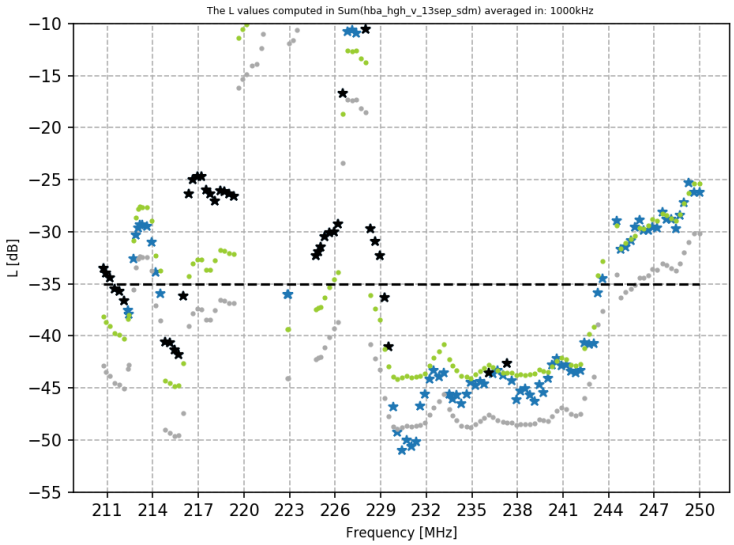

HBA_HIGH SDM (V)
13 September

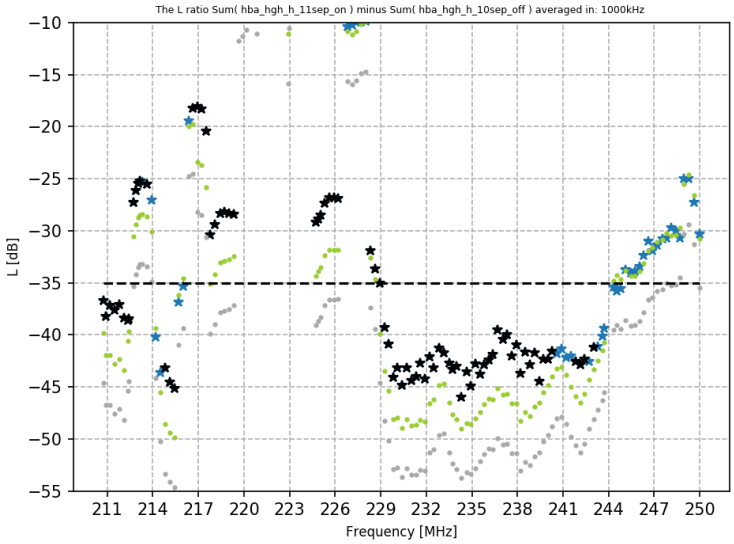

HBA_HIGH H (ON - OFF)
11 -10 September

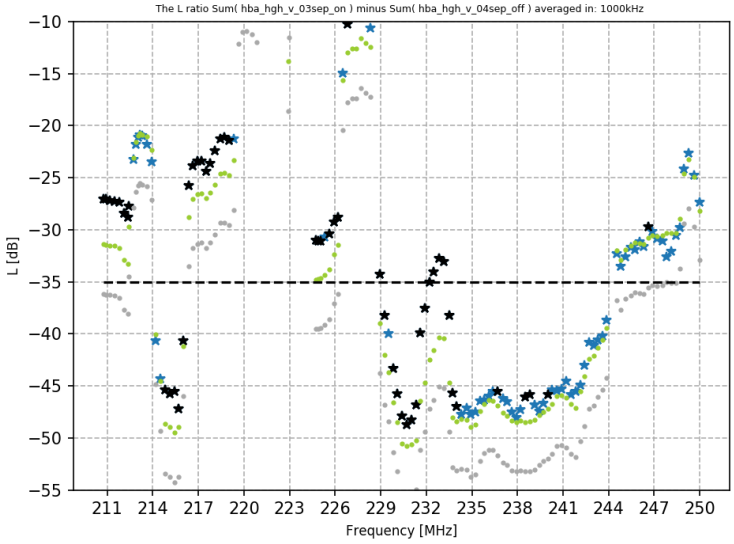

HBA_HIGH V (ON - OFF)
3 - 4 September

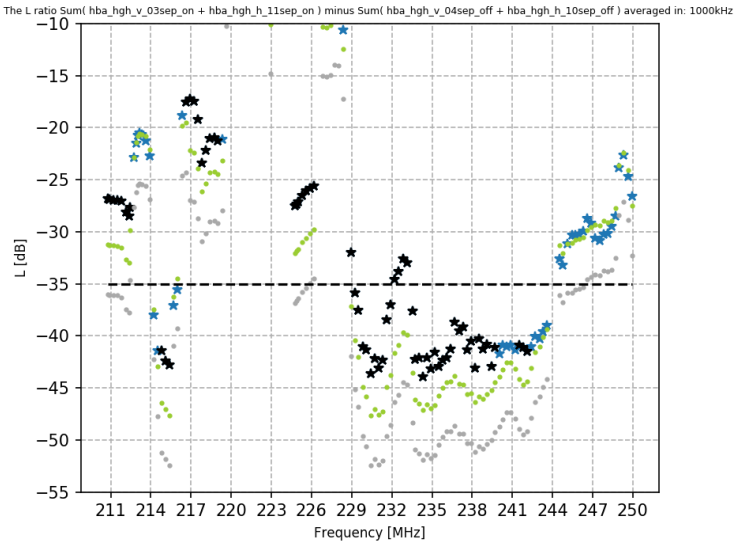

HBA_HIGH ON (H+V) – HBA_HIGH OFF (H+V)
(3+11) – (4+10) September

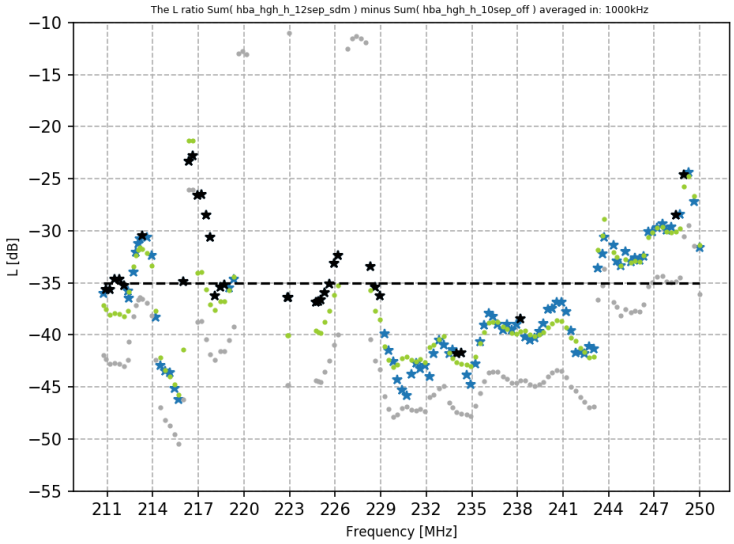

HBA_HIGH H (SDM - OFF)
12 -10 September

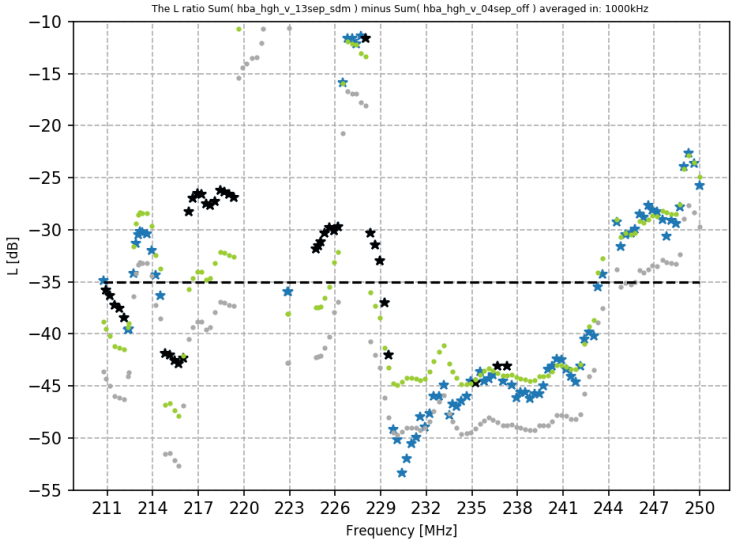

HBA_HIGH V (SDM - OFF)
13 - 4 September

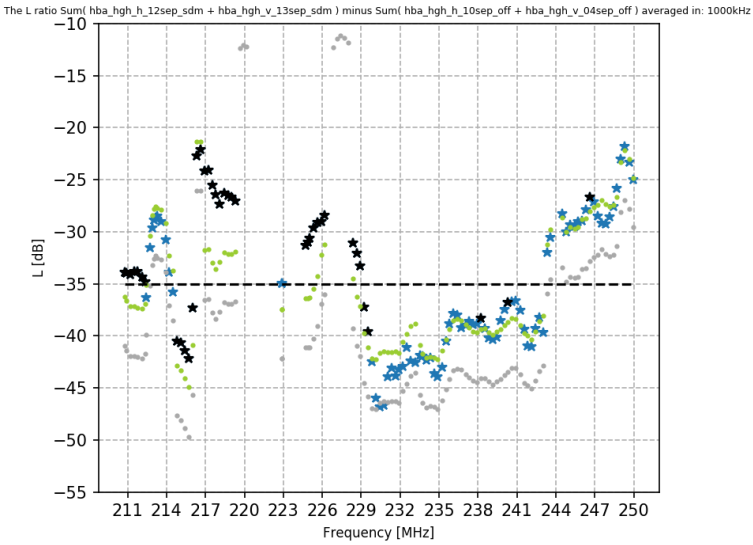

HBA_HIGH SDM (H+V) – HBA_HIGH OFF (H+V)
(12+13) - (4+10) September

5 Summary of results and conclusions

This report describes the measurements on the wind turbine DEE-2.1, which were carried out during the first two weeks of September 2019, and subsequently reports on the analysis results of these measurements. In particular, the measurements were analysed to find an excess of -35 dB as stated in the covenant [Cov].

These measurements were performed with a measuring instrument built by S&T and ASTRON. During the design and construction of the measuring instrument, ASTRON and AT were kept informed and checked both the design and the code. ASTRON and AT also have been informed and included in the execution of the measurements and in the analysis of the resulting data.

Therefore ASTRON, AT and S&T state together that:

1. The complete measuring instrument, with LOFAR as the measuring instrument, has proven to meet the requirements and conditions described in the system requirements document [SRD] and the functionality as laid down in the Architectural Design Document [ADD], both based on:
   - The Measuring method [MeasMeth], developed by Agentschap Telecom,
   - The Statement Of Objectives [LMEMI], written by ASTRON, for usage or LOFAR as a measurement device and
   - The WTEM Memorandum: L-formula [L-Form-upd], written by ASTRON.
2. The execution of the measurements and the analysis of the resulting data were performed correctly.

The observations that can be made with respect to the measurements and analyses are:

- All data has been backed up so that the results can be re-analyzed if necessary.
- The main analysis results per frequency band are:
  - **LBA:**
    - Around 70 MHz (in the LBA frequency band) we seem to have found evidence for a wideband signal whose source is believed to be found inside the WTG.

      Further analysis regarding a suspected UPS shows that indeed it contributes significantly to the measured interference.
    - Other signals exceeding the -35 dB limit are either caused by insufficient sensitivity of the equipment, excessive environmental noise, or cannot unambiguously assigned to a source inside the WTG, but more likely to a reflection of a source outside the WTG.
    - For the combination of H-pol and V-pol data, we added both H-pol signal and the V-pol signal. We notice then when the UPS is switched off, the H+V signal is at the -35 dB limit, whereas when the UPS is still operational, the H+V signal exceeds the -35 dB limit with 3 dB. Note, the operational version of the DEE-2.1 will be modified such that the UPS will have its impact reduced on the signal strength.
  - **HBA-LOW:**
    - The majority of the HBA-LOW band doesn't show a significant disturbance, except for a set of IM-products originating from the nonlinear character of the LOFAR receiver chain itself. At the higher frequencies, we see the effect of reflections of DAB emissions outside the WTG itself.
  - **HBA-MID**:
    - The HBA-MID is almost completely contaminated by DAB emissions. No disturbances from the WTG have been found.
  - **HBA-HIGH:**
    - The lower frequencies of this band are contaminated by DAB emissions just like the complete HBA-MID band. Other disturbances that can be found in the averaged L-plot cannot be unambiguously assigned to a source inside the WTG, but are more likely to be a reflection of a source outside the WTG.

- The summations of the H-polarization and V-polarization components (H+V) have been performed. What can be concluded from the results is:
    - For those ranges where there is a signal from the WTG detected (e.g., around the 70 MHz) we notice the expected increase in signal power of approximately 3 dB (the signal being more-or-less unpolarized).
    - In the HBA frequency range there is no signal higher than -35 dB value at the frequencies where the signal in individual H-polarization and V-polarization component is under -35 dB level, i.e., no new exceedances of the -35 dB level are introduced by the summation.

Conclusion:

One signal has been found around the 70 MHz that is believed to originate from the WTG. This issue has been further investigated and it was shown that the signal can be linked to the workings of one of the UPS systems inside the WTG. This has been validated by processing the data for those time period for which it is certain that the UPS was not operative anymore. This analysis resulted indeed in evidence that the UPS contributes to the signal found at 70 MHz.

Other signals exceeding the -35 dB limit are either caused by insufficient sensitivity of the equipment, receiver characteristics, excessive environmental noise, or cannot unambiguously assigned to a source inside the WTG, but more likely to a reflection of a source outside the WTG.

Also, after the required summation of the polarization components (H-pol and V-pol) we have seen:

- A considerable improvement has been obtained is by switching off the UPS as part of the modification the WTG. The measured signal strength is then at the -35 dB limit for the 70 MHz region.
- Currently, no other frequency is suspected to exceed the -35 dB llimit value where the WTG must be assumed to be the source of the measured noise level.

Figure 34 gives a graphical overview of the main measurement results over entire frequency range.

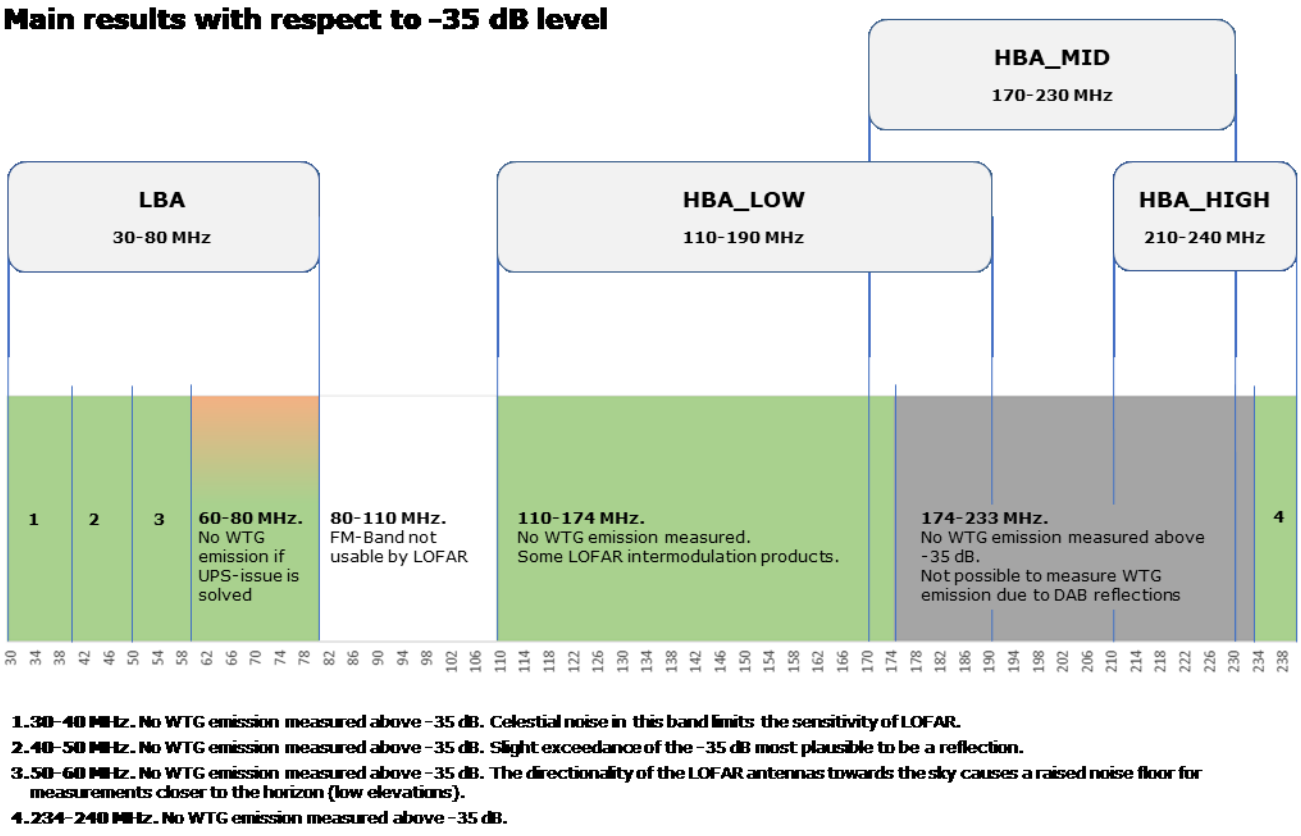

Figure 34: Overview of main measurement results over entire frequency range

6 Appendices

6.1 Appendix: Measurement schemes

The measurement schemes used for the September measurements are given in a separate document:

- ST-WDMO-WTEM-TN-004 Appendix - Measurement schemes September 2019

6.2 Appendix: Analysis reports

Table 9 lists the automated analysis reports, described in section 4.2, that belong as appendices to this Final Report.

L-value plot legend:

- **Orange** Reference source level "0 dB" level (it deviates a bit from the 0 dB value because the narrow band signal characteristic of the source)
- **Light grey** Measured noise floor
- **Light green** 3-sigma line
- **Light blue** Measured maxima outside centre cube
- **Black** Measured maxima inside centre cube
- **Red** Window around frequency attention

The above L-value plot legend applies to all L-value plots in the analysis reports in Table 9

Table 9: List of analysis reports*

Analysis report	Report name
1. V-pol, 3-sep-2019, Normal operation, LBA	wtem_report_lba_v_03sep_on.pdf
2. V-pol, 3-sep-2019, Normal operation, HBA_LOW	wtem_report_hba_LOW_v_03sep_on.pdf
3. V-pol, 3-sep-2019, Normal operation, HBA_MID	wtem_report_hba_MID_v_03sep_on.pdf
4. V-pol, 3-sep-2019, Normal operation, HBA_HIGH	wtem_report_hba_hgh_v_03sep_on.pdf
5. V-pol, 4-sep-2019, Wind turbine off, LBA	wtem_report_lba_v_04sep_off.pdf
6. V-pol, 4-sep-2019, Wind turbine off, HBA_LOW	wtem_report_hba_LOW_v_04sep_off.pdf
7. V-pol, 4-sep-2019, Wind turbine off, HBA_MID	wtem_report_hba_MID_v_04sep_off.pdf
8. V-pol, 4-sep-2019, Wind turbine off, HBA_HIGH	wtem_report_hba_hgh_v_04sep_off.pdf
9. V-pol, 13-sep-2019, EMC Shutdown, LBA V-pol, 13-sep-2019, EMC Shutdown, LBA, UPS reduced	wtem_report_lba_v_13sep_sdm.pdf wtem_report_lba_v_13sep_sdm_UPS_RED.pdf
10. V-pol, 13-sep-2019, EMC Shutdown, HBA_LOW	wtem_report_hba_LOW_v_13sep_sdm.pdf
11. V-pol, 13-sep-2019, EMC Shutdown, HBA_MID	wtem_report_hba_MID_v_13sep_sdm.pdf
12. V-pol, 13-sep-2019, EMC Shutdown, HBA_HIGH	wtem_report_hba_hgh_v_13sep_sdm.pdf
13. H-pol, 10-sep-2019, Wind turbine off, LBA	wtem_report_lba_h_10sep_off.pdf
14. H-pol, 10-sep-2019, Wind turbine off, HBA_LOW	wtem_report_hba_LOW_h_10sep_off.pdf
15. H-pol, 10-sep-2019, Wind turbine off, HBA_MID	wtem_report_hba_MID_h_10sep_off.pdf
16. H-pol, 10-sep-2019, Wind turbine off, HBA_HIGH	wtem_report_hba_hgh_h_10sep_off.pdf
17. H-pol, 11-sep-2019, Normal operation, LBA	wtem_report_lba_h_11sep_on.pdf
18. H-pol, 11-sep-2019, Normal operation, HBA_LOW	wtem_report_hba_LOW_h_11sep_on.pdf
19. H-pol, 11-sep-2019, Normal operation, HBA_MID	wtem_report_hba_MID_h_11sep_on.pdf
20. H-pol, 11-sep-2019, Normal operation, HBA_HIGH	wtem_report_hba_hgh_h_11sep_on.pdf
21. H-pol, 12-sep-2019, EMC Shutdown, LBA H-pol, 12-sep-2019, EMC Shutdown, LBA, UPS reduced	wtem_report_lba_h_12sep_sdm.pdf wtem_report_lba_h_12sep_sdm_UPS_RED.pdf
22. H-pol, 12-sep-2019, EMC Shutdown, HBA_LOW	wtem_report_hba_LOW_h_12sep_sdm.pdf
23. H-pol, 12-sep-2019, EMC Shutdown, HBA_MID	wtem_report_hba_MID_h_12sep_sdm.pdf
24. H-pol, 12-sep-2019, EMC Shutdown, HBA_HIGH	wtem_report_hba_hgh_h_12sep_sdm.pdf

*: All analysis reports have been updated for Final Report version 1.2, except the ones with grey highlighting.

6.3 Appendix: Analysis description

6.3.1 Pipeline overview

The overview of the processing pipeline is given in the figure below. The upper left part (left of the red dotted line; covering only approximately a tenth of the figure's width) represents the pre-processing performed by ASTRON. The upper right part (covering .9 of the figure's width) represents S[&]T's implementation of the processing pipeline.

The bottom half of the figure explains the phase calibration process in bit more detail.

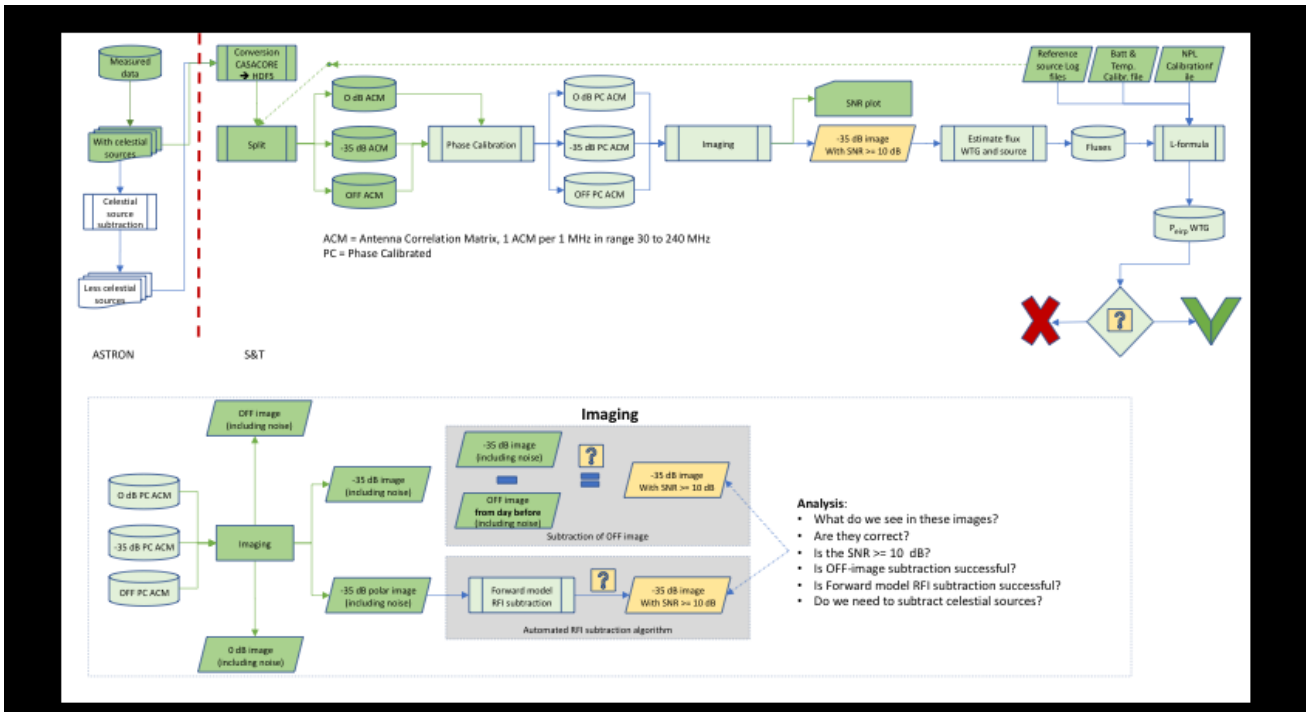

Figure 35: Processing pipeline overview

6.3.2 ASTRON Pre-processing

The following pre-processing is being performed:

- Cross correlation of the antenna signals, for the LBA data, and the three frequency ranges of the HBA data.
- Depending on the type of data:
  - Flagging of RFI affected data.
  - Flagging of RFI affected data and subtraction of the signals as produced by a selected set of celestial bodies.
- Averaging of the data, where flagged data are ignored in the calculation of the average.

6.3.3 Conversion CASACORE -> HDF5

The conversion of CASACORE to HDF5 format is basically a translation from one representation (CASACORE) to another (HDF5). There is no addition of data / information occurring at this step.

6.3.4 Split

The log file of the RS provides information about the state of the RS. These states include.

- 0dB: The output of the RS corresponds to the reference value of the covenant: In Article 1: "The (equivalent of) the limit values in EMC norm EN55011 for class A group 1, of 50 dBµV/m in a bandwidth of 120 kHz (this is equivalent with – 0,8 dBµV/(m · Hz)) at 10 m distance of the wind turbine nacelle at 100m height, are used as reference for the agreement in this covenant ("Norm")."

- OFF signal. No signal is emitted by the RS.

The RS is controlled remotely in a repeating pattern of 0dB and OFF signals (originally it was intended to use the 0 dB, -35 dB and OFF signals but the use of the -35 dB signal was discontinued):

- 0dB: This signal is clearly visible by the ACMs (care must be taken as the flagging algorithm of the pre-processing will see this signal as RFI), and can be used as a bright source for the calibration algorithm (see Section 6.3.5.1) that will focus the image correctly.
- The OFF-signal leads to a voxel image cube where the WTG is emitting and the RS is quiet. This will allow us to correctly estimate the WTG flux value.

A typical schedule for the controlling is as follows (for typically 2 hours):

- 0dB (12 sec), OFF (48 sec),
- 0dB (12 sec), OFF (48 sec),
- …etc…

The split-process, divides in the input data in parts of 0dB samples and OFF samples.

These subsets will be handled as follows:

- For each data set of 1 minute:
  - Take the 0dB samples and use these to phase calibrate the ACM data, i.e., compute the complex gains of the antenna system (see Section 6.3.5.1).
  - The phase calibration results will be used to construct the images of the OFF situation.
- Take all the OFF images during a 2hr measurement, and average the images for OFF situation.
- The OFF averaged image provides information for the flux emitted by the WTG.

In this way, variations in the environment and the equipment will be compensated.

6.3.5 Imaging and calibration

Further to the description in Section 3.1, the workings of the reference source is such that it emits repeatedly a signal of 0dB (roughly corresponding to 50 dBμV/m in a BWcov = 120 kHz band width at 10 m distance) for 12 s followed by a period of 48 s where no signal is emitted. During the 12 s of operation, the use of the reference source is threefold:

- The emitted signal is well-known and is related to the covenant limits (related to 50 dBμV/m in a BWcov = 120 kHz bandwidth at 10 m distance) as it is calibrated by NPL. As we measure the flux at both the reference source location and the WTG location, the known output of the reference source can be used to relate the measured WTG-flux to the covenant limit (using what we have called the L-formula).
- The reference source can be used to compensate for changes in the propagation path as the signal of the reference source and of the WTG travel approximately the same path.
- It can be used to calibrate the receiver antenna system for electronic fluctuations, as the 0dB signal is that it dominates the EM noise and disturbances for most of the situations.

The periods that the reference source emits no signal (those periods with a duration of 48 s) are being used to measure the output of the WTG. In this case, we are sure that the Reference Source doesn't affect the measurement at the WTG location.

The estimation of the signal strength at both the Reference Source location and the WTG location will be performed by a process called (near-field) imaging. In order to explain this process, think about (the slightly easier) problem of "simulation". For example, the Reference Source may be considered a point source. If we now define a 3D (spatial) grid around the Reference source, then we can simulate the behaviour of the electrical signals by describing the (a) attenuation of the signal, and (b) the phase behaviour of the signal, for first the elements (which are called "voxels") directly neighbouring the point source, next, for the voxels neighbouring these first cells, and so forth until the antennas of the LOFAR system are being reached. The imaging problem now, is the inverse of the simulation problem. From the antenna signals (that is, the cross correlations between each of the antenna pairs), the signal sources in the area around the Reference Source and the WTG must be computed. A strong source, such as the Reference Source, will be visible as a "hot spot" in the voxel cube. This hot spot is distorted (elongated) due to the point spread function of the receiving equipment. The following figure depicts such an elongated hot spot, where the figure on the right represents the voxel cube seen from above, and the figure on the left is the antenna information used to construct this image.

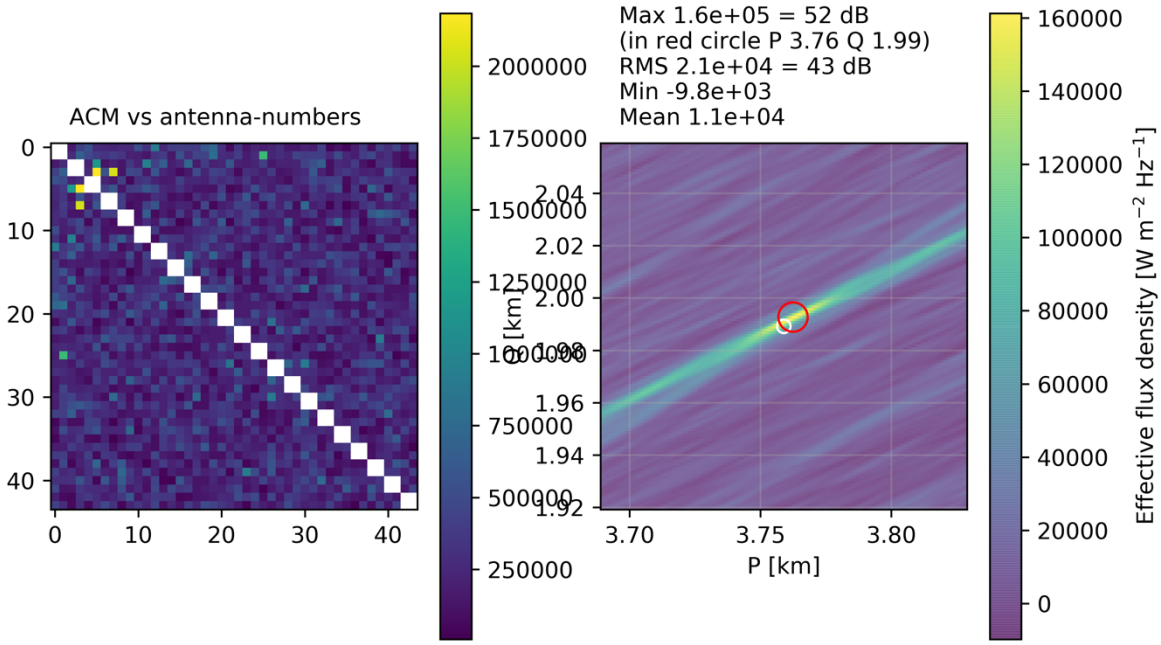

Figure 36: Imaging (right) of the Reference Source signal strength based on the Antenna Correlation Matrix information (left)

To summarize, based on the periodic signal of the reference source, we have the following analysis steps:

- The 12 s signal for which the reference source emits the 0-dB signal (modulo the differences as captured by the NPL-calibration) is used for calibrating the electronics of the receiving system.
  - This calibration estimates the (complex[9]) gains of each antenna element by iteratively adjusting these differential gains so that the measured signal corrected for the differential gains corresponds to the theoretical signal as computed by a forward model (predicting the measured signal based on the reference source's output and an ideal measurement system).
  - These calibration gains can then be used to create an image of the EM-sources in the area of the reference source. As the reference source emits a strong signal from a single point, the imaging process creates a 3D-image where the source is visible as point source distorted by the so-called point spread function of the receiving system. This image can be used to compute the signal flux at the reference source location.
- The 48 s where no signal is emitted by the reference source:
  - The calibration gains as just computed using the preceding 12 s signal are then used to image the area around the WTG. Again, if the WTG emits a strong signal, we will see in the voxel area these emitting points (again distorted by the point spread function of the receiving system).

This computation will be performed for each frequency within the range of 30 … 240 MHz, with an interval of 43 kHz.

As described previously, to reduce the thermal and systematic noise, a typical measurement duration takes two hours (thus, the 12 – 48 s sequence is repeated 120 times) for a single frequency band (LBA, HBA-LOW, HBA-MID, and HBA-HIGH). The reference system flux and the WTG flux are determined by averaging the voxel cubes that are computed for each of the 12s and 48s periods.

The reference source may be safely assumed to be a point source in the voxel cube describing the fluxes around the source. As an estimate for the flux of the reference source, the maximum value is taken at the location that is close to the reference source's location (i.e., within a radius of 15 m).

[9] Thus, phase and gain calibration.

The WTG isn't necessarily a point source, and depending on the nature of the disturbances be better modelled as a composite of multiple point sources (e.g., a source at the nacelle of the WTG, and a source at half of the mast). In this report, however, we assume a single source of EM-emission, and as a consequence, we take the same approach as for the reference source (simply, take the maximum value at the WTG location in the voxel cube). During the investigations of the estimated powers of the WTG, we made multiple 3D representations of the voxel cubes for those frequencies where substantial power values are seen, and for those frequencies we haven't identified a case where the WTG is assumed to be the source of the measured signal and multiple emission sources are visible in the 3D voxel cube.s

6.3.5.1 Phase Calibration

Phase calibration is performed by using a "forward model" that uses the Antenna Correlation Matrix (ACM) as input. Let us call this model calculate_acm_model (…); it computes the predicted ACM_p based on the location of the RS. The antenna gains g_i (complex values) are now iteratively adjusted such that the predicted ACM_p agrees with the measured ACM_0. The estimated gains are stored for further processing.

The calibration is performed for each of the frequencies for which a 0dB image / signal is available; thus, for every 1MHz frequency, except for the 10 MHz multiples (and possibly other frequencies that are affected by RFI such as DVB-T transmissions). The gains capture a number of "disturbances" of the antenna system, including the electrical and geophysical distance between the RS and the individual antennas. Assuming this distance-difference dominates the gain-estimation, we can use a straight-line approximation to estimate the noise in the individual gain estimation (e.g., due to RFI) and provide a gain-estimate the frequencies for which no 0dB signal is available.

Flagging

Note that the gains must be estimated using the 0dB data, using the strong 0dB signal. One of the ASTRON pre-processing involves the flagging of the data. The 0dB signal is, however, recognized as RFI, and being flagged. Flagged samples are also being removed from the dataset. The result is that the strong signal that is being used as calibration signal is being removed from the dataset. As a consequence, the unflagged data must be used for calibration, even in the case that flagged data is being used to compute the WTG signal strength.

Subtraction of background noise

The pipeline supports the possibility to subtract the background noise that has been measured previously. During a period that both the RS and the WTG are OFF (no electrical emission), the nominal RFI background can be measured and averaged over a certain period of time (measured over a period with the same sidereal date must also compensate for the celestial bodies).

Supported pipeline options.

The pipeline supports the following uses of the calibration data (i.e., the estimated gains)[10]

- No calibration, i.e., the OFF images are being generated without a gain correction. This mode of operation can be used for quick-look investigations.
- For those frequencies *f* for which 0dB signal is available, the OFF images are being corrected using the gains that are computed for that frequency *f*.
- Using the straight-line approximation of the gains, the OFF images are being corrected.

Implementation of the calibration function

The algorithm for the implementation of the calibration function is ANTSOL [ANTSOL]. The samples of the 12s period where the Reference Source is emitting the so-called 0 dB signal are being used to estimate the calibration gains.

6.3.5.2 Imaging

The basic imaging makes use of a phasor definition (i.e., describing how the phase behaves over distance).

The phasor relationships are described by the following piece of code:

[10] Note that although the measurements of September 2019 used only two modes of operation of the Reference Source (i.e., 0 dB signal and NO signal), the processing software is able to process also the mode that the Reference Source emits a signal of -35 dB.

```
def station_phasors(voxel_pqr, station_pqr, freq_hz):
    '''
    For each voxel in the voxel_pqr array, calculate a phasor for every station location.
    :param voxel_pqr: PQR coordinates of all voxels with shape ((xpixels+1) * (ypixels+1) * (zpixels+1), 3)
    :param station_pqr: PQR coordinates of all stations with shape (num_stations, 3)
    :param freq_hz: Frequency in Hz
    '''
    dist: np.float32          # distance between the station and the voxel
    wavenumber: np.float32    # wavenumber = (frequency / speed of light)

    wavenumber = freq_hz/c
    num_stations = station_pqr.shape[0]
    num_voxels = voxel_pqr.shape[0]
    result = np.zeros((num_voxels, num_stations), dtype=np.complex64)
    for v in nb.prange(num_voxels):
        v_pqr = voxel_pqr[v, :]
        for i in range(num_stations):
            pqr = station_pqr[i, :]
            dist = 0.0
            for j in range(3):
                dist += (pqr[j] - v_pqr[j])**2
            dist = np.sqrt(dist)
            result[v, i] += np.exp(1j*2*pi*wavenumber*dist)
    return result
```

And the construction of the images, i.e., the voxel cube, based on the ACM (auto correlation matrix) data. The imaging is described by the following python code:

```
def near_field_imager(acm, phasors_per_voxel):
    '''
    For every voxel in the phasors_per_voxel, loop over all stations and calculate the sum of
      (the ACM of that station) * (the phasor between the voxel and that station)
    Of the resulting sum take only the real value (i.e. the amplitude) and divide it by
    the square of the number of stations. The resulting array contains a float-value for every
    voxel which is called the flux of that voxel.
    '''
    fluxes = np.zeros(phasors_per_voxel.shape[0], dtype=np.float32)
    n2 = phasors_per_voxel.shape[1]**2
    for ix in nb.prange(phasors_per_voxel.shape[0]):
        p = phasors_per_voxel[ix, :]
        # pylint: disable=no-member
        fluxes[ix] = (np.dot(np.dot(np.conj(p), acm), p)).real
    return fluxes/n2
```

The pipeline processor constructs an image for the data of the XX polarization of the antenna, and an image of the YY polarization of the antenna. The images of the XX and YY data are then added.

6.3.5.3 Estimate flux of the WTG and Source

The flux of the WTG and Source are computed as follows:

- The RS flux is derived by finding the maximum flux value in the neighbourhood (within 15m) of the RS location, using the voxel cube centred around the RS that is constructed using the 12 s interval.
- The WTG flux is derived by finding the maximum flux value the neighbourhood (within 15m) of the WTG location, using the voxel cube centred around the WTG that is constructed using the 48s interval.

6.3.5.4 L-formula

According to [L-Form-upd] (which updates [MeasMeth]), the formula that in the end will be used to compute the covenant level equals:

$$L = R - 10 \cdot log_{10}(B) + 10 \cdot log_{10}(W) - 10 \cdot log_{10}(C) - 20 \cdot log_{10}(Dw/D\tau) + 0.8$$

Where B is the band width of the channel containing the reference source signal (9.155 kHz in 200 MHz clock mode, and 7.324 kHz in 160 MHz clock mode as of this writing), R is the e.i.r.p of the relevant reference source signal, as measured by NPL, in units of dBµV/m at 10 m distance (e.g. +47.2), W is the WTG's power flux density in correlator units as read from the Measurement Set, C is reference source's power flux density in correlator units as read from the Measurement Set, and Dw and Dc are the distance towards the superterp's centre of the WTG, respectively the reference source.

The computation of the value of R depends on the following variables:

- Battery voltage
- Setting of the Reference Source's attenuation
- Inside temperature
- Calibration table (from the absolute power calibration).

All these items are being read from the RS log file (for the battery voltage, RS attenuation, and Inside Temperature), and the calibration file from NPL.

The value L must be determined for the observations with the wind turbine fully powered off, as well as fully powered on. The radiated level is then estimated by $L_{radiated}$ = 10 log ($10L_{on}/10$ - $10L_{off}/10$). We basically perform the calculation according to the previous formula twice, the subtraction lets us with the wind turbine emission only. Results are found in section 4.3.11.

6.4 Appendix: Change list

6.4.1 Changes version 1.1

This version 1.1 is an update based on review remarks on version 1.0 and the outcome of the discussion of the report on 23 September 2019. Additionally, H+V-plots have been added as planned.

In general, the outcome of the discussion on the 1.0 version of the report on 23 September 2019 was that, based on the disturbances in some of the L-value plots, according to ASTRON and AT no conclusions can be made whether the wind turbine is free from radiation, or at least radiates below -35dB, apart from the radiation by the discovered UPS.

The disturbances in some of the L-value plots are caused by exceptional high values in the ACM's, which in turn originate from values in the original data of ASTRON. To prevent these extremes, the processing pipe line already applied a 5-sigma filter over the ASTRON time series data. Any value above the 5-sigma value is discarded. Apparently, it is necessary to apply this filter also on the set of baselines in the ACM, to filter out complete baselines with extreme values (applied to DXX and DYY separately). This filter has now also been applied, with the restriction to filter out a maximum of 3 baselines per frequency. The results have been added to this document (see Table 11: Updated L-value plots, Updated L-value plot analysis results and Updated analysis reports).

In a phone call on 25 October ASTRON was not convinced that a disturbance around the 47 MHz in LBA is not caused by the wind turbine. A section has been added with a further investigation of that suspect disturbance.

In Table 10 the list is given of review remark documents that were received on version 1.0 of this report and handled in the current version. Table 11 lists the changes in this report.

Table 12 lists review remarks that have not been implemented (yet).

Table 10: List of review remark documents received

Reviewer	Review document
(ASTRON)	ST-WDMO-WTEM-REP-005 End Report-MAB.pdf
(AT)	• RE_ WTEM End Report for internal review.msg • Misleidend zij aanzicht.msg
(AT)	ST-WDMO-WTEM-REP-005 End Report_.docx
(S&T)	Various spelling and grammatical improvement suggestions

Table 11: List of changes in this version of the report

Change	Location	Originator
Added new sections:		
• **Further analysis around 47 MHz (LBA)**	Ssection 4.3.1 and Section 4.3.5	ASTRON
• **H+V**	Section 4.3.11 H+V	S&T
Updated L-value plots:		
• **V-ON LBA (3 sept)**	Section 4.3.1 V-polarization LBA	ASTRON/AT
• **V-OFF LBA (4 sept)**	Section 4.3.1 V-polarization LBA	ASTRON/AT
• **V-SDM LBA (13 sept)**	Section 4.3.1 V-polarization LBA	ASTRON/AT
• **V-SDM LBA (13 sept) – Zoomed, All Data**	Section4.3.10.2 Results 13 September (LBA reduced dataset)	ASTRON/AT
• **V-SDM LBA (13 sept) – Zoomed, UPS reduced data**	Section4.3.10.2 Results 13 September (LBA reduced dataset)	ASTRON/AT
• **V-OFF HBA_LOW (4 sept)**	Section 4.3.2 V-polarization HBA-LOW	ASTRON/AT
• **V-ON HBA_HIGH (3 sept) ???**	Section 4.3.4 V-polarisation HBA_HIGH	ASTRON/AT

Change	Location	Originator
• **V-OFF HBA_HIGH (4 sept)**	Section 4.3.4 V-polarisation HBA_HIGH	ASTRON/AT
• **H-OFF LBA (10 sept)**	Section 4.3.5 H-polarization LBA	ASTRON/AT
• **H-ON HBA_LOW (11 sept)**	Section 4.3.6 H-polarization HBA_LOW	ASTRON/AT
• **H-OFF HBA_LOW (10 sept)**	Section 4.3.6 H-polarization HBA_LOW	ASTRON/AT
• **H-SDM HBA_LOW (12 sept)**	Section 4.3.6 H-polarization HBA_LOW	ASTRON/AT
• **H-ON HBA_HIGH (11 sept)**	Section 4.3.8 H-polarization HBA_HIGH	ASTRON/AT
• **H-OFF HBA_HIGH (10 sept)**	Section 4.3.8 H-polarization HBA_HIGH	ASTRON/AT
Updated L-value plot analysis results:		
• **V-LBA: Remarks on plots and analysis**	Section 4.3.1 V-polarization LBA	ASTRON/AT
• **V-HBA_LOW: Remarks on plots and analysis**	Section 4.3.2 V-polarization HBA-LOW	ASTRON/AT
• **V-HBA_HIGH: Remarks on plots and analysis**	Section 4.3.4 V-polarisation HBA_HIGH	ASTRON/AT
• **H-LBA: Remarks on plots and analysis**	Section 4.3.5 H-polarization LBA	ASTRON/AT
• **H-HBA_LOW: Remarks on plots and analysis**	Section 4.3.6 H-polarization HBA_LOW	ASTRON/AT
• **H-HBA_HIGH: Remarks on plots and analysis**	Section 4.3.8 H-polarization HBA_HIGH	ASTRON/AT
• **V-SDM LBA (13 sept): Remarks on plots**	Section4.3.10.2 Results 13 September (LBA reduced dataset)	ASTRON/AT
Updated automated analysis reports:		
• **1. V-pol, 3-sep-2019, Normal operation, LBA**	Section 6.2 Appendix: Analysis reports, Table 9	ASTRON/AT
• **5. V-pol, 4-sep-2019, Wind turbine off, LBA**	Section 6.2 Appendix: Analysis reports, Table 9	ASTRON/AT
• **6. V-pol, 4-sep-2019, Wind turbine off, HBA_LOW**	Section 6.2 Appendix: Analysis reports, Table 9	ASTRON/AT
• **8. V-pol, 4-sep-2019, Wind turbine off, HBA_HIGH**	Section 6.2 Appendix: Analysis reports, Table 9	ASTRON/AT
• **9. V-pol, 13-sep-2019, EMC Shutdown, LBA, UPS reduced**	Section 6.2 Appendix: Analysis reports, Table 9	ASTRON/AT
• **13. H-pol, 10-sep-2019, Wind turbine off, LBA**	Section 6.2 Appendix: Analysis reports, Table 9	ASTRON/AT
• **14. H-pol, 10-sep-2019, Wind turbine off, HBA_LOW**	Section 6.2 Appendix: Analysis reports, Table 9	ASTRON/AT
• **16. H-pol, 10-sep-2019, Wind turbine off, HBA_HIGH**	Section 6.2 Appendix: Analysis reports, Table 9	ASTRON/AT
• **18. H-pol, 11-sep-2019, Normal operation, HBA_LOW**	Section 6.2 Appendix: Analysis reports, Table 9	ASTRON/AT
• **20. H-pol, 11-sep-2019, Normal operation, HBA_HIGH**	Section 6.2 Appendix: Analysis reports, Table 9	ASTRON/AT
• **22. H-pol, 12-sep-2019, EMC Shutdown, HBA_LOW**	Section 6.2 Appendix: Analysis reports, Table 9	ASTRON/AT
Review remarks:		

• **Changed text "VENTOLINES" to "the three companies building DMO".**
• **Removed text: "(representing the future owners of the wind farms)"**
• **Added text: "These parties are:**
  • **Raedthuys Windenergie B.V.,**
  • **Duurzame Energieproductie Exloërmond B.V.,**
  • **Windpark Oostermoer Exploitatie B.V."**
	Section 1, first paragraph
	Section 2.2, first paragraph
		ASTRON/ AT/ VENTOLINES

Change	Location	Originator
• **Added text: "so called (pre-)validation"**	Section 1, third paragraph	AT
• **Changed text "around 70 MHz" to "in the range of 60 to 85 MHz"**	Section 1, Conclusion	ASTRON
• **Updated tag "[L-form]" to "[L-Form-upd]"**	Section 2.2, bullet: The Memorandum of ASTRON	AT
• **Updated issue date of [L-form-upd] to 2019/10/11**	Section 2.4, [L-form-upd], issue date	AT
• **Updated version and issue date of [UNCERT]**	Section 2.4, [UNCERT], issue date	ASTRON
• **Changed text "XX" to "YY" and vice versa**	Section 3.2, two bullets + paragraph below the two bullets	AT
• **Added references to [ADD] and [MeasMeth]**	Section 3.3., Figure 1 and Table 3	AT
• **Added text: ", on suggestion of Dick Harberts (Philips) who is supporting WTG project development,"**	Section 3.2, last paragraph	ASTRON
• **Changed text "HBA_MID" to HBA_LOW"**	Section 3.5.3, fourth paragraph	ASTRON
• **Updated according to the outcome of uncertainty assessment version 1.1 [UNCERT]**	Section 1, uncertainty values Section 3.7 and table 6	ASTRON
• **Added text: ", statistically with 88.9% probability, by Chebyshev's inequality[3]. For unimodal distributions the probability of being within the interval is at least 95% by the Vysochanskij–Petunin inequality[4]. There may be certain assumptions for a distribution that force this probability to be at least 98%[5] and here for 3σ: 99,73%[5]."**	Section 4.1.1, third bullet	AT
• **Updated L-formula (swopped numerator and denumerator)**	Section 4.1.2, L- formula	AT
• **Deleted first paragraph of Reflection about blade reflection, including the two bullets and original example figure 7.**	Section 4.1.3, Reflection, below figure 6	AT
• **Changed "4 MHz" to "1.5 MHz"**	Section 4.1.3, Reflection, fourth paragraph	AT
• **Changed the second bullet to "Analogue TV uses VHF frequencies from 47 MHz to 68 MHz and 174 to 230 MHz"** • **Changed footnote 2 to "http://www.frequentieland.nl/omroep/tv.htm"**	Section 4.1.3, Reflection, second bullet	ASTRON
• **Changed text "LOFAR system" to "measurement system"**	Section 4.1.3, Noise floor is higher than -35 dB	AT
• **Finished the sentence with "individual measurements show."**	Section 4.1.3, Signal from the WTG second bullet	AT
• **Added text "(using 5 times MAD)" with a reference in a footnote**	Section 4.2, bullet WTG data	S&T
• **Updated "Orange" explanation**	Section 4.3, L-value plot legend Section 6.2, L-value plot legend	AT
• **Whole section cleaned from -35 dB parts**	Section 6.3.4 Section 6.3.5.1	S&T/AT
• **First sentence changed to: "Phase calibration is performed by using a "forward model" that uses the Antenna Correlation Matrix (ACM) as input. Let us call this model calculate_acm_model (…); it computes the predicted ACMp based on the location of the RS."**	Section 6.3.5.1, first paragraph, first sentence	AT
Various • **Spelling and grammatical changes reported from all review remark documents.** • **Minor textual changes**	Whole document	S&T AT

Table 12: Review remarks not implemented (yet)

Remark	Location	Discussion	Status	Originator
The SRD document is out-of-date, leave it out or update it to what was really done	Section 2.4, [SRD]	S&T: This is the latest version. Please state what updates are missing.	OPEN	AT
Maybe helpful to point at WTG location and at the measured maximum	Section 4.1.3, figure 6	S&T: WTG location is 0,0. Implementing showing the measured maximum, was not requested at the time and is at this point in time too much work as it means regenerating all these images	CLOSED	AT
ODD sharp boundary	Section 4.3.1, figures 8 and 9	MB: This was resolved. It's because the maximum is at the edge of the box at those lines of sight	CLOSED	ASTRON

6.4.2 Changes version 1.2

This version 1.2 is an update based on review remarks on version 1.1 and the outcome of the CoCo-meeting 30 October 2019. All added and changed images have been processed with the latest pipeline software version, including the ACM filter to filter excessive values form the ACM.

In Table 13 the list is given of review input documents that were received on version 1.0 of this report and handled in the current version. Table 14 lists the changes in this report.

Table 13: List of version 1.1 review remark documents received

Reviewer	Review input document
(ASTRON)	Email "Re: Word versie Eindrappport v1.1." dated Tue 05/11/2019 22:05
(AT)	Verslag coördinatiecommissie_30_10_2019.docx
(AT)	ST-WDMO-WTEM-REP-005 End Report 1.1 rev.docx

Table 14: List of changes in this version 1.2 of the report

Change	Location	Originator
New sections		
• **H+V HBA_LOW**	Section 4.3.11.2 HBA_LOW	S&T
• **H+V HBA_HIGH**	Section 4.3.11.3 HBA_HIGH	S&T
Updated L-value plots:		
• **V-SDM HBA_LOW (13 sept)**	Section 4.3.2	S&T
• **V-ON HBA_HIGH (3 sep)**	Section 4.3.4	S&T
Updated automated analysis reports:		
• **All analysis reports have been updated, except:** ○ the HBA_MID reports and ○ V-pol, EMC Shutdown, LBA (incl. UPS) ○ H-pol, EMC Shutdown, LBA (incl. UPS)	Sections 4.2 and 6.2	S&T
Review remarks		
• **Updated version and issue date of [UNCERT]**	Section 2.4, [UNCERT], version and issue date	ASTRON/AT
• **Updated uncertainty figures with the figure for H+V (note: not yet in the v1.2 draft version)**	Section 1: paragraph 6, first bullet Section 3.7: Between 1st and 2nd paragraph	ASTRON
• **Added additional analysis of the in the 160 … 170 MHz range, regarding the additional signal structure (on top of the "IM product")**	Section 4.3.6	ASTRON
• **Added additional analysis of a signal (lower than -35 dB) at the frequencies 230 MHz and higher**	Section 4.3.8	AT
• **Updated with statements describing the cooperation between ASTRON, AT and S&T, the compliance of the measurement instrument, the method of measurement and correctness of measurement execution and data analysis**	Section 1, fourth and fifth paragraph Section 5, first three paragraphs	Chairman CoCo
• **Updated result en conclusions regarding H+V analysis**	Section 1, second bullet of "The results of the summations of the H-polarization and V-polarization components (H+V) are;", page 7 Section 5, second bullet of "What can be concluded from the results is:", page 76	S&T

Change	Location	Originator
• **Added Overview of main measurement results over entire frequency range , using a linear frequency scaling**	Section 1, figure 1 Section 5, figure 34	ASTRON Chairman CoCo
• **Updated text with some editorial improvements. All suggestions have implemented** ST-WDMO-WTEM-REP-005 End Report 1.1 revBS.docx	Sections 1 and 5	AT
• **Updated text with all of the suggested improvements, except for the suggestion to shift paragraphs in section 4.3** Email "Re: Word versie Eindrappport v1.1." dated Tue 05/11/2019 22:05	Sections 3, 4, 5 and 6	ASTRON

6.4.3 Changes version 1.2 Final

This version 1.2 Final is an update based on review remarks on version 1.2 draft. During the skype meeting of Monday 18 November 17:00 hours, the remarks were discussed and outcome has been updated in this document. With these updates, version 1.2 Final of this document, has been approved by all parties, being ASTRON, AT, Ventolines and S&T.

In Table 15 the list is given of review input documents that were received on version 1.0 of this report and handled in the current version. Table 16 lists the agreed changes in this report. Table 17 lists review remarks that have not been implemented, as agreed.

Table 15: List of version 1.2 draft review remarks received

Reviewer	Review input document
(AT)	Email "RE: Final report versie 1.2 draft" dated Mon 18/11/2019 16:51
(ASTRON), (AT)	Orally, during skype meeting Monday 18 November 17:00 hours: no further comments, the changes have updated according the remarks made on version 1.2 draft.

Table 16: List of changes in this version 1.2 Final of the report

Change	Location	Originator
• **Removed the words "and successfully"**	Section 1, list number 2 of the 5th paragraph (ASTRON, AT and S&T statement)	AT
• **Updated uncertainty values conform [UNCERT]**	Section 1, 6th paragraph, 1st bullet	ASTRON
• **Updated version and issue date of [UNCERT]**	Section 2.4, [UNCERT]	S&T
• **Updated uncertainty values conform [UNCERT]**	Section 3.7: • 1st paragraph • Table 6	ASTRON
• **Removed the words "and successfully"**	Section 5, list number 2 of the 3rd paragraph (ASTRON, AT and S&T statement)	AT

Table 17: Review remarks not implemented

Remark	Location	Discussion	Status	Originator
Remarks on the text: Therefore ASTRON, AT and S&T state together that: 1. The complete measuring instrument, with LOFAR as the measuring instrument, has proven to meet the requirements and conditions, **as good as possible within the given constraints**, described in the system requirements document [SRD] and the functionality as laid down in the Architectural Design Document [ADD], both based on: • The Measuring method [MeasMeth], developed by Agentschap Telecom, • The Statement Of Objectives [LMEMI], written by ASTRON, for usage or LOFAR as a measurement device and • The WTEM Memorandum: L-formula [L-Form-upd], written by ASTRON. 2. The execution of the measurements and the analysis of the resulting data were performed correctly ~~and successfully~~.	Section 1 and 5	The text addition **", as good as possible within the given constraints,"** in list number 1 was not added, after discussion in the skype meeting of Monday 18 November. AT pleaded themselves that the addition already is contained in the ADD and SRD. ASTRON agreed. The words "and successfully" have been removed from the text, as they may be subjective.	CLOSED	AT

< End of Document>